AKENTEN APPIAH-MENKA UNIVERSITY OF SKILLS TRAINING AND ENTREPRENEURIAL DEVELOPMENT

EXPLORATION OF AVOCADO SEEDS AS MATERIAL FOR THE ELIMINATION OF TOXIC METALS IN GROUNDWATER IN SOME COMMUNITIES IN THE SEFWI WIAWSO MUNICIPALITY, GHANA

ASOMU, ADER BLONDY

2025

AKENTEN APPIAH-MENKA UNIVERSITY OF SKILLS TRAINING AND ENTREPRENEURIAL DEVELOPMENT

EXPLORATION OF AVOCADO SEEDS AS MATERIAL FOR THE ELIMINATION OF TOXIC METALS IN GROUNDWATER IN SOME COMMUNITIES IN THE SEFWI WIAWSO MUNICIPALITY, GHANA

BY

ASOMU ADER BLONDY

(8211440005)

A Thesis Submitted to the Department of Chemistry Education of the Faculty of Science Education, Akenten Appiah-Menka University of Skills Training and Entrepreneurial Development, in partial fulfilment of the requirements for the award of a Master of Philosophy Degree in Chemistry Education.

AUGUST, 2025

DECLARATION

Candidate's Declaration

I hereby declare that this thesis, with the exception of quotations and references contained in published works which have all been duly acknowledged, is the result of my own original work, and that no part of it has been presented for another degree at this university or elsewhere.

Candidate's Name: ASOMU ADER BLONDY

Signature: …… Date:……

Supervisor's Declaration

We hereby declare that the preparation and presentation of the thesis were supervised in accordance with the guidelines on supervision of thesis as laid down by the Akenten Appiah-Menka University of Skills Training and Entrepreneurial Development.

Principal Supervisor's Name: DR. AGYAPONG EMMANUEL ASARE

Signature:…… Date:…….

Co-Supervisor's Name: PROF. EMMANUEL DARTEY

Signature: ……. Date:……

ACKNOWLEDGEMENTS

I thank the Almighty God for his protection, direction and mercy throughout my life during this research work. My special thank you to my supervisors, Dr. Emmanuel Agyapong Asare and Prof. Emmanuel Dartey, lecturers in the Department of Chemistry, Akenten Appiah-Menka University of Skills training and Entrepreneurial Development, Mampong campus, for their fathering role, technical guidance and encouragement throughout this research work. Another thanks goes to Godfred for his help and valuable inputs to this work. A distinctive thanks goes to my mother, Ehiman Abah Therese and all my friends who helped in any other way to make this work possible. A special thanks also to Lydia Amachie Blay for her love, encouragement, financial support and prayers to see me through this work. Finally, I would also like to recognize with much love, my children, Teddy Darius Blondy, Doritha Ablemma Asomu, Eliana Abah Blondy and Inez Deloris Asomu for their indefatigable support.

DEDICATION

This research is dedicated to my wife, Mrs. Lydia Amachie Blay, and my family.

TABLE OF CONTENTS

LIST TABLES

LIST OF FIGURES

ABSTRACT

The use of activated avocado seeds for adsorption is an environmentally safe, effective and affordable technique for cutting back heavy metal levels in water. In this study, activated carbon was produced from avocado seeds, characterised, and tested for its adsorptive capacity on As, Cd and Pb in selected groundwater resources at Sefwi Wiawso Municipality in the Western North region of Ghana. A physical activation method was used to obtain the activated avocado seeds. Surface properties of the activated avocado seeds produced were assessed by XRF, FTIR and SEM-EDX spectroscopy before and after use in the adsorption process. Surface characterisation analysis showed that the activated avocado seeds were potentially good adsorbents for selected heavy metals. Except for turbidity levels, the physicochemical properties of the water samples used were below WHO permissible limits. As, Cd, and Pb levels in the water samples also exceeded the WHO permissible limit. Over 90% of the ions of the heavy metals were removed from the water samples. The metal ions investigated were removed from the water samples. The Freundlich isotherm and the second-order pseudo-kinetic models best fitted the equilibrium adsorption data of the study. The kinetics studies showed that the adsorption process was chemisorption, whilst the thermodynamics studies found the adsorption to be spontaneous and exothermic. This study recommended a study into the production of activated carbon from other agricultural waste products and assesses their adsorptive capacities on metal-ion removal in water resources.

CHAPTER ONE

INTRODUCTION

1.1 Background to the Study

Sprouting of industries as well as modernized agriculture activities are major sources of water contamination, and this, in recent years, has been a concern to the world. Through pollution, several societies worldwide have been denied access to a clean and fresh water supply (UNICEF, 2025). Approximately four billion individuals are subjected to a severe form of water shortage at least once a year (Mekonnen & Hoekstra, 2016).

The exploitation of fresh water sources is problematic due to mining activities, particularly in Africa, where vast quantities needed for the purification of ore, pollutants from mining waste, as well as seepage of water into tailings and waste rock dumps (Boateng et al., 2020; Armah et al., 2016). Inefficient utilization of these assets has made us realise how our safe and usable water resources might run out due to mismanagement by human beings.

Even though, target 6.1 of the Sustainable Development Goals requires that everyone enjoys fair access to potable and reasonably priced drinking water, there is an estimated value of approximately four hundred and thirty-five million people across the world who consume unprotected water, such as wells and springs (WHO, 2019). Numerous African communities depend on environmental ground and surface water resources polluted by wastewater and other contaminants for their domestic needs (UNICEF, 2021; WHO, 2020). Notwithstanding the vital and significant roles played by water in our daily lives, potable water has no value in the eyes of illegal miners and some farmers in Ghana.

Industrial operations such as paint productions, glass manufacturing, electroplating, batteries fabrication and mineral extraction activities have progressively released large volumes of non-biodegradable metals to contaminate water bodies (Suja et al., 2024). Over time, demand for metallic elements in modern society has remarkably increased. In attempts to satisfy these needs, poisonous and hazardous metals, including chalcophiles, have continuously increased in aquatic systems and the broader environment (Armah et al., 2014).

Artisanal gold mining activities (galamsey) in Ghana have also destroyed most natural resources including water (Kuffour et al., 2018). Such informal processes happen in most regions of the country including Sefwi Wiawso and adjacent communities in Western North, Ghana (Owusu-Nimo et al., 2018). Among the 195 settlements in Sefwi Wiawso Municipality, which are equally affected by mining activities, are Amafie, Kojina and Wiawso (GSS, 2000).

The toxic chemicals employed in the mining process by miners during mining activities not only degrade land and water resources but also become altered as they absorb metallic contaminants within the ecosystem and pollute water resources through percolation and overland flow (Hilson,2002; Kuma & Younger, 2004; Obiri et al., 2016; Tarras-Wahlberg et al., 2001). Hazardous substances like cadmium, mercury, lead and arsenic are released from mining sites, and these metals have been linked to endocrine disruption (Iavicoli et al., 2009; Tchounwou et al., 2012; Diamanti-Kandarakis et al., 2009). The endocrine-disrupting metals have tearing effects on the normal functioning in humans and other living organisms (Iavicoli et al., 2009; Sargis, 2020; Diamant-Kandarakis et al., 2009).). For instance, cadmium is linked to low progesterone and

prolactin levels in humans and lower testosterone in men (Hou et al., 2022). In addition, cadmium results in kidney and hepatic impairment, acute pulmonary oedema, testicle injury and osteomalacia (Gouilleux et al., 2017; Fouladi-Nashta et al., 2020).

Chronic exposure to lead has been found to cause harmful effects on both female and male reproductive systems in humans (Telisman et al., 2007). High amount of arsenic exposure is also reported to have a neurological effect, chronic lung disease, vascular disease, arteriosclerosis, renal disease, and cardiovascular diseases (Rahaman et al., 2021). Exposure to rising arsenic content is associated with several health complications, including several types of cancers, cerebrovascular disorders, and reproductive health impacts (Rahaman et al., 2021).

Toxic metallic contaminants in aquatic resources pose danger to the health of the people, more so to the developing countries that lack adequate technological knowledge in the remediation of metals (Obiri et al., 2010). It is therefore crucial to take measures to reduce and eliminate these pollutants from the natural water resources and the environment (Mohan & Gandhimathi, 2009).

According to Meunier et al. (2006), among the commonly applied approaches for treating water resources contaminated with metals are electrolytic process, membrane technology, resin-based treatment, adsorption, coagulation process, as well as chemical treatment, among others. Although some of the approaches adopted by different researchers from previous studies provided some positive outcomes in eliminating metal contaminants (Gautam et al., 2014). However, Dawam et al. (2025) pointed out that some of the strategies for the remediation of high levels of metal ions are costly. Therefore,

there should be an attempt to devise effective, non-hazardous, innovative, and affordable procedures for extracting and recovering these metals in polluted water bodies (Joseph et al., 2019). Adsorption has been identified to be a highly efficient elimination approach, largely attributed to its economic viability (Malik et al., 2016; Sandhya Babel et al., 2003). Various materials are employed in the remediation of heavy metals (Raji et al.,2023), with commercial examples including carbon nanotube, graphene, and activated carbon. The naturally occurring: clay, zeolites. Another group is bio-adsorbents, which include chitins and chitosan, peat, yeasts, fungal and bacterial biomass, and agricultural, animal, and industrial waste products, also form a beneficial source of adsorbent material (Chakraborty et al., 2020).

Among the different treatment strategies for heavy metal removal in aquatic environments, activated carbon adsorption is considered one of the most reliable methods due to its economic feasibility, green characteristics, and strong adsorption capacity (Raji et al., 2023; Crini et al., 2019). Activated carbon is a carbonaceous material with a highly porous structure through which slightly small holes have been introduced in the material as a result of controlled heating or chemical treatment, which causes its surface area to expand significantly and enable it to adsorb with more capacity (Hupian et al.,2023) Activated carbon is composed of several constituents which typically include starches, simple sugars, proteins, lipids, hydrocarbons, hemicellulose, in addition to water, with these constituents providing functional groups such hydroxyl, amino, carboxyl, and ester (Ioannidou & Zabaniotou, 2007). Such functional groups enable the adsorbent to undergo a process of eliminating the pollutants through binding heavy metals in the water, and creating metal complexes on its surface (Chen et al., 2013). Activated carbon application aimed at treating contaminated surface and groundwater resources involves replacing

existing ions on the activated carbon surfaces with metal ions in aqueous systems (Chen et al., 2013).

Most of the currently known activated carbons are the products of agricultural wastes, which include, among others, cobs and sawdust, shells of palm kernel fruits, and coconuts. They have also been successfully used as clean-up agents towards contaminated water (Buah et al., 2016; Onundi et al., 2010, and Gaikwad, 2004). There has been no concerted effort in Ghana, so far, to utilize activated avocado seeds to extract heavy metals in water bodies across the country, as avocado seeds are readily available in the Southern Region of the country (Adams et al., 2016), and they stand out as a cost-effective, eco-friendly, and highly efficient biosorbent. Their surface area, chemical functionality, and renewable nature make them a strong alternative or complement to other biosorbents like coconut shells, plantain peels or maize cobs in water purification and heavy metal removal processes. Considering that activated avocado seeds exhibit a potential to eliminate heavy metals present in polluted groundwater, it is vital to conduct a comprehensive study of the adsorption and characterization of such material and assess its effectiveness in the remediation of farming and artisanal small-scale mining communities in the Sefwi-Wiawso Municipality.

1.2 Statement of the Problem

The widespread dependency of chemicals in the extraction cycle adds to the toxic metal contaminants in the surroundings. The movement of such metals is gradual, evading the processing centres and eventually finding their way to groundwater reservoirs or draining through the surface runoff and hence polluting such water resources (Donkor et al., 2018; Agyarko et al., 2014).

Certain heavy metals that enter the groundwater system are absorbed into the bodies of aquatic organisms, causing bioaccumulation of such chemicals over long periods and eventually disrupting the local food chain (Engwa, 2019). Although this problem has existed, very few attempts have been made in Ghana to remove these harmful metals (Buah et al., 2016). The technologies that have been employed in most cases were too expensive, inefficient at remediating high levels of heavy metals, or produced huge sludge (Alfara et al., 2014; Gunatilake, 2015). The transformation of avocado seeds into an effective adsorbent, which has the ability to clean up toxic metals in polluted water bodies, would also be an important addition in the quest to find cost-effective and efficient adsorbents to use in cleaning up heavy metal's contamination.

1.3 Objectives of the Study

The present work focuses on the production of avocado seed, characterises it, and assesses its ability to adsorb some chosen heavy metals (which are in the groundwater of Sefwi Wiawso Municipality and the neighboring communities).

1.3.1 Specific objectives of the study

The research seeks to:

1. Produce and characterise activated avocado seeds using XRF, FTIR, and SEM-EDX analysis.
2. Utilize the activated avocado seeds to treat groundwater samples and reduce As, Cd, and Pb concentrations.
3. Investigate how contact time, adsorbent dosage, solution pH, and temperature influence the adsorption capacity of the activated material.

4. Study isotherms, kinetics, as well as thermodynamic processes that occur during the investigation.

1.4 Significance of the Study

Research by Jaishankar et al. (2014) indicates that long-term exposure to heavy metals may cause unfavourable effects to individuals when the levels of exposure are not fatal and occur in the long term. Farming and artisanal mining towns in Ghana are mostly poor, and inhabitants cannot afford clean potable water from their already low income (Asare et al., 2018) and depend on water resources within their communities for their water needs. These water resources have been contaminated by excessive accumulation of heavy metals, which originate from illegal gold mining activities in these communities (Kuffour et al., 2018).

Recent studies conducted consecutively in mining areas in Ghana (Arah 2015; Ewusi et al., 2017; Kuffour et al., 2018) have shown that these water sources are heavily polluted. My research, therefore, aims at designing an effective evidence-based solution to reducing As, Cd, and Pb in such water sources so as to improve access to safe and hygienic water for community members.

1.5 Justifications of the Study

The existence of illegal gold mining, poor waste management systems, and poor farming activities has significantly increased the release of toxic metals into both water resources and the broader environment, affecting public well- being (Tom-Dery et al., 2012; Anim-Gyampo et al., 2021). Although a myriad of measures has been taken in a bid to utilize the available remediation technologies to decontaminate polluted water, these methods

seem either ineffective in decontaminating the toxic metals when they are at high levels or have provided a very high cost that cannot be accepted by most developing countries including Ghana, whose resource base cannot withstand the high cost of implementation. The current study is quite promising since avocado-seed-obtained adsorbents can substitute purchased adsorbents. In Ghana, no such or limited efforts have been implemented to develop, characterise or use such adsorbent material in remediating heavy metals in water sources. Nevertheless, there have been related studies in Ghana, but two cases, relatively costly and chemically activated preparation techniques were used, and in one case, the yielded adsorbents were too large (Boadu et al., 2018) (potentially leading to the inability to collect and transport needed volumes of treated water). Groundwater remediation in this work targets arsenic (As), cadmium (Cd), and lead (Pb) through adsorption, with activated avocado seed-derived adsorbents serving as the treatment medium.

CHAPTER TWO

LITERATURE REVIEW

This presents literature that relates to related studies. It also addresses works of other authors on the water quality and low-cost activated material utilization.

2.1 Water Quality

Access to water is a fundamental human requirement, and as part of sustainable development, quality water should be provided for human consumption (UN SDG6, 2015). Positive health effects are related to the consumption of clean and safe water and vice versa (WHO, 2018).

Water serves more purposes than contributing to the agricultural and industrial processes, but is also essential for maintaining environmental balance, promoting human well-being, and conserving natural resources (Ghana Water Resource Review, 2018). Although water is a very crucial life compound, there exist some inherent health risks in the use of contaminated or polluted water (Adutwum et al., 2022). The suitability of water is defined by its planned use (Bashir et al., 2020). The parameters regarding the evaluation of water quality assessment have been studied (Gibilla et al., 2011; Lamptey et al., 2013). Water quality, as known by humans, entails the healthiness of water as suitable to be consumed by humans, serve industries, or agricultural purposes (Rahmanian et al., 2015). Water quality is compromised by contaminants and, hence, human health (Rahmanian et al., 2015).

Water contaminations are initiated by geological conditions, industrial activity, farming, and water treatment plants. There are mainly three kinds of water contaminants:

microbial, radiological, and toxic chemical sources (EPA, 2025). Pollutants on the ground and the surface are either natural or man-made. Brackish water, poor surface water, and mineral deposits are all regarded as naturally occurring water contaminants. When the anthropogenic factors come into play and disturb the balance between the natural environment, especially the mineral resources and resulting in acid mine drainage, the depletion of aquifers and saltwater intrusion, and releases of hazardous chemicals due to the leaching of pollutants because of the excessive irrigation, these natural sources of water contamination become extremely severe (Su et al., 2020). Pollution of ground and surface water also occurs with the help of anthropogenic activities, including farming activities (fertilizers, manure application), domestic activities, manufacturing and mining activities (He &Wu, 2019; Jhariya et al, 2016). Comparative research in Ghana revealed that water sources provide water that has contaminants like toxic metals (Fianko et al., 2007; Attua et al., 2014)

2.2 Water Quality Parameters

The physical and chemical characteristics influencing water quality encompass pH, temperature, turbidity, dissolved oxygen concentration, salinity, nitrate levels, phosphates, and high levels of dangerous metals, among others (Agbalagba and colleagues, 2011; Samie and colleagues, 2013; Rahmanian and colleagues, 2015).

2.2.1 pH

The pH scale, which ranges from 0 to 14, determines the acidity or basicity of water, with pH 7 indicating neutrality, pH values over 7 signifying alkalinity, and pH values below 7 indicating acidity. Drinking water could have a permissible range of pH that ranged between 6.5 to 8.5 (WHO, 2010). The life of some aquatic organisms is fatal towards the

water that has pH levels below 4.5 and above 9.5 (IEPA, 2014). Acidic water causes corrosion of water pipes (Agbalagba et al., 2011), and when water from those pipes is consumed, it may have health effects on nerve receptors and the gastrointestinal tract (Obiefuna & Sheriff, 2011; Ojekunle et al., 2020). Water pH affects the solubility of organic compounds, metals, and salts (IEPA, 2014). PH values outside 6.5 and 8.5 may be harmful to aquatic organisms and can cause corrosion of water infrastructure, which in turn releases toxic metals into water (IEPA, 2014). The implication of taking water with low pH continuously may lead to complications like acidosis and gastrointestinal tract injury (Asamoah et al., 2011).

2.2.2 Temperature

Water temperature has a significant impact on dissolved oxygen in water, a factor that makes temperature a very important parameter to water quality (IEPA, 2014). Warming of water reduces quantities of dissolved oxygen (IEPA, 2014). At 0 ºC, water contains up to 14.6mg of oxygen per litre, whereas 30 °C water holds only up to 7.6mg/L (IEPA, 2014).

An increase in water temperature could promote the growth of microorganisms such as coliform bacteria (Adefemi & Awukuni, 2010). These microorganisms could impart taste, odour, and colour to the water and cause corrosion problems (Adefemi & Awukuni, 2010).

2.2.3 Turbidity

According to Azis et al. (2015), turbidity is a measurement of granules such as clay, silt, microscopic matter, algae, dissolved coloured organic matter, plankton, and other minute

organisms that are engulfed in water. Particles that are in suspension are typically introduced to the aquatic environment through the effluent of the sewage plants and industry, leading to soil erosion (Azis and colleagues, 2015). Suspended solids in surface water, particularly rivers, is found to be high in the rainy season (Azis et al., 2015). Environmental degradation due to deforestation from agricultural practices, mining operations, whilst ignoring conservation rules, has played a major role in modifying river flow and increasing water cloudiness (Azis et al., 2015). Allowable turbidity of water for human consumption is 5 NTU (Meride & Ayenew, 2016).

A high turbidity of water resources brings a health hazard to human beings who use it for drinking since turbid water normally has total suspended solids that contain micro-organisms and other vectors that cause disease outbreaks (Oluyemi et al., 2010; Samie et al., 2013). Suspended particles clog the mouthparts and gills of aquatic organisms such as fish and thus suffocating them (Mann et al., 2007). Pollutants such as nutrients and pesticides sometimes combine with suspended solids and settle in the sediments (Mann et al., 2007). High turbidity also interferes with disinfection as microorganisms hide under suspended matter (Jia et al., 2020).

2.2.4 Salinity

Salinity, as defined by Beattricevet et al. (2019), is the amount of dissolved salt in water. Salinity likely rises when the flow and degree of water are reduced. The measurement of salinity can also apply to the total dissolved solids as a total salt concentration of a water source (Maju-Oyovwikowhe et al., 2019).

The electrical conductivity (EC) of substances is what makes them be used as a channel or medium through which electricity is conducted (Ojekunle et al., 2020). Therefore, the EC is the measure that shows the overall levels of the soluble salts in the water (Sarala & Mageswari, 2014).

Salty water is an ideal electrolyte, and it has a better ability to conduct electricity compared to purer water (Ojekunle et al., 2020). An electrical conductivity for groundwater is defined by Jakhrani et al. (2019) as the capacity of water to conduct an electric current, measured in micro-Siemens per centimetre (µS/cm) at 25°C. Thus, electrical conductivity (EC) is dependent on total dissolved solids (Sarala & Mageswari, 2014). The EC of pure rain water is less than15µs/cm, whereas that of brackish water measures 1,600 to 4,800µS/cm (Ojekunle et al., 2020).

2.2.5 Levels of chemicals

Chemicals that can arise in water resources due to activities of industry include polychlorinated biphenyls (PCBs), Chlorine, Phosgene, Hydrogen sulphide, Arsine, Phosphine, Formaldehyde, and Arsenic trichloride (Peng et al., 2013). When water with PCB concentrations is consumed, the compound, benzodioxin-phenols, influences human immune, reproductive, nervous and endocrine systems (Peng and others, 2013).

2.2.6 Levels of metals

Naturally occurring metals like copper, manganese, and zinc, among others promote biochemical reactions required by living organisms (Bobade & Eshtiagi, 2015). Nonetheless, the concentration of these and other metals/metalloids like mercury,

cadmium, lead and arsenic in water bodies is fatal to both animals and human beings who utilise them (Arivoli et al., 2008).

2.3 Water Pollution

Fresh and clean water to be used by people has been in demand as the population growth has been expanding rapidly (Mandal, 2014). The Anthropogenic factors that can be traced to urbanization, agriculture, industrialization and population growth have also caused the dropped or deteriorated water quality around the globe in an accelerated manner. (Xiaolong et al., 2010).

2.3.1 Sources of water pollution

Pollution sources can be categorized into point sources and non-point sources (Chaudhry & Malik, 2017). Point sources are directly linked to specific locations, such as industrial sites, storm drains, and sewage treatment facilities, which discharge pollutants into the environment (Chaudhry & Malik, 2017).

Non-point pollution sources, however, originate from sources of different origins and they enter groundwater or surface water resources from different sources, including but not limited to runoffs from agricultural fields and urban waste (Moss, 2008).

Transboundary pollution is pollution that occurs in a particular environment and displays its effect over hundreds or thousands of miles away (Zulum et al., 2017). A typical example of transboundary pollution is nuclear material from processing plants in a specific country that can spread through ocean currents, posing a risk to nearby nations. (Zulum and colleagues, 2017).

2.4 Heavy Metals

Lead, cadmium, mercury and cobalt are dense metallic elements characterised by specific gravity (Bobade & Eshtiagi, 2015). They have density between 3.5 and 8.65 g/cm^3 and are also toxic at even sublethal concentrations (Gautam et al., 2014). Introduction of high amounts of metallic elements into the world environment has been due to technological enhancement of the industries in the recent decades (Abidemi, 2011).

The buildup of metallic elements in groundwater and other water resources has been a global concern, bearing in mind that they are highly toxic (Sekabira et al., 2010). By their nature of persistence, the human body does not metabolise heavy metals and therefore bio-accumulates on the human system (Es'haghi et al., 2011). They are hazardous metals, either in metallic or ionic state, which move towards human beings in the food chain (Ehi-Eromosele & Okiei, 2012). Most of the toxic metallic contaminants in the aquatic systems, are anthropogenic, including mining of minerals, tanneries, household painting activities, production of car radiators and agricultural application of fertilizers and fungicides (Arivoli et al., 2007).

Unlike other organic and inorganic compounds, toxic metals with high density are not ecologically friendly and can be bioaccumulated by human and other organisms (Arivoli et al., 2007). They have caused diseases and disorders in different bioaccumulation, as reported by Arivoli et al. (2007). Certain heavy metals, such as Iron, copper, zinc and manganese, play important roles in human health when they are consumed in minimal quantities (Arivoli et al., 2007).

2.5 Beneficial heavy metals

Sulyman and colleagues (2015) identified iron, manganese, and other trace metals occurring in very small amounts in biological systems. These are nutritionally essential to human beings in small quantities (Sulyman et al., 2015). They can be found primarily in food, fruits, and vegetables and commercially obtained multivitamin products (Sulyman et al., 2015).

2.6 Toxic heavy metals

The human body cannot process and excrete certain metals effectively, causing them to build up in the soft tissues and potentially leading to health complications (Es'haghi and colleagues, 2011). Introduction of metallic elements to the human body happens when humans ingest polluted food, water, or inhale polluted air containing heavy metals, or also through absorption on the skin when exposed to heavy metals through agricultural activities, manufacturing, pharmaceutical, industrial, or residential environments (Es'haghi et al., 2011).

Elements like arsenic (As), cadmium (Cd), and lead (Pb) lack any biological significance in humans and their consumption, even in very low dosages can prove to be fatal (Yahaya et al., 2010; Gautam et al., 2014). The three main sources contributing to the presence of metallic contaminants in the environment include atmospheric deposition, sewage disposal and metal extraction.

2.7 Cadmium chemistry

Cadmium is a silver-white, non-essential, soft, ductile metal having atomic number 48 (Chakraborty et al., 2020). It is under group pentuple (in the d block and period 5) and

with a material specific gravity of 8.65g/cm^3 (Sharma et al., 2015). Naturally, cadmium forms part of the earth's surface layer (Sharma and colleagues, 2015). Its electronic structure represents [Kr] 4d^{10} 5s^2 and the abundance of the crustal layer is approximately 0.15 ppm (Sharma et al., 2015).

Greenockite forms the largest cadmium mineral of the Earth's crust, and it is a by-product obtained at increased levels of sulphide resources especially lead, zinc and copper deposits (Sharma et al., 2015). In other industries, cadmium finds its use in batteries, phosphate fertilisers, coating, plating and alloys, among others (Chakraborty and others, 2020).

2.7.1 Cadmium emissions

The emission of cadmium is due to the burning of non-renewable energy sources, the extraction of steel and iron, cement and nonferrous metals manufactories, incineration of waste, smoking, and application of fertilisers among other activities (Sharma and others, 2015; Chakraborty and others, 2020). The volcanic eruption, as well as mining, are some of the other activities that lead to indirect cadmium emission from the earth crust to human immediate environment that could also affect the human negatively (Sharma et al., 2015).

Rechargeable batteries (nickel-cadmium) are widely utilised compounds (studies of cadmium). Cadmium is widely used as a pigment and in anticorrosion agents (Chakraborty et al., 2020). Cadmium is also added in the form of stearate Ba-Cd- Zn as stabilisers to polyvinyl chloride (Folarin & Sadiku, 2011). Cadmium is present in the aquatic system either through ecological or man-made operations like the urban run-off and agricultural practices (ATSDR, 2009). The effects of breakdown and washing away

of cadmium-bearing rocks have also been discovered to be key sources through which cadmium gets out into the environment (ATSDR, 2009).

2.7.2 Cadmium impact on human health

Cadmium is among the known metallic elements present in the environment which are hormone disruptors (El-Kady & Abdel-Wahhab, 2018). According to EI-Kady and Wahhab (2018), and Satarug et al. (2017), human beings are subjected to cadmium through breathing or swallowing of polluted air (e.g., polluted cigarette smoke), foods (polluted fish, coffee etc.). When cadmium oxide forms fumes, inhalation of such particles is highly irritating to the respiratory system (Chakraborty et al., 2020). Cadmium causes decreased progesterone and prolactin hormones and suppresses men's testosterone (Chakraborty et al., 2020). There is a report of lung and renal dysfunction among industrial workers following air-borne cadmium which is around 200 0ug/g (OSHA, 2005). Excessive levels of Cadmium result in coughing, headache, and vomiting among a population exposed to it (El-Kady & Abdel-Wahhab, 2018). Cadmium may also cause an accumulation in the liver, the kidneys and even replace calcium in the bones, causing painful bone diseases like osteomalacia and osteoporosis and renal failure (Chakraborty et al., 2013). WHO, USEPA, and EC have established a maximum cadmium concentration of 0.003,0.005 and 0.005 mg/L in water to be used as drinking water (WHO, 2011; USEPA, 2009; Adesiyan et al., 2018)

2.8 Lead chemistry

EI-Kady and Abdel-Wahhab (2018) present lead as a poisonous, odourless, and silver to bluish white metal, which is naturally found in the earth's surface layer. Lead is soft, very malleable, ductile and a very poor conductor of electricity. Lead is resistant to corrosion

but becomes tarnished when left exposed to the air (NTP, 2004). Lead (Pb) is characterised by +2 and +4 oxidation states (NTP, 2004). The inorganic lead compounds normally have lead in the +2 oxidation state. It is like other members of group 2 metals such as beryllium, magnesium, calcium, strontium, and barium, (NTP, 2004). Lead compounds are categorised into water-soluble and water-insoluble (HSDB, 2009). The soluble lead compounds include $Pb(C_2H_3O_2)$, $(Pb(C_2H_3O_2).3H_2O)$, $(PbCl_2)$ and $(PbNO_3)$ (HSDB, 2009). The major insoluble lead compounds consist of lead arsenate $(Pb(AsO_2)_2)$, lead azide $(Pb(N_3)_2)$, lead bromide $(PbBr_2)$, lead fluoride (PbF_2), lead phosphate $(Pb_3(PO_4)_2$, lead stearate $(C_{36}H_{70}O_4Pb)$ and lead sulphate $(PbSO_4)$, among others and they occur as white powders, crystals, or needles (HSDB, 2009).

2.8.1 Lead emissions

The greatest origins of lead to the environment around the globe are atmospheric lead (major source is automobile emissions), paint chips, used ammunition, fertilizers and pesticides and lead acid batteries and other industrial products (World Health Organization, 2020). Lead emissions into the global environment also originate from the manufacturing of electronic products, metal processing, electroplating, leather tanning and mining industries (WHO, 2020). Lead-containing fuels played a major role in spreading lead into the global environment (Ye & Wong, 2006). The burning of leaded fuel also emits traces of lead particles in the air which remain for a very long time (Ye & Wong, 2006). These lead particles eventually drop and become part of the soil and dust (Ye & Wong, 2006).

2.8.2 The impact of lead on human health

Lead is a type of toxic metal that occurs naturally and has been recorded to be a neurotoxin and a long-term negative health impact on human beings (Ye & Wong, 2006). Youngsters who come into contact with lead, may have hindered physical and mental growth (Agwaramgbo et al., 2011). In adults, excessive lead intake could cause damage to various vital organs in the body (Agwaramgbo et al., 2011). Lead poisoning results in cognitive impairment in adults and negatively affect the male and female reproductive systems (WHO, 2024). WHO, USEPA and EC have standards of 0.01 mg/L, 0.015 mg/L and 0.01 mg/L respectively, as the acceptable level of lead in drinking water from groundwater and surface water sources (WHO, 2011; USEPA, 2009).

2.9 Chemistry of Arsenic

Arsenic, a metalloid, is highly toxic, bright silver-grey and with no odour (Mohan & Pittman, 2007). Its specific gravity is 5.73 and its melting point of 817ºC (Haynes, 2016). It occurs in four oxidation states, +5 (as arsenate), +3 (as arsenite), 0 (elemental arsenic) and -3 (as arsine) (Mohan & Pittman, 2007). The boiling point and vapour pressure of arsenic are also 613°C and 1 mm Hg respectively, at 372° C (Mohan & Pittman, 2007). At atmospheric pressure, elemental arsenic sublimes when heated in the presence of air, producing a yellow vapour (Mohan & Pittman, 2007). Nevertheless, when arsenic is heated in the air, the white smoke of arsenic trioxide results (Kesici, 2016).

Arsenic contamination comes from both natural and human-related processes. In nature, it is released through volcanic activity, hydrothermal emissions, and the wearing away of rocks. Human-made sources include mining and smelting of metals and fossil fuel combustion, petroleum refining, steel and industrial manufacturing, and agricultural

application (Ei-Kady & Abdel-Wahhab, 2018; Masuda et al., 2018; Patel et al. 2023; Zhao et al., 2024; Bhat, 2024). The lasting use of arsenical pesticides also leads to rise in arsenic levels in agricultural soils and the environment (Cupa et al., 2013; Shahid et al., 2017; Patel et al., 2023; Bhat, 2024). As it can be found in the environment either as arsenite (AsO_3) or as arsenate (AsO_4), however, the most prevalent form of arsenic in groundwater sources is As (III) (Kesici, 2016).

2.9.1 Arsenic emission

Arsenic is a metalloid that is naturally formed during volcanic activities or even through man-made ways such as during the extraction and processing of metals such as gold, lead, copper, and nickel and fossil fuel combustion, steel manufacturing and other industrial activities (IARC, 2012). Other anthropogenic activities, such as agricultural production, pesticides application, industrial waste disposal, the use of feed additives, ceramics, veterinary medicine, metallurgy, electrical generation, leatherwork and fabric also release substantial quantities of arsenic into the environment (Wang et al., 2017). Naturally, weathering of rock containing arsenic also contributes to arsenic levels in water (WHO, 2010).

2.9.2 Impacts of arsenic on health

The rising exposures to arsenic by consuming contaminated food and drinks pose a dangerous health risk to mankind (WHO, 2010). Arsenic exposure to humans happens through two main pathways, which are the ingestion of tainted food and water (El-Kady & Abdel-Wahhab, 2018). According to Kesici (2016), the clinical effects of acute poisoning with arsenic include gastrointestinal complications, neurological implications and tingling of the extremities, painful muscle cramps and some cases death.

Prolonged contact with excessive amounts of arsenic leads to alteration in the pigmentation of the skin that results in the development of lesions as well as rough patches on the hands and feet of the body (Patlolla & Tchounwou, 2005). There are other effects with continuous interaction of high levels of inorganic arsenic with the skin, which causes various cancers, and also creates conditions such as cardiovascular diseases, diabetes, developmental toxicity and increased mortality in young adults (WHO, 2022). Cancer of the skin, bladder and the lung can also occur resulting from excessive exposure to high amounts of arsenic (El-Kady & Abdel-Wahhab, 2018).

Pregnant women exposed to arsenic-contaminated drinking water chronically, have an elevated risk of adverse reproductive outcomes (WHO, 2010). During the fetal and early stages of development, arsenic exposure, has also been associated with the complications of lung cancers and bronchiectasia (WHO, 2010). WHO, USEPA and EC differentiate the controllable levels of arsenic in drinking water as 0.01, 0.01 and 0.01 mg/L respectively (WHO, 2011; USEPA, 2009)

2.10 Heavy Metals Remediation

According to the European Environmental Agency (2025), remediation is an activity that has the purpose of cleaning-up or mitigating, correcting, abating, minimising, eliminating, controlling and containing or preventing a release of contaminants into the environment so as to avoid the adverse effects on human health and environment. Remediation also involves measures taken to look into, or evaluate, read or presumed control of the release of contaminants (Burlakovs & Vircavs, 2011).

2.11 Some available remediation technologies

Numerous studies, which include remediation methods for arsenic and other metals, like chemical precipitation techniques, membrane filtration (reverse osmosis), ion exchange and adsorption have been thoroughly researched (Smedley & Kinniburgh, 2002; Mohan & Pittman, 2007, Naidu et al., 2019). However, the usage of these technologies in the remediation of arsenic and metallic elements, is not frequent because of their high cost and low feasibility (Sorg et al., 2015; Ighalo et al., 2024; Asad et al., 2024). Nevertheless, adsorption tends to be widely regarded as a cost-effective and efficient method for heavy metal removal, especially when using low-cost or green adsorbents, the preferred method of heavy metal removal because of high efficiency and low cost (De-Gisi et al., 2016; Hussain et al., 2021).

2.11.1 Chemical precipitation

Heavy metal uptake in industry effluents is performed through chemical precipitation (Saloua et al., 2020). It is through this method that the metal compounds are rendered insoluble through reaction with dissolved metals in solutions and other sources (Saloua et al., 2020). Chemical precipitation is straightforward to perform, uses low-cost and readily available materials and pH management of the process is not complicated Nonetheless, the chemical precipitation process requires excessive chemicals and the operational cost of this method is very high.

2.11.2 Coagulation and flocculation

It is a proven century-old technology that uses trivalent metal salts as a means of precipitating chemicals through either coagulation or flocculation (Johnson, 2008). The physico-chemical technique that is frequently implemented in the process of treating

contaminated wastewater is coagulation-flocculation (Kastali et al., 2020). It removes colloidal particles, some soluble substances and ultra-fine solid suspensions that are found into the wastewater initially, through a process of destabilization and floc formation (El-Gaayda et al., 2021). The coagulation technology of metal remediation decreases the net surface charge of the colloidal particles that are stabilized by electrostatic repulsion mechanisms, thereby enabling them to aggregate and be effectively removed. During the flocculation process, particles continue to attain a larger size as a result of more and more collisions and stretching, along with contact with the inorganic polymers that are generated by the organic polymers dispensed (Gunatilake, 2015). It is complicated by the fact that the process generates a large volume of sludge despite the simplicity of the process.

2.11.3 Electrochemical treatments

Electrochemical process involves electricity, which works as current flows through the metal-laden solution that is aqueous with a cathode plate and a non-soluble anode (Gunatilake, 2015). It includes the formation of heavy metals in weak acidic or neutralized catholyte as hydroxides, and it uses electro-deposition, electrocoagulation, electro-flotation, as well as electro-oxidation. Electrochemical process involves the use of sizeable quantities of chemicals to convert metals to acceptable levels that would allow them to be released.

Nevertheless, the method creates massive sludge and also reduces the rates of metal precipitation, inappropriate settlement, floc caking of metal precipitates, and environmental impacts of sludge.

2.11.4 Ion exchange

The most popular method in the water treatment industry is the ion exchange technique applied to remove heavy metals which draws soluble ions out of the liquid phase to the solid phase (Abo-Farha et al., 2010). During this process, cations or anions with a special ion exchanger are employed in the removal of metal ions in solutions (Abo-Farha et al., 2010; Wikipedia, 2025). Synthetic organic ion exchange resins are widely used ion exchangers and apply to low-concentration metal solutions only, and the technique is excessively delicate to the pH of the aqueous phase.

In this method, water-insoluble solid ion exchange resins are utilized and can adsorb either positive or negative ions of an electrolyte solution and produce other equal and opposite charges of the same charge into the solution in a corresponding quantity (Cobzaru & Inglezakis, 2015). In cationic resins, e.g., hydrogen and sodium ions that have positive charges, positive charges like nickel, copper and zinc ions are replaced by the solutions (Dardel & Arden, 2008). On the same note, negatively charged ions like chromate, sulphate, nitrate, cyanide and dissolved organic carbon can exchange with the negative ions in the resins; hydroxyl can be replaced by the chloride ions (Dardel & Arden, 2008). The ion exchange process operates conveniently, utilises cheap resources, and is a metal-selective process with fewer numbers of metal ions getting removed (Dardel & Arden, 2008).

2.11.5 Membrane filtration

Membrane filtration is an effective method of getting rid of suspended matter, organic and inorganic substances, including heavy metals, and it is carried out based on the size of the particle which might be retained. As a result, three major methods are used

consistently to remove heavy metals from wastewater treatment via ultrafiltration, nanofiltration, and reverse osmosis (BBRC, 2021). Membrane filtration has an advantage compared with other methods of wastewater treatment, such as the reduced driving force, smaller footprint because it has high packing density, among other advantages (Trivunac & Stevanovic, 2006). However, it is frequently considered costly, and its efficiency becomes worse in case of high levels of contaminants (Alfarra et al., 2014).

2.11.6 Reverse osmosis

Reverse osmosis is a technique of separation, which is based on pressure to pump a solution through a membrane. The membrane keeps the solute on one side and also lets the pure solvent through to the other side. The process will serve as a molecular sieve and its removal efficiency exceeds 99% of all soluble minerals (Akpor & Muchie, 2010). The membranes are semipermeable and they enable the flow of solvent but retain the metals. The membranes in reverse osmosis possess thick barrier layers within the polymer materials where separation is usually done (Gunatilake, 2015). The procedure is able to eliminate numerous classes of molecules, such as bacteria and ions in solutions. Reverse osmosis is applied in the treatment of various industrial effluents which include electroplating, textile, tanneries, and pulp and paper industries (Al-Obaidi et al., 2020; Pizzichini et al., 2005). It relies on pressure and solute concentration to separate, and it has a diffusive mechanism (Gunatilake, 2015) which is reverse osmosis. No matter how good it works, membranes involved in reverse osmosis are rather costly to acquire and maintain (Akpor & Muchie, 2010).

2.11.7 Adsorption techniques

Adsorption involves separation that entails the process by which contaminants of a given medium attach themself to the adsorbents surface. The approach may be chemical or physical in nature as the adsorbates commonly known as contaminants interact with the active surfaces of adsorbents. Such interaction can be feeble Van der Waals forces or result in chemical bond formations. Even its modern application in Horticultural Transformation has the barrier of cost (Xia et al., 2019). Adsorption takes place when the adsorbates accumulate on the surface of an adsorbent to cause the formation of molecular, ionic or atomic film and occurs in the presence of two phases of liquid-liquid, gas - liquid,or gas - solid interface. The adsorption of gases and liquids on the surface of the adsorbent usually becomes multilayered and monolayered, respectively (IUPAC, 2001). The driving forces of adsorption processes include affinities between surfaces of adsorbent towards metal ions, position of metal ions and adsorbent, pH of the adsorption medium, adsorbent surface area and adsorption medium surface tension (Singh et al., 2021; Raji et al., 2023). Physical adsorption is enhanced by weak Van der Waals forces between the adsorbent surfaces and the adsorbates. Gaseous adsorptions mostly imply condensation of the gaseous adsorbate into the pores of the adsorbent. Among the various adsorbents used in the adsorption and remediation of heavy metals, the use of chitosan (Upadhyay et al., 2021), natural zeolites (Delkash et al., 2015), clay (Liu et al., 2021) and bacteria (Asare et al., 2018) is most popular. The use of agricultural waste (Tizo et al., 2018), industrial waste (Sun et al., 2021), and activated carbon (Onundi et al., 2010; Bernard et al., 2013; Buah et al., 2016) are also effective. Low-cost adsorbents like natural materials, agricultural and industrial byproducts are beneficial in many aspects than the traditional method of treating heavy metals (Alfara et al., 2014). They comprise

less expensive adsorbents economically and possess excellent metal selectivity and have the capability of regeneration, too, as reported by Alfara et al. (2014).

2.12 Adsorbents Used in Adsorption Process

Adsorption is a widely applied method in the process of treating water contaminants (Satyam & Patra, 2024). This adsorption process is based on the characteristics of the adsorbent employed. Research on some of the most commonly used adsorbents includes chitosan, natural zeolites, clay, industrial waste, agricultural waste and activated carbon. This review also illuminates the recent research on multiple adsorbents when it comes to the treatment of water pollutants.

2.12.1 Chitosan adsorbent

Chitosan is a cheap adsorbent that is excellent in metal-binding capacity (Upadhyay et al., 2021). Chitosan is a long-chain polysaccharide that includes randomly distributed units coded within 1-4-linked D-glucosamine and N-acetyl D-glucosamine within the shells of shrimp and different crustaceans in response to sodium hydroxide. Nevertheless, Upadhyay et Al., 2021, have the opinion that the adsorbent chitosan is readily soluble in acid, and this impacts its work.

2.12.2 Natural zeolites as adsorbents

Zeolites are naturally occurring crystals formed as a result of aluminosilicates (Al_2SiO_5), which have a structure composed of tetrahedral molecules that are bonded together through the sharing of oxygen atoms (Grace, 2010). Zeolites have internal crystalline and complex structures, which provide them with high specific surface area, making them effective adsorbents (Gedik & Imamoglu, 2008). Natural zeolites have higher ion-

exchange capability, they function as a molecular sieve, they are very abundant, low- cost and they also function as agents for photocatalysts and their ability to adapt to the environment makes zeolites favourable for wastewater treatments (Delkash et al., 2015). Zeolites also have less or no corrosive properties, no waste or disposal problems but have high thermostability (Delkash et al., 2015). On the other hand, it is impossible to use micro-porous zeolites to synthesise bulky molecules (Delkash et al., 2015). The strong polarities of its functional groups, make it even harder to utilise shape selectivity of zeolites through their reaction (Delkash et al., 2015).

2.12.3 Clay as adsorbent

Savic et al., (2014) note that clay's high adsorption capacities stem from its inorganic nature, extensive surface area, and strong ion exchange capabilities. Clay's structure comprises multiple layers of tetrahedral and octahedral arrangements of silicon, aluminium, magnesium, oxygen, and hydroxyl ions (Savic et al., 2014). These layers are separated by interlayer spaces, where surface groups with either positive charges (due to excess Si, Al, or Mg) or negative charges (due to excess oxygen or hydroxyl) are present (Kennedy et al., 2018). The interlayer spacing comes in handy during the adsorption of various cations, anions or perhaps, other molecules located in wastewater (Savic et al., 2014). The adsorption capability of the clay is influenced by the level of the charges on the surfaces of clay and the balancing ions of the excess charges (Kennedy et al., 2018). Clays have pesticides, herbicides, pathogens and adsorptive ability of inorganic sulphate and Phosphate as well as Nitrate (Kennedy et al., 2018). Clays such as montmorillonite, bentonite, and kaolinite differ in their SiO_2/Al_2O_3 composition, with montmorillonite exhibiting the highest cation exchange capacity and are being effective, low-cost adsorbents for wastewater treatment (Yu & H an, 2015, Kennedy et al., 2018; ElBastamy

et al., 2021; Aljlil & Alsewailem, 2014, Liu et al., 2014). The distinction can be found in the percentage mineral composition of Al_2O and SiO_2 layers of each of the types of clay (Nshimiyimana et al., 2020; Wang et al., 2022). An efficient and effective wastewater treatment using clay adsorbent was reported by ElBastamy et al. (2021), who studied the first six territories and Aljlil & Alsewailem (2014) studied the sixth territory (2021). The use of clay adsorbent is a very simple and low-cost available material with a cost-attractive alternative solution compared to the regular treatment of water (Liu et al., 2014).

2.11.4 Industrial waste as adsorbents

Cheaper adsorbents that are applied in heavy metals elimination are the industrial waste adsorbents (Ahmaruzzaman, 2011). The wastes which are generated by industries are refined so as to improve their ability to adsorb contaminants. (Ahmaruzzaman, 2011). By-products produce these wastes and are provided in great amounts (Sun et al., 2021; Ahmaruzzama, 2011). Blast furnace sludge, fly ash, waste slurry, lignin, iron (III) hydroxide and red mud are industrial wastes tested to seek out remediation possibilities on toxic heavy metal elimination in wastewater (Sun et al., 2021; Ahmaruzzaman, 2011). Other industrial waste used in heavy metal removal in wastewater, and are effective and low-cost include coffee husks, Areca waste, tea factory waste, sugar beet pulp, waste pomace of olive oil factory waste, battery industry waste, waste biogas residual slurry, sea nodule residue (Ahmaruzzaman, 2011). Industrial Fly ashes have also found their application widely as a low-cost adsorbent for heavy-metal remediation (Ahmaruzzaman, 2011). Liu et al. (2017) stated the successful application of fly ash in lead and chromium uptake from aqueous solution. Proceeding in the same way, Bhatnagar & Minocha (2009) successfully used blast furnace sludge waste to clean up

lead and cadmium in the wastewater. Genc-Fuhrman et al.(2004) also gave an effective use of red mud in the extraction of Arsenic ions out of the wastewater.

2.11.5 Adsorbent of plant origin

Recently, agricultural wastes have found application in the treatment of water using them as low-cost adsorbents, including rice husk, corn cobs, palm kernel shells, coconut shells and egg shells (Khan et al., 2004; Eruola & Ogunyemi., 2014; Tizo et al., 2018). These researchers analyzed the adsorptive capacities of such agricultural wastes (Tizo et al., 2018). The lignin and cellulose are the typical components composing agricultural wastes and contain -OH and -COOH groups (Pyrzynska, 2019). The OH and COOH groups can interact with the metal ions by delivering electron pairs to them to form metal complexes (Pyrzynska, 2019).

The applications of agricultural waste adsorbents in wastewater treatments are both simple to perform and require minimal processing with high adsorption of the waste (Sud et al., 2008). Agricultural wastes possess both selective capacities of contaminants and they are cheap, readily accessible, environmentally friendly, and, hence, can be readily recreated (Sud et al., 2008). Nonetheless, using untreated agricultural wastes as adsorbents can be problematic because of their low adsorption capacity and high levels of organic pollutants, which can reduce their ability to effectively adsorb substances (Liu et al., 2022; Demirbas, 2009).

2.12.6 Activated carbon adsorbents

Activated carbon is an amorphous processed carbon (Kennedy et al., 2018), and they have enlarged pore sizes, which multiply their surface area segment where adsorption

can take place (Tadda et al., 2016). The activated carbons are associated with some carbon family that comprises charcoal, nuclear graphites, carbon fibres and their composites or electrode graphite among others (Kennedy et al., 2018).

2.13 Preparation of activated carbon

Biomass, forestry and plant-based waste are considered as effective sources for preparing activated carbon (Bubanale & Shivashankar, 2017). The precursors should contain high levels of carbon so that they can be used for the activation (Prahas et al., 2008; Xu et al.,2014) .The production of activated carbon can be obtained through two processes: physical activation and chemical activation (Xu et al., 2014; Prahas et al., 2008). Physical activation involves two main steps, viz, carbonisation of raw materials and activation of carbonised charcoal (Tadda et al., 2016). The carbonisation takes place at 400 to 800ºC whilst the activation takes place at 800 to 1000ºC (Bubanale & Shivashankar, 2017). Physical activating agents commonly used include carbon dioxide and steam (Bubanale & Shivashankar, 2017).

The chemical method of activated carbon preparation involves a single step of both carbonisation and activation (Tadda et al., 2016). The material to be activated, is mixed with a chemical agent and kept at a very high temperature for activation (Bubanale & Shivashankar, 2017). The chemical agents, viz: potassium hydroxide (KOH), potassium trioxocarbonate (IV) (K_2CO_3), zinc chloride ($ZnCl_2$), tetraoxophosphate (V) (H_3PO_4), among others act as oxidants and dehydrating agents (Bubanale & Shivashankar, 2017).

2.14 Morphology of activated carbon

The structural characteristics of activated carbon have a close connection with adsorption ability, and the latter is correlated with pore volume, distribution of pores, and surface area (Xu et al., 2014). According to research, activated carbon has about 15 % ash, which is basically mineral matter (Xu et al., 2014). Activated carbons have varied pore structures in terms of dimension and geometrical, shape (Bubanale & Shivashankar, 2017). The size of the pores ranges between tens of nanometers (10nm) and thousands (1000nm) (Bubanale & Shivashankar, 2017). Activated carbons have pore categories based on their average pore width, which is defined as the distance between the walls of a slit-shaped-pore or the radius of a cylindrical-pore- (Prahas et al., 2008; Xu et al., 2010; Bubanale & Shivashankar, 2017). The microcrystalline structure is created as a result of carbonisation of precursor material (Bubanale & Shivashankar, 2017). In this way, the activated carbon structure undergoes a radical change compared with graphite in terms of interlayer spacing (Bubanale & Shivashankar, 2017). While the interlayer spacing of graphite is 0.335 nm, activated carbons have interlayer spacing of 0.34 to 0.35 nm (Bubanale & Shivashankar, 2017; Moreno-Pirajan & Giraldo_Gutierrez, 2008). Activated carbons are categorised into graphitising carbons and non-graphitising carbons denpending on the orientation of the interspacing layers (Bubanale & Shivashankar, 2017). In graphitising carbons, the graphene layers are oriented parallel to each other (Bubanale & Shivashankar, 2017). The carbon contents are delicate due to weak cross-links between neighbouring micro-crystallites and have less developed porous structures (Bubanale & Shivashankar, 2017). Non-graphitising carbons are usually hard due to strong cross-links between crystallites and they have well-developed micro-pores which enhance their surface area and adsorption ability (Bubanale & Shivashankar, 2017).

Even though adsorption capacities of activated carbons are determined by their porous structures, the relatively small amounts of chemically bonded heteroatoms (oxygen and hydrogen) strongly influenced their adsorption capabilities (Xu et al., 2014). Activated carbons show differences in the distribution of an electron cloud in an organic carbon skeleton (Bubanale & Shivashankar, 2017). Regions of electron deficiency are created because of such arrangements and this creates unpaired electrons and valences that are not fully satisfied. It is these electronic structure asymmetries that determine the high adsorption of polar compounds by activated carbons.

2.15 Applications of activated carbon

Actively used activated carbons included the filtration of automotive fluids, the adsorption of harmful constituents in tobacco during the production of cigarettes, and the provision of catalytic support or in catalytic roles. To top it off, they play a major role in the process of removing mercury, cadmium, lead, and any other metal ions through water treatment (Zhou et al., 2016). The process of the attachment of these compounds to the activated carbon can be either physical or chemical depending on the character of the interactions of adsorbates and adsorbents (Wang et al., 2020). This interaction can be well compacted within the relatively weak Van der Waals forces (Physical) or stronger chemical bonds (chemical) that bind adsorbates to the adsorbents, depending on the nature of the adsorbent and the adsorbate (Foo & Hameed, 2010).

2.16 Dynamics of Adsorption

The process of adsorption occurs in a series of stages which are discrete (Foo & Hameed, 2010). The sequence begins with the diffusion of adsorbates from the bulk solution to the outer surface of the adsorbent, passing through the liquid boundary layer, described as

external diffusion (Foo & Hameed, 2010; Crini & Lichtfouse, 2019). This is followed by mass transfer across the interface via pore diffusion, connecting the external surface of the adsorbent to the interior porous structure (Mohan & Pittman, 2007; Foo & Hameed, 2010). Subsequently, the adsorbates diffuse further along the porous surface, eventually binding to the active sites on the inner surface of the pores (Mandal et al., 2014; Crini & Lichtfouse, 2019).

2.16.1 Physisorption

Physical adsorption refers to a process where the adsorbate adheres to the adsorbent due to weak intermolecular forces, specifically Van der Waal interactions (Foo & Hameed, 2010; Kralik, 2014). The physical adsorption provides a situation where the adsorbent is covered with multilayers of adsorbates (Xia et al., 2019). The enthalpy of this adsorption mode is low (2040 kJ/mol) and this process, in general, occurs below the boiling temperature of the adsorbate (Xia et al., 2019). However, the increase in temperature enhances the process of physisorption (Xia et al., 2019). Porous structured materials like mesoporous silica, zeolites and activated carbon that eliminate metal ions from aqueous solution by means of physical adsorption take advantage of their large surface area and their pore volumes (Xia et al., 2019). Such porous materials are prepared using different agricultural wastes and residues which provide high surface area and porosity for pollutant elimination (Xia et al., 2019). The physical adsorbents, while effective for contaminant elimination, are sometimes unfriendly to the environment and tend to be easily engineered.

2.16.2 Chemisorption

Chemical adsorption involves the attraction forces that chemically bind adsorbates to the surface of the adsorbent, resulting in the formation of multiple layers of adsorbates on the adsorbent's surface, where both the adsorbent and contaminants interact through chemical complexation (Foo & Hameed, 2010).

Most inorganic adsorbents are made up of metals and oxygen, which have high affinity towards adsorbing cations or molecular species due to their great affinity. The inorganic active sites (i.e., oxides formed by metals, or a composite) also provide an excess amount of surface adsorption sites, which allow the metal ions to be anchored by the coordination with oxygen atoms (Guilherme et al., 2015).

Common organic adsorbents include such macromolecules as polymers, carbohydrates, lipids, proteins, and nucleic acids (Staneva et al., 2017). These adsorbents have functional groups, such as carboxyl and hydroxyl, which are the active binding sites for the metal ions (Staneva et al., 2017). Compared to physical, chemical adsorption has a faster removal rate and high removal efficiency of metal ions in solution. Chemisorption gives high adsorption enthalpy and can be worked upon at any temperature (Xia et al., 2019). Nonetheless, the speed of chemisorption grows with rising temperatures, and the general extent of adsorption increases exponentially to reach the equilibrium point.

2.17 Determinants of Adsorption of Heavy Metals

The elimination of heavy metals found in wastewater through adsorbent materials relies heavily on numerous factors such as contact time, the amount of adsorbent, pH, adsorbate concentration, temperature, and agitation rate.

2.17.1 Contact time on adsorption

Duration of contact is a critical parameter of the adsorption systems (Bernard & Jimoh, 2013). It refers to the time that is used to attain the adsorption equilibrium (Onundi et al., 2010). The lengthening of this interval increases the rate at which the active sites of adsorption on the surfaces of the adsorbent hold contaminants (Eruola & Ogunyemi, 2014).

As revealed by Buah et al. (2016), removal of Pb2+ showed a significant rise within the first 15 minutes, and then the amount of Pb2+ adsorbed reduced at a steadily declining rate. Other studies, such as the one done by Onundi et al. (2010) in parallel, observed a rapid decline in nickel (Ni), copper (Cu), and lead (Pb) from the initial 5 minutes after coming into contact with palm shell activated carbon, but then gradually decreased until equilibrium was achieved. The first 5 minutes rapid removal ability of the adsorbent is attributed to the difference in concentration between adsorbates in the system and those available active sites on the adsorbent surface (Onundi et al., 2010).

The second rise in the adsorption and achievement of the equilibrium is explained by the low number of metal ions that can move between the solution and adsorbent due to mass-transfer processes on the external adsorbent surface (Onundi et al., 2010). Additionally, the surface functional groups' interactions with the metal ions in the solution, depending on the pH, contact time, and adsorbent dosage, determine the fate of adsorbing metal ions on an adsorbent (Onundi et al., 2010).

2.17.2 Adsorbent dose

Onundi et al. (2010), demonstrated the relationship between adsorbent dose and the mass of adsorbates, describing it as a direct relationship between adsorbent mass and metal ion removal efficiency. Bernard et al. (2013) found out from their investigation that when the adsorbent dosage was increased from 0.2g to 1.0g, while maintaining other conditions constant, the adsorption of Pb^{+2} increased by 100%, Fe^{+2} by 84.10%, Cu^{+2} by 78.16% and Zn^{+2} by 34.77%. Increasing the adsorbent from 1.0 g did not result in any meaningful removal of these ions, indicating that 1.0g was the optimum dosage for effective removal of these ions (Bernard et al., 2013).

These can be explained by the high level of adsorbent concentration during the study of adsorption (Bernard et al., 2013). This is because increasing the amount of adsorbent offers more active sites for the metal ions, which improves the adsorption rate (Ezeh et al., 2017; Gkika et al., 2025). Therefore, the removal rate increases with the adsorbent dosage until an optimal dose is reached, beyond which further increases do not significantly improve efficiency (Li et al., 2022; Zhang et al., 2020). The reduction in the occupation of active sites leads to the acceleration of metal uptake (Eruola & Ogunyemi, 2014). On the other hand, the maximum adsorption capacity reduces when active sites are filled up (Onundi et al., 2010).

2.17.3 pH

PH of the solution has a significant bearing on the adsorption of heavy metals (Haas et al., 2013). Adsorbent surface charge, degree of ionization, and speciation of the adsorbates are pH-dependent (Haas et al., 2013). The adsorption of the metal ions of the adsorbents increases with pH between 2 and 5 (Haas et al., 2013). The adsorbent/ heavy-metal uptake mechanism in the presence of pH is an aspect that allows the mobility of

H+ + ions during lower pH (1-2) to favour the H+ adsorption as opposed to the other metal ions (Haas et al., 2013). Therefore, on lower PH conditions, the adsorbent surface is surrounded by H ions (H+), which in turn do not allow contact between metal ions and binding sites on adsorbent surfaces (Haas et al., 2013). The adsorbents have a negative surface, which is revealed as the pH changes to assist in metal ions uptake (Haas et al., 2013; Jimoh et al., 2011). Moreover, when pH exceeds 7, the alkalinity of the adsorption medium limits the level of protonations of functional groups on adsorbents and hence, a smaller number of metal ions is eliminated (Gorzin & Ghoreyshi, 2013).

2.17.4 Adsorbate concentration

The concentration of adsorbate also contributes, to an extent, to the adsorption of metal ions. As the heavy metal concentration gets higher, more and more metal ions are adsorbed into them up to the optimum amount, when the rate of adsorption will start decreasing (Asare et al., 2018). Such an observation can be attributed to the reduction in the amount of active adsorption sites on the surface of the adsorbent (Tumin et al., 2008). With the adsorbent surface, the adsorption rate decreases due to the exhaustion of available active sites when metal ions are bound to the surface (Gorzin & Ghoreyshi, 2013). Not all metals have the same uptake of metal ions, but it depends on the size of the ion in a metal, the atomic mass, and the mechanism involved during the interaction of the metal ions and the adsorbent (Tumin et al., 2008; Gorzin & Ghoreyshi, 2013).

2.17.5 Temperature

According to experimental data, the adsorption ability of adsorbents and their capability to remove heavy metals from wastewater grow proportionally to temperature (Gaikwad, 2014; Gorzin & Ghoreyshi, 2013; Nabi et al., 2015). An increment in temperature

enhances the level of diffusion of the cations towards the active places that are present on the adsorbent (Nabi et al., 2015). However, at a certain optimum temperature, adsorption will start falling away, an outcome that is often due to a reduction in the chemical interactions of the active sites on the adsorbent with the adsorbate (Gaikward, 2004).

CHAPTER THREE

METHODOLOGY

The methodology would be described in this part of the research. The analytical details of the area, procedure for sampling, chemical and physical parameters of the samples, treatment as well as elemental analysis are elaborated. Moreover, the application of the activated avocado seeds, characterisation and evaluation of its applicability are also highlighted.

3.1 Description of Study Area

Sefwi Wiawso Municipality lies in the North Eastern part of the Western Region between latitudes 6°N and 6°N 30°N and longitudes 2° 45° W and 2° 15° W as reported in the Ghana Statistical Service 2010 Population and Housing Census. The Brong Ahafo region (The Ahofo and Bono East Regions) shares a boundary with it to the North and Juaboso and Bia to the West, Aowin-Suaman to the south, Bibiani-Anhwiaso-Bekwai district to the East and Wassa Amenfi West to the Southeast, as indicated in the Ghana Statistical Service 2010 Population and Housing Census.

The Municipality covers an area of 1,1011.6 sq.km (GSS, 2010) and has Sefwi Wiawso as its capital. The major occupation of the area is farming, which includes but not limited to cocoa, maize and vegetable production, light manufacturing, lumbering and agro-processing. However, artisanal mining, popularly known in Ghana as galamsey, has also taken over in recent times, as reported in the Ghana Statistical Service 2010 Population and Housing Census.

The Sefwi Wiawso District was established by Legislative Instrument (L.I) 1386 as the Sefwi Wiawso Distict on November 23, 1988 under the PNDC Law 207 which was later replaced by the Local Government Act 493, 1993. During this replacement, the district was elevated to a Municipal status on March 21, 2012 under the Legislative Instrument, (L.I) 2015, as indicated in the Ghana Statistical Service 2010 Population and Housing Census. The Municipality has a population of 139,200, comprising 69,753 males (50.10%) and 69,477 females (49.9%) of the population.

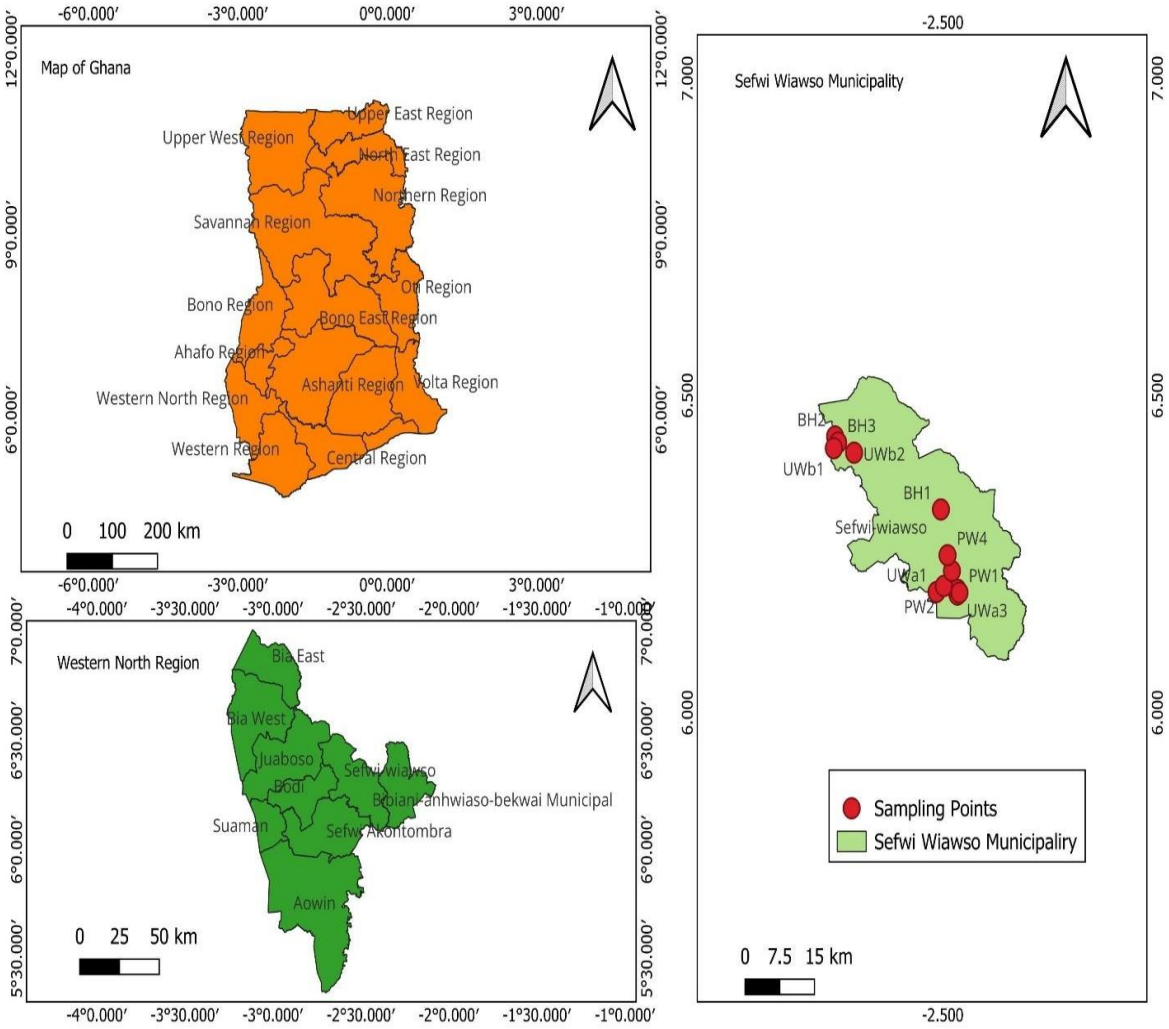

Figure 1: Image showing map of study area

3.1.1 Climate conditions of the study area

The Sefwi Wiawso is within the tropical rainforest climate zone with temperatures between 25°C and 30°C throughout the year (GSS, 2010). Humility is relatively high, about 90% at night falling to 75% during the day (GSS, 2010). It has two long wet seasons separated by relatively short dry season. The dry season is marked by relatively low humidity with hazy conditions occurring from December to February (GSS, 2010).

3.1.2 Vegetation of the study area

The Sefwi Wiawso Municipality is also in the moist semi-deciduous forest zone of Ghana. It covers most of Ashanti, Western, Bono, Ahafo and Eastern Regions (GSS, 2010). The forest type is a Celtic Triplochiton association. The most common plant species are Onyina, Odum, Wawa, Mahogany, Sapele, Emire Asamfina, and red cedar, among others (GSS, 2010). The forest is degraded at a faster rate, and due to that, a large portion of the forest has been lost as a result of bad farming activities and artisanal mining activities (GSS, 2010). Due to this, a large section of the forest, totalling 612.22 km, has been put under reserve. The Municipality has three (3) forest reserves, which include Muro in Boako (167.8Km), Suhuma in Old Adiembra/Amafie (359.8km) and Tano Suhien in Punikrom (84.6km) as indicated in the Ghana Statistical Service 2010 Population and Housing Census.

3.1.3 Topography of the study area

The Sefwi Wiawso Municipality, which forms part of the Western North Region of Ghana, was previously under the Western Region of Ghana. Most of the Municipality is generally undulating and lies between 152.4m and 510m above sea level. The

highest point, the Krokoa peak, which is 510m above sea level, lies roughly to the South-West of Sefwi Wiawso (GSS, 2010). The main drainage feature is the Tano River and its tributaries. The Tano River runs roughly in a North-South direction and enters the sea in La Cote d´ivoire. The major tributaries include the Suhien, Kunuma, Sui and the Yoyo (GSS, 2010). The level of flow (volume of these rivers) is affected greatly by persistent clearing of forest areas of the rivers and streams for farming and illegal mining purposes (GSS, 2010).

3.2 Avocado Seeds Collection and Preparation

The avocado seeds used were collected at random from some avocado sellers in the study area. In the laboratory, they were cleaned by washing with copious volumes of distilled water. The washing was repeated thrice each with large volume of distilled water to remove any pulp or skin that was attached to the seed. The seeds were dried in an electrical oven at 70°c for 24 hours to remove excess moisture.

3.2.1 Grinding and Sieving of dried Avocado seeds

The seeds were ground into a fine powder using a stainless laboratory grinder. The powder was sieved through a mesh filter to obtain a uniform particle size ranging between 0.5 – 1mm.

3.2.2 Hydrogen Peroxide Treatment of Sieved Avocado Seeds Powder

The sieved avocado seeds powder was treated with a 30% hydrogen peroxide solution at the ratio 1:10 w/v. The sieved avocado seeds powder-hydrogen peroxide mixture was stirred for 24 hours using a magnetic stirrer to allow the hydrogen peroxide to penetrate the seed powder particles and open up the pores structure.

After the hydrogen peroxide treatment, the mixture was rinsed twice each with large volume of distilled water to remove excess hydrogen peroxide.

3.2.3 Activation of the Peroxide-Treated Avocado Seeds Powder

The dried hydrogen peroxide-treated avocado seed powder was kept in an electrical oven at 60°C for 24 hours to remove excess moisture. The powder was further dried in an electrical furnace at 80°C for 2 hours to enhance its adsorption capacity. The final product was stored in an airtight plastic container in order to preserve its adsorption capacity.

3.2.4 Granulation of the Seed Powder

The activated avocado seed powder was mixed with a previously prepared Sodium trimetaphophate. The sodium trimetaphosphate, a cross-linking agent is reacted with starch molecules to form phosphate ester bonds, thereby reducing its solubility in water and improving its stability. The activated avocado seed powder was treated with the binding agent at a ratio of 9:1 w/w. The mixture was granulated by feeding it into a pellelizer, and then compressed into pellets hereafter referred to as extrusion. The granules were discharged from the pelletizer and stored in an airtight plastic container.

3.3 Characterisation of Activated Avocado Seeds Powder

Surface properties of the activated carbon produced using avocado seeds collected were investigated before and after its use in the metal ions remediation processes. The surface characterisation was done using an analytical Scanning Electron Microscope spectroscope, JSM-6380 USA, Rigaku NEX CG II Energy Dispersive X-Ray Spectroscope, X-ray fluorescent spectroscopy and Shimadzu, IR Affinity 1 Fourier Transform Infrared spectroscopy.

3.3.1 Surface morphology determination with SEM-EDX

The Surface morphology of the activated avocado seeds was also studied before and after their application in the adsorption process. The SEM-EDX images of the activated avocado seeds produced were captured on a JOEL analytical Scanning Electron Microscope (JSM6380, USA) with gold coated (300Å) ion sputtering device. A particle of the activated avocado seeds produced (approximately 0.5 mm in diameter) was mounted onto an aluminium stub with double-sided carbon adhesive and then placed into the sample cup holder. This in turn was put into the scanning Electron microscopy (JSM- 6380, USA) to obtain an optical image at a wavelength of 358 μm.

An electronic image was produced from the optical image by pressing an electronic image button on the SEM (JSM-6380, USA). Focusing, magnification, contrast and brightness of the electronic image were adjusted to produce a better electronic image of high resolution (1024 pixels) at a wavelength of 358 μm. The SEM images of the activated avocado seeds were taken before and after the activated avocado seeds were used in the metal ions remediation process (Figures 4.1 and 4.2).

3.3.2 Analysis of activated Avocado seeds with X-Ray fluorescence

The activated avocado seeds were analyzed quantitatively and qualitatively using the X-ray Fluorescence spectroscope (Rigaku NEX CG II, USA). This was aimed at finding the major oxides as well as the elemental constitution of the activated seeds, both before and after being used in processes of metal-ions adsorption. Four grams (4g) of the powdered activated avocado seeds were weighed onto a Whatman filter paper (grade 1), which was then placed in the sample cup of the X-Ray Fluorescence

spectroscope. In order to prevent the surface analysis window from being contaminated, the weighed sample in the filter paper was transferred quantitatively into the sample cup. The lid cup was then put on top of the sample cup and inserted into the X-Ray fluorescence (XRF) spectroscope sample chamber to be analyzed. The process was performed in the basic parameters' application mode.

3.3.3 Surface functionalities Determination of the activated avocado seeds produced

To investigate possible functional groups on the surfaces of the activated avocado seeds, Fourier transform infrared (FTIR) analysis was conducted to investigate the possible functional groups on the surfaces of the activated avocado seeds. Ten grams (10 g) of dried activated avocado seed powder was added to 100 mg of KBr pellet in a ceramic mortar, and the mixture was ground into fine powder. The grounded powdered sample was loaded into a sample holder and processed into a translucent sample disc. The sample disc was inserted into the FTIR spectroscopy (Shimadzu, IR Affinity1, Japan) and then scanned at 400 to 4000 cm^{-1} to generate the FTIR spectrum. This process was repeated on the activated avocado seeds produced after it has been used in the metal-ion adsorption processes.

3.4 Collection of water samples

Sterilised 1L plastic bottles were used to store collected water samples. Wells were sampled using a plastic bucket with a long rope tied to the open end. The bucket was lowered deep into the well and progressively filled with water. The bucket was pulled up and its content was poured back into the well. This was repeated thrice to ensure that well-mixed water samples were obtained as described in Asare et al. (2018). In sampling

water from boreholes, the water was pumped out of the borehole and allowed to flow out for 15 minutes before samples were collected into 1 L high-density sterilised plastic bottles. This was done in order to avoid water resident in the piping system of the borehole from being taken as a sample. Water samples collected were put into high-density plastic bottles, sealed tightly and then labelled.

3.5 Physico-Chemical Parameters of Sampled Water

The physico-chemical parameters (temperature, pH, turbidity, electrical conductivity and total dissolved solids) of various water samples were determined using the probe method as used in Samie et al. (2013), Christine et al. (2018) and Maju-Oyovwikowhe & Shuaib (2019).

3.5.1 Temperature

Temperatures of water samples were determined on-site using a Hanna Checktemp pocket thermometer (HI 98501, USA) immediately after sampling. Prior to the determination of the temperature of the water samples, the pocket thermometer probe was calibrated. A sterilised beaker was filled with a crushed ice block of deionised water. Cold deionised water was added until the beaker was full. The electrode of the thermometer probe was inserted in the centre of the beaker of iced water (without touching the bottom or sides of glass). The water was slightly stirred, then waited until the temperature indicator on the thermometer read 0 °C. Fifty millilitres (50 mL) of each water sample was put into 12 different 100 mL beakers. The thermometer was immersed in each water sample in each beaker. The meter readings were noted and recorded when the readings were stable. Triplicate values of the temperatures were read for each water sample, and the mean value was reported.

3.5.2 pH

Samples of water were examined against pH using the pH meter Hanna (HI 83141, USA), whose accuracy was ±0.01. This was done before the measurement took place because the instrument was calibrated using three known buffer solutions which included a pH value of 4.01, 7.00 and 10.01. It was observed that the 3-point calibration is achieved as expressed by Motsara and Roy (2008). To obtain the 50 mL water sample, 50 mL of water was taken in different 100 mL beakers. The calibrated electrode was placed into the water and stirred up so that there was proper mixing. The values of the pH were measured after equilibrium was achieved. This was analysed three times, and the mean pH value of each of the water samples was then reported as mentioned by Motsara and Roy (2008).

3.5.3 Electrical conductivity

A potable conductivity meter Hanna (HI 9828, USA) was used to measure the electrical conductivity (EC) of the water samples; this was calibrated to have a precision of ± 0.01. It was run through an aqueous solution of KCl three times before taking a reading of 50 mL of the aqueous solution containing a concentration of 0.01 M KCl. The temperature compensation dial was set to 0.0191/C and the instrument read-off 1412 micro-ohms per centimetre. The cell constant was calculated using Equation (1).

$$Kc = 1412 - X[0.0191(T - 25) + 1], \quad (1)$$

where Kc is the cell constant (cm^{-1}), C_{KCl} is the measured conductance (μΩ), and T is the observed temperature of the standard KCl solution (°C).

After calibration, the electroconductivity of each of the samples was obtained by washing out the cell of the apparatus with 50 mL of the sample being studied. The liquid temperature was later kept at 25° C using the built-in thermometer. Then the cell was inserted into a 50 mL sample, and the readings indicated on the meter were noted and documented.

3.5.4 Total Dissolved Solids

The total dissolved solids in the water were measured through the use of a Potable Total Dissolved Solids (TDS) Hanna (HI98312, USA) meter. The procedure used in calibration of the instrument followed the guidelines provided by Christine et al., (2018) and Maju-Oyovwikowowhe & Shuaib (2019). Three standard solutions were used namely: distilled water, low-standard aqueous solution (1400 ppm) of KCl and high-standard (12900 ppm) aqueous solution of KCl. A 50 mL of distilled water was placed on an electrode tip, and the meter reading 0.00 ppm was observed. The electrode was rinsed with a low concentration of KCl solution. Then it was placed in 50mL of the low-standard aqueous solution (1400 ppm) of KCl, and the reading of the meter was taken as 1.4 uS. This was carried out with 50 mL of a high standard of aqueous solution (12900 ppm) and this gave a reading of 12.9uS on the meter. After calibration was completed, the electrode was cleaned with deionized water, followed by its immersion in 50 mL of the sample. The measurements were taken and put in the dataset as instructed in Christine et al., (2018). The Total dissolved solids were computed using the following formula, (equation 2).

TDS (µS/cm) = meter reading x1000, **(2)**

3.5.5 Turbidity

Turbidity of the samples of water was obtained using a turbidity meter (WAGTECH 7100, UK). The instrument was calibrated by placing the probe in a standard solution with a value of 0.01 and 1.00 Nephelometric Turbidity Unit (NTU) units of turbidity. The probe electrode was then washed three times and inserted into the water samples. The readings were read and recorded. Each of the eight water samples was run through the whole process 3 times, and the mean turbidity was computed and reported.

3.6 Preparation of Samples for Elemental Assessment

Freshly prepared aqua regia (HNO_3 (16 M) and HCl (12 M), 1:3 v/v) was used in the preparation process using the method reported by Hu & Qi (2014). Twenty millilitres of each water sample were measured into 8 set of 50 mL Pyrex beakers. Ten millilitres of the freshly prepared solution of HNO_3 and HCl was added to the contents in each beaker. The content in the beakers were mixed by a gentle swirling of the beakers. The beakers and their contents were put on a hot plate at 180^{o}C and then boiled to dryness. The beakers were moved from the hot plate and cooled to ambient temperature. Next, twenty millilitres of deionised water were poured into each beaker and the mixture thoroughly shaken so as to rehydrate the mixtures. After the mixtures were reconstituted, they were sieved using gravity Whatman No. 1 filter paper and filtered into individual 50 mL volumetric flasks. The beakers were then washed three times with five millilitres of deionised water and subsequent washings were added to the identically matched content on each of the over 50 mL volumetric flasks. Deionised water was then added to the filtrates to increase the volume to 50 mL, and

the samples were analysed for the respective heavy metals. All the analyses were in triplicate, and the mean was determined.

3.6.1 Blank samples

In the blank samples' preparation, three sets of 50 mL beakers were run through with ten millilitres of aqua regia first. Then, it was followed by 20 mL of deionised water for each vessel. The contents of each beaker were then further added with 10 mL of aqua regia. The mixtures were stirred in a gentle-swirling fashion and left to digest according to the reported concurring procedure.

3.6.2 As, Cd and Pb reference standard solutions preparation

A set of arsenic, cadmium and lead standard solutions of 1000.00 mgL^{-1} was prepared as follows: 1.00 mL^{-1} of 1000.00 mgL^{-1} of each metal stock solution was added to 1.00 L volumetric flasks, and then deionised water was added to increase the volume of solutions to the mark. Serial dilutions were carried out to get 10, 20, 40, 60, 80, 100, 120, 140 and 160 ugL^{-1} standards of each metal. These standard solutions were analysed with the reference samples at 228.80 nm, 283.31 nm, and 193.70 nm of cadmium, lead, and arsenic, respectively, as described previously (Lakshmi et al., 2015), Cd or Pb were analysed using the Atomic Absorption Spectrometer (VARIAN AA 240FS, Germany) in acetylene-air flame at the Ghana Energy Commission, Environmental Laboratory (Accra, Ghana).

3.7 Adsorption study on the activated avocado seeds

Adsorptive ability of the activated avocado seeds produced was studied on As, Cd and Pb in the samples. Eight samples from a borehole (2), an unprotected $well_a$ (2), a

protected well (2), and an unprotected $well_b$ (2) were used, after background study of the metal ions and physicochemical properties of the samples. Twenty millilitres of each of the water samples selected was put into 4 sets of 50 mL Pyrex beakers. One gram of the activated avocado seeds produced was put into a Whatman No. 1 filter paper and then made into an activated avocado seeds bags.

The activated avocado seed bags were put into the water samples in each beaker at pH 7. The beakers containing the activated avocado seeds bags and the water samples were placed onto a flask shaker (SK-O180-Pro, China) and operated at 200 rpm speed for 60 minutes at 25 ºC.

After 60 minutes, the activated carbon bags were removed and the water in them was allowed to drain for 10 minutes into respective beakers. The procedure was triplicated and treated water samples were digested for residual metal analysis using the digestion procedure as described for the untreated water samples.

Removal efficiency of the activated avocado seeds was determined using Equations 3 and 4

$$\text{Amount of metal removed} = \frac{(Co-Ce)}{m}\ v\ , \qquad (3)$$

$$\%\ \text{efficiency of metal ion removed} = \frac{(Co-Ce)}{Co} \text{ x } 100\ \%\ , \qquad (4)$$

Where C_o and C_e denote concentrations (mgL^{-1}) of metal ions in water samples at initial and final stages of the adsorption process respectively, V represents the volume (L) of water samples used and m is the mass of the activated avocado seeds used as described in similar studies (Bernard et al., 2013; Asare et al., 2018; Niu et al. 2020).

3.8 Factors Influencing Adsorption Capacity of Activated Avocado Seeds

The current research paper discusses the factors that affect the activation of avocado seeds in adsorbing metals, as Bernard et al. (2013), Gorzin & Ghoreyshi (2013) and Anyika et al. (2017) report. A batch adsorption experiment was conducted using water from the study site and systematic variation of parameters of duration, dosage of adsorbent, pH and temperature.

3.8.1 Contact time effect on adsorption capacity of the activated avocado seeds

The impact of the contact duration on the adsorption capacity was evaluated by raising the contact period between 20 and 100 min in increment of 5 min and keeping other parameters unchanged using activated avocado seeds. 4g of activated avocado seeds each was placed in 4 different Whatman No 1 filter-papers, and these bags were then placed in 4 beakers that each contained 20 mL of one of the four selected samples of water, at pH 7. The beakers were placed on a flask shaker (SK-O180Pro, China) and then agitated at 100 rpm for 20 minutes at 25 ºC. The procedure was repeated at contact time ranges of 40, 60, 80 and 100 mins. At the end, the samples were taken from the flask shaker, filter paper bags removed, and the water in them was allowed to drain for 10 minutes into the respective beakers. The procedure was triplicated, and the treated water samples were digested for residual metal analysis using the digestion procedure as described for the untreated water sample above.

3.8.2 Impact of Adsorbent Dosage

The impact of activated avocado seeds dosage on the metal adsorption process was also investigated. The adsorbent dose was varied whilst other parameters were kept

constant. Four filter paper bags containing 1.0 g of activated avocado seeds were put into the four different Pyrex beakers containing 20 mL each of the water samples selected at pH 7. The beakers and their contents were placed onto a rotary flask shaker (SK-O180-Pro, China) at 25 ºC and operated at 100 rpm for 60 minutes. The filter paper bags were removed from the beakers. Water in the filter paper was allowed to drain into the respective beakers for 10 minutes. The procedure was repeated for one and a half grams, two grams, two and a half grams, and three grams adsorbent dose. The process was repeated three times with each dose of the adsorbent, and the contents of each beaker after the activated avocado seeds treatment were digested via the procedure used on the untreated water samples.

3.8.3 pH effect on the adsorption capacity of the activated avocado seeds

The impact of pH on the adsorption ability of activated avocado seeds was considered within the range 5-9. pH 5 and 6 were obtained by carefully adding 0.1M HCl solution, and pH 8 and 9 solutions were reached by comparable additions of 0.1M aqueous NaOH. One litre of sampled water of pH 5 was dispensed in four 100-ml portions to which 1.0g of activated carbon was added, which had been produced in a Whatman Number one filter paper bag. The beakers were then put in a flask shaker (SK-O180-Pro, China) and rotated at 100 rpm at 25°C, 60 min. Following the removal of the filter paper bags, the water in them was allowed to drain into the beakers for 10 min. The same was duplicated with sampled water at pH 6, 7, 8 and 9. Each sample was replicated three times, and then the drained water samples were digested as described above for the untreated water samples.

3.8.4 Temperature effect on adsorption capacity of the activated avocado seeds

Impact of temperature on the adsorption capacity of activated avocado seeds was investigated at a range of 25 to 45°C, with the contact time, dosage, pH and agitation speed being kept constant. In four of the beakers containing the respective water samples, 1g of activated avocado seeds was weighed into four filter paper bags and inserted into the 4 sets of beakers containing each water sample. These beakers, together with their contents, were stirred on a flask agitator (SK-O180-Pro) at 100 rpm in 60 min at 25° C. When this was done, the activated avocado seeds were taken off the beakers and the water in them was allowed to drain in a different set of beakers for 10 minutes. The same procedure was done using 30, 35, 40, and 45° C temperatures. The analysis was performed, in triplicate, and the water samples that had undergone the treatment were then analyzed after following identical procedures that were applied to the untreated water samples.

3.9 Modelling of activated avocado seeds

The study assessed the adsorption capacity of the activated avocado seeds by applying the Langmuir and the Freundlich isotherms to investigate the interactions of As, Cd, and Pb in aqueous solution. The parameters of each of the models were obtained through linear regression analysis of the corresponding isotherms using the Microsoft Excel version 2018 spreadsheet program.

3.9.1 Linear modelling of Langmuir isotherm

By using the linear representation of the Langmuir model, the determination of the Langmuir isotherm properties was done. According to Anyinka et al., (2017) and Edet

& Ifelebuegu (2020), surface adsorption of metal ions by the activated avocado seeds can be well explained as monolayer adsorption through the Langmuir model onto localised active sites. According to Loi et al., (2021), adsorbates do adsorb at fixed (homogeneous) surface sites with occupancy adsorption energy that is the same. Langmuir adsorption isotherm lacks the migration of the metal ions in the plane of adsorption surfaces (Edet &Ifelebuegu, 2020). In addition, it presupposes equal energy spreading across the monolayer via the adsorbed metal ions on the surface of the adsorbents according to Edet and Ifelebuegu (2020). Graphical representations that were used in the study are based on the linear form of the Langmuir isotherm (Equation 5) as indicated by Jimoh et al., (2011); Salam et al., (2011); Eruola & Ogunyemi, (2014), Anyinka et al., (2017).

$$\frac{Ce}{Qe} = \frac{Ce}{Qm} + \frac{1}{b(Qm)}, \qquad (5)$$

b = Langmuir constants, Qm = maximum amounts of metal ions removed at equilibrium, Ce (mg / L) = amounts of metal ions in water samples at equilibrium, and Qe (mg / g) = amounts of metal ions removed at equilibrium.

3.9.2 Linear modelling of Freundlich isotherm

By using the linear version of the Freundlich isotherm model (Equation 6), the Freundlich isotherm parameters were determined. Freundlich isotherm was also used to determine the possibility that the metal ions adsorbed on the activated carbon used were part of a multilayer adsorption process, Jimoh et al. (2011); Salam et al., (2011); Eruola & Ogunyemi, (2014); Anyika et al., (2017); Edet & Ifelebuegu, (2020).

The linear version of the Freundlich isotherm model, Equation (6):

$$Logqe = LogK + \frac{1}{n}LogCe, \quad (6)$$

Ce (mg/g) = quantity of metal ions presents in the equilibrium water sample, qe (mg/g) = the quantity of adsorbed, metal ions at equilibrium per gram of adsorbent, and k = Freundlich constant and n = the adsorption intensity.

3.10 Kinetics Analysis

The kinetic analysis of adsorption provides extensive insight into the processes involved in metal-ion exchange and the step that controls the transfer process (Gorzin and Ghoreyshi, 2013). Established kinetics models, such as the ones used by Gorzin and Ghoreyshi (2013), Edet and Ifelebuegu (2020), have been used by many researchers to model the adsorption of heavy metals on various adsorbents. The current work used the first-order pseudo kinetic along with the second-order pseudo kinetic linear models to describe the absorption of As, Cd, and Pb onto activated avocado seeds. First-order model generally relates to the physical adsorption where metal ions have low affinity to the adsorbent and there is no strong chemical bonding. Radnia et al., (2012) endorse this premise. Mathematically, it has the form of equation (7), qe and qt being the equilibrium and time-dependent concentrations of adsorbed metal ions and k_1 the adsorption rate constant (measured in terms of min -1):

$$In(qe - qt) = In(qe) - k_1 t, \quad (7)$$

On the contrary, the second-order model as given by equation (8), defines adsorption through a strong chemical interaction between the adsorbent surface and the metal ions:

$$\frac{t}{qt} = \frac{1}{k^2 qe^2} + \frac{t}{qe}, \quad (8)$$

qe and qt indicate the equilibrium and time (t) dependent concentrations of adsorbed metal ions with t minutes, respectively, and k_2 indicates the pseudo-first order rate constant of adsorbed metal-ion concentration at equilibrium. Rate constants k_1 and k_2 can be determined with the help of linear plots constructed based on equations (7) and (8). The obtained coefficients of determination (R^2) of the two models would determine the model that best fit the adsorption kinetics.

3.11 Thermodynamic Assessment of Adsorption Process

The thermodynamic investigation of the metal-ion adsorption process involved in this study was conducted. This was vital in order to establish the feasibility of the adsorption process as reported by Gorzin & Ghomeshi, (2013), Asare et al. (2018), and Edet & Ifelebuegu (2020). Thermodynamic assessment of the process was also important as it would predict the possible mechanism(s) involved in the metal ion adsorption process. Thermodynamic parameters investigated in this study were Gibbs free energy (ΔG^o), enthalpy (ΔH^o), and entropy (ΔS^o) as reported by Ilkunur & Hanife (2013), Gorzin & Ghoreyshi (2013), Asare et al. (2018) Edet & Ifelebuegu (2020).

Thermodynamic parameters $\Delta H°$ and $\Delta S°$ were also computed from the plot of Van't Hoff (Equation 9) and $\Delta G°$ was calculated using Equation (10) as used by Gorzin & Ghoreyshi (2013), Asare et al. (2018) and Edet & Ifelebuegu (2020).

$$InKeq = \frac{\Delta H^\circ}{RT} + \frac{\Delta S^\circ}{R}, \quad (9)$$

$$\Delta G° = \Delta H° - T\Delta S° , \quad (10)$$

Where Kc is the equilibrium constant, T is the absolute temperature (K) and R is the universal gas constant (8.314 J/mol/ K).

CHAPTER FOUR

RESULTS AND DISCUSSION

This part of the research contains the description of the results and a discussion of the investigation done. It analyses data relating to the activated avocado seeds, physicochemical properties of untreated samples used, the quantities of metal ions tested and the outcome of analyses conducted on the activated avocado seeds treated water samples. Additionally, the chapter details the application of the isotherm models, kinetic models, and the thermodynamic parameters computed for the processes on activated avocado seeds.

4.1 Characterisation of Activated Avocado Seeds

The activated avocado seeds were characterised in terms of surface properties, and they were assessed to determine their pore structure, size and volume, chemical components and surface functionalities before as well as after the application of the activated avocado seeds in the adsorption process. Before and after application, an electronic Scanning Microscope- Energy Dispersive X-ray (JSM-6380, USA) was used to provide an image of the surface, as well as X-Ray Fluorescent spectrometry (Rigaku NEX CG II, USA) to provide the elemental image composition. The surface functionalities of the activated avocado seeds were identified and compared to those of activated avocado seeds after their use using Fourier Transform Infrared Spectroscopy (Shimadzu IR Affinity1, Japan).

4.1.1 Activated avocado seeds characterisation with SEM-EDX study

Surface morphology and elemental composition of the activated avocado seeds were investigated with Scanning Electron Microscope, Energy Dispersive X-ray spectroscopy

(SEM-EDX) before and after use in the selected metal-ion adsorption process, and results presented (Figures 4.1,4.2, 4.3 and 4.4).

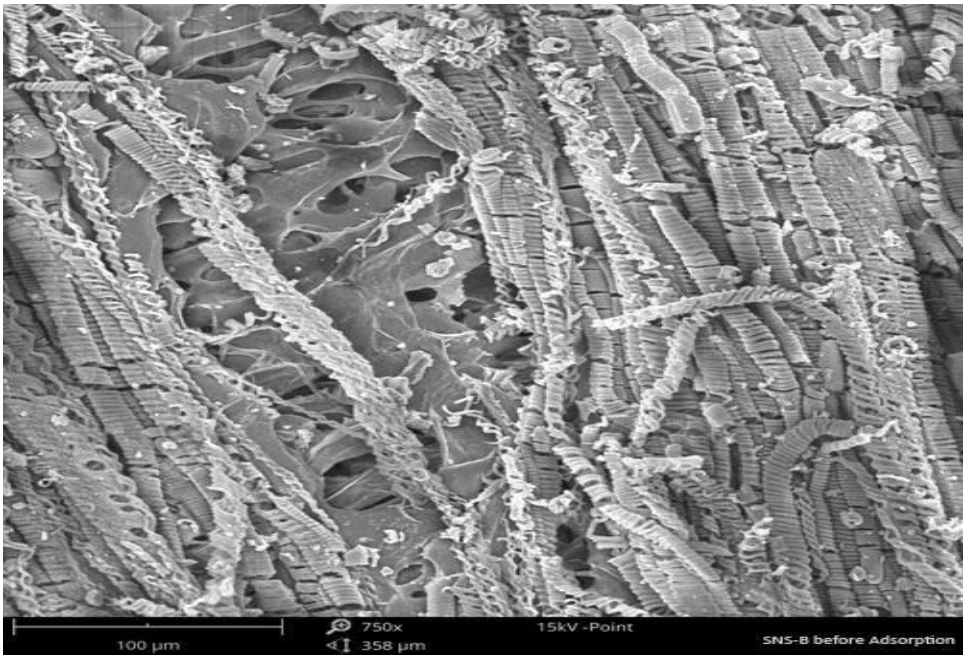

Figure 4.1: SEM image of activated avocado seeds before its application

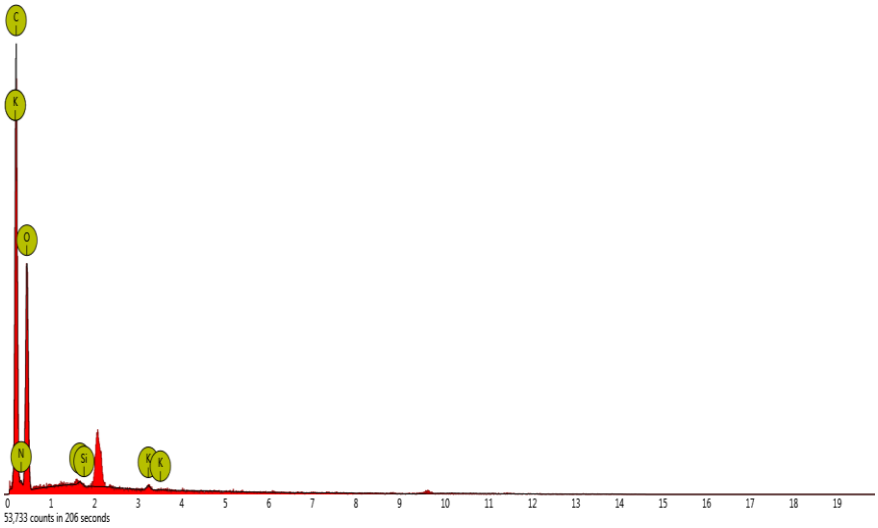

Figure 4.2: EDX analysis of activated avocado seeds before its application

The surface morphology of the activated avocado seeds prior to their use in the treatment process (Figure 4.1) exhibited irregular, elongated, and porous structural features, as described in Wang et al. (2020). This porous surface and its associated irregular surface projections indicate that the activated avocado seeds could be a potential and effective adsorbent for contaminants removal as reported by Hazourli et al. (2009) and Vafakhah et al. (2014).

High porosity and irregularity of the surface of the activated avocado seeds might contribute to its large surface area and large pore volume observed in the characterisation process. These observations were similar to those reported by Bernard et al. (2013), Vafakhah et al. (2014) and Buah et al. (2016). The variation in pore sizes seen on the surface of the activated avocado seeds could enhance its adsorption capacity as also seen in similar studies (Hussein et al., 2015; Buah et al., 2016 and Anyika et al., 2017). These surface properties of the activated avocado seeds could also enable their uptake of high concentrations of adsorbates, as reported in Hussein et al. (2015).

Energy Dispersive X-ray analysis (EDX) was also conducted to determine the elemental composition of activated avocado seeds. The EDX spectrum obtained (Figure 4.2) showed the constituent elements in the activated avocado seeds before its application in the adsorption process. Carbon, potassium and oxygen atoms recorded higher peaks (Figure 4.2). Carbon constituent of the activated avocado seeds immobilises the metal ions at ambient conditions by providing an adsorptive surface to the metal ions (Bashkova et al., 2005). Surface oxygen groups provide acidic carbon surfaces (Bandosz et al., 2006). The decomposition of acidic groups creates

active sites at the edges of the graphene layer (Bandosz et al., 2006) which enhances the uptake of adsorbates. Elevated potassium component with oxides and hydroxides provides alkaline surfaces of the activated avocado seeds (Williams & Aydinlik, 2021). The alkaline surfaces of the activated avocado seeds provide negatively charged surfaces of the adsorbent, which attract positive ions (metal-ions) in the adsorption process (Williams & Aydinlik, 2021).

Therefore, higher peaks of carbon, potassium and oxygen could contribute to the efficiency of the activated avocado seeds to adsorb metal-ions as reported in Uddin & Nasar (2020).

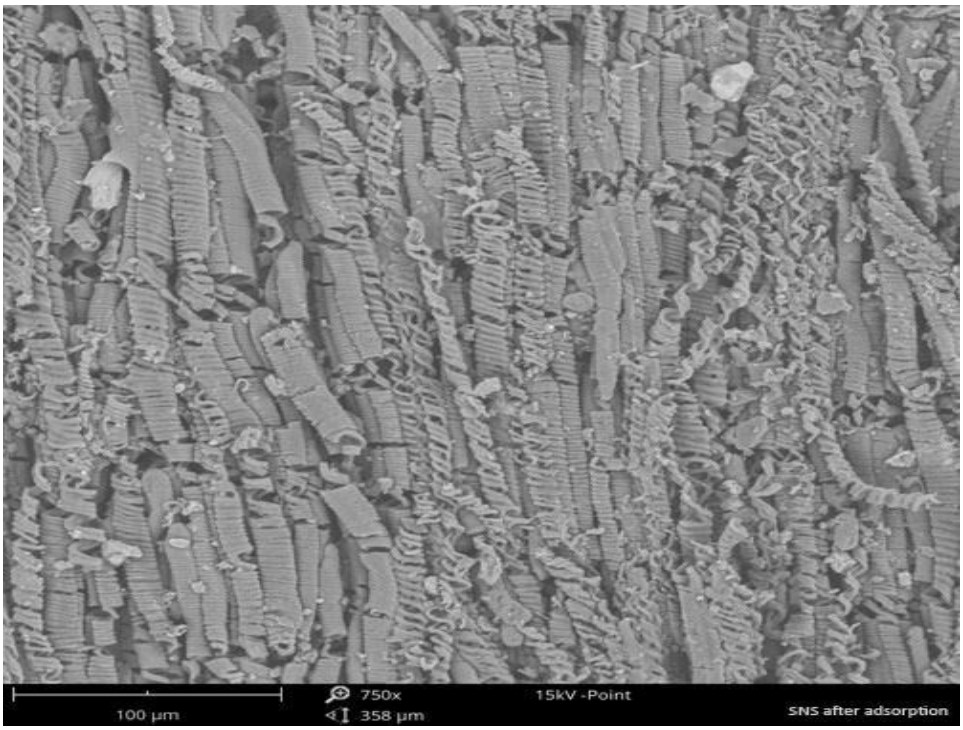

Figure 4.3: SEM image of activated avocado seeds after its application

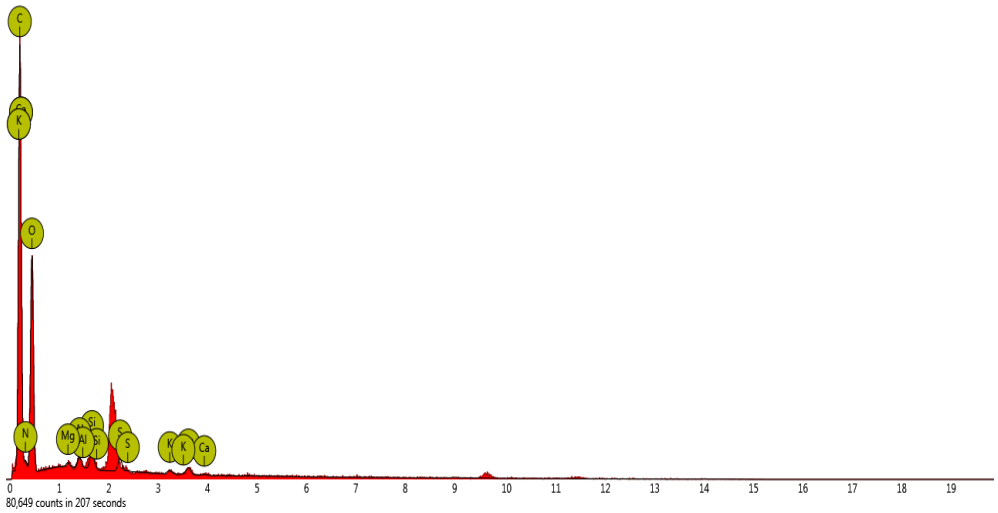

Figure 4.4: EDX analysis of activated avocado seeds after its application

Surface morphology of the activated avocado seeds after its application in the water treatment process (Figure 4.3), showed a relatively smooth surface when compared with that seen before its use in the adsorption process (Figure 4.1). This surface smoothness might be due to surface coverage of the activated avocado seeds by the selected metal ions as reported in similar studies (Gorzin & Ghoreyshi, 2013; Ezeokonkwo et al., 2018).

The EDX spectrum obtained after the activated avocado seeds have been used in water treatment (Figure 4.4) showed carbon, calcium, potassium and oxygen to have higher peaks. The changes seen in the EDX spectrum might have been caused by surface coverage of the activated avocado seeds by the metal ions as reported by Gorzin & Ghoreyshi (2013), Uddin & Nasar (2020) and Yin et al. (2020).

Comparison of the EDX spectra recorded for the activated avocado seeds before and after their use in the adsorption process (Figures 4.2 and 4.4) showed that surface coverage of the activated avocado seeds by metal ions As, Cd and Pb is obvious after

the adsorption process (Gorzin & Ghoreyshi, 2013; Yin et al., 2020). This observation also agrees favourably with findings reported by Uddin & Nasar (2020), and Yin et al., (2020).

4.1.2 Characterization of activated avocado seed powder with XRF

X-Ray Fluorescence characterisation of the activated avocado seeds was also performed to obtain their chemical and elemental compositions. The data obtained were treated statistically and the mean values reported (Tables 4.1 and 4.2). The XRF assessment was done before and after the activated carbon was used in the adsorption process.

Table 4.1: Chemical Constituents of Activated Avocado Seeds prior to and after their Application

	Chemical constituents (mg/kg)		% change in composition
	Prior to appl	After appl.	After appl.
Constituent			
MgO	9.39 ± 0.12	5.41 ± 0.13	42.39
Al_2O_3	7.98 ± 0.11	7.34 ± 0.04	8.02
SiO_2	24.3 ± 0.07	23.1 ± 0.00	5.14
P2O5	5.84 ± 0.04	3.19 ± 0.02	45.38
SO_3	8.56 ± 0.04	4.54 ± 0.02	46.96
K_2O	0.23 ± 0.21	0.23 ± 0.00	1.71
CaO	44.0 ± 0.01	25.2 ± 0.14	42.73
MnO	0.70 ± 0.01	0.23 ± 0.02	6.77
Fe_2O_3	0.86 ± 0.03	6.40 ± 0.07	86.56

The results obtained from the XRF investigations (Table 4.1) showed that the activated avocado seeds contain 44.0 ± 0.01 $mgkg^{-1}$ CaO with 24.3 ±0.07 $mgkg^{-1}$ SiO_2 as the main constituent oxides. Other compositions were 9.39 ± 0.12 $mgkg^{-1}$ MgO, 8.56±0.04 $mgkg^{-1}$ SO_3, 7.98 ± 0.11 $mgkg^{-1}$ Al_2O_3 and 5.84 ± 0.04 $mgkg^{-1}$ P_2O_5 (Table

4.1) were also significant of the activated avocado seeds. 0.86 ± 0.03 $mgkg^{-1}$ Fe_2O_3, 0.70 ± 0.01$mgKg^{-1}$ MnO and 0.23 ± 0.21 $mgKg^{-1}$ K_2O constituents of the activated avocado seeds were present at trace quantities (Table 4.1).

Similarly, the XRF analysis results after the activated avocado seeds have been used in the adsorption process showed that 25.2 ± 0.14 $mgkg^{-1}$ Cao, 23.1± 0.00 $mgkg^{-1}$ SiO_2, 7.34 ± 0.04 $mgkg^{-1}$ Al_2O_3, 4.54 ± 0.02 $mgkg^{-1}$ SO_3, 6.40 ± 0.07 $mgkg^{-1}$ Fe_2O_3, 5.41 ± 0.13 $mgkg^{-1}$ MgO and 3.19 ± 0.02 $mgkg^{-1}$ P_2O_5 were the major constituents (Table 4.1). 0.23 ± 0.02 $mg^{-1}kg$ MnO and 0.23 ± 0.00 $mgkg^{-1}$ K_2Owere present in small quantities (Table 4.1).

The activated avocado seeds were also found to contain high lime content that has the potential to make them have high neutralising capacity for acidic effluents, as reported by Siemak et al. (2024). The high lime content of the activated avocado seeds can also precipitate metal ions as reported by Rao et al. (2009). Aluminium oxide, silicon oxides, Iron (III) oxide and Magnesium oxide play key roles in interfacial processes such as mineral precipitation and dissolution as stated by Leite et al. (2017). These elements also serve as contaminant transport in the adsorption process, as reported by Goldberg et al. (2007). Sulphur trioxide (SO_3) and Phosphorus pentoxide components of the activated avocado seeds give its surface charge characteristics, which provide more negative ionic adsorption sites for metal-ion adsorption and also enhance the adsorption capacity of the activated avocado seeds towards ionic pollutants, as indicated by Goldberg et al. (2007). The surface characteristics of the activated avocado seeds due to the presence of a significant quantity of SO_3 and P_2O_5 also promote their selective adsorption (Kim et al., 2016).

Thus, the main constituents of the activated avocado seeds were Al_2O_3, CaO, MgO, P_2O_5, SiO_2 and SO_3, which favourably agree with similar work done by Kaga et al. (2024); Elizalde-Gonzalez et al. (2007). These components could be the reason why it is capable of extracting chosen heavy metal ions in metal-polluted sources of water. Little variation occurred in the oxide quantities in the activated avocado seeds after their application in the adsorption process. Except for Iron (III) oxide (Table 4.1), which had an increased composition, the oxide had a decline in quantities after the application (Table 4.1). These variations in the composition of the activated avocado seeds after use might be due to the interaction of the activated seeds with metal ions, as reported by Ezeokonkwo et al. (2018). These interactions may have led to the deposition of metal ions onto the porous surface of the activated avocado seeds to be adsorbed on active adsorption sites, as observed in the study performed by Ezeokonkwo et al. (2018); Siemak et al. (2023).

The factor of elemental compositions of activated avocado seeds employed in the present study was also determined prior, and after its utilisation during the process of investigation. Elemental composition was studied by X-Ray Fluorescence analysis, as done by Park et al. (2019). Statistically, the obtained results were treated, and the mean values were reported (Table 4.2). None of the investigated metals, arsenic (As), cadmium (Cd) and lead (Pb), was a constituent of the activated avocado seeds before its use in the metal-ion adsorption process (Table 4.2). This observation might indicate that the metals As, Cd and Pb were absent or lower than the detection limit registered by the XRF instrument. Nonetheless, the XRF analysis of the activated avocado seeds after the adsorption process showed that $0.27 \pm 0.02 mgkg^{-1}$ Pb was a constituent of the activated avocado seeds. The XRF analysis of the activated avocado seeds showed

before its use in the adsorption process, Vanadium, Chromium, Lead, Thallium, Nickel, Tantalum, and Antimony were either absent as components of the activated avocado seeds or below the detection limit of the XRF used (Table 4.2). Yet, after the activated avocado seeds have been used, the XRF analysis showed Vanadium, Chromium, Lead, Thallium, Tantalum and Antimony as elemental constituents of the activated avocado seeds (Table 4.2). 611.0 ± 2.83 $mgkg^{-1}$ Zirconium, 99.9 ± 1.20 $mgkg^{-1}$ Scandium and 57.9 ± 0.64 $mgkg^{-1}$ Chlorine were also found to be major elemental constituents of the activated avocado seeds before their application (Table 4.2).

Table 4.2 : Elemental Composition of Activated Avocado Seeds prior to and post Application

Element	Mean metal conc. (mg/kg)		
	Prior	Post	% Change in concentration
Cl	57.9 ± 0.64	76.5± 0.71	24.3
Ti	21.0 ± 1.56	80.8 ± 3.46	74.0
V	-	11.7 ± 0.71	100.0
Cr	-	1.62 ± 0.00	100.0
Co	2.70 ± 0.21	11.3 ± 0.64	76.1
Ni	-	0.80 ± 0.00	100.0
Cu	5.46 ± 0.15	6.52 ± 0.47	16.2

Table 4.3 : Elemental Composition of Activated Avocado Seeds prior and post Application

Element	Mean metal conc. (mg/kg)		
	Prior	Post	% Change in concentration
Zn	11.2 ± 0.28	31.8 ± 0.07	64.8
Rb	11.9 ± 0.14	16.6 ± 0.28	2.5
Sr	13.9 ± 0.07	24.2± 0.07	42.3
Sn	9.17 ± 0.21	7.84 ± 0.17	14.5
Te	8.84 ± 0.00	5.99 ± 0.00	32.2
Au	0.899 ± 0.00	37.5 ± 0.12	97.6
Sc	99.9± 1.20	178.0± 6.36	43.9
Zr	611.0 ± 2.83	633.0 ± 21.92	3.5
Pb	-	0.276 ± 0.02	100.0
Tl	-	2.60 ± 0.00	100.0
Ta	-	1.7 ± 0.00	100.0
Sb	-	2.73 ± 0.00	100.0

But,11.9 ± 0.14 $mgkg^{-1}$ Rubidium, 21.0 ± 1.56 $mgkg^{-1}$ Titanium, 13.9 ± 0.07 $mgkg^{-1}$ Strontium, 11.2 ± 0.28 $mgkg^{-1}$ Zinc, 9.17 ± 0.21 $mgkg^{-1}$ Tin and 8.84 ± 0.00 $mgkg^{-1}$ Tellurium were the minor elemental constituent (Table 2). Copper and Gold occurred in trace quantities in the activated avocado seeds before their application (Table 4.2).

Again, 633.0 ± 21.92 $mgkg^{-1}$ Zirconium, 178.0 ± 6.36 $mgkg^{-1}$ Scandium and 76.5 ± 0.71 $mgkg^{-1}$ Chlorine were observed to be major elemental constituents of the activated avocado seeds after its use in the adsorption process (Table 4.2). 16.6 ± 0.28 $mgkg^{-1}$ Rubidium, 80.8 ± 3.46 $mgkg^{-1}$ Titanium, 31.8 ± 0.07 $mgkg^{-1}$ Zinc, 24.2 ± 0.07 $mgkg^{-1}$ Strontium, 7.84 ± 0.17 $mgkg^{-1}$ Tin and 5.99 ± 0.00$mgkg^{-1}$ Tellurium, 6.52 ± 0.47 $mgkg^{-1}$ Copper and 37.5 ± 0.12 $mgkg^{-1}$ Gold were also seen as major elemental constituents of the activated avocado seeds. 2.73 ± 0.00 Antimony, 2.60 ± 0.00 $mgkg^{-1}$ Thallium, 11.7 ± 0.71 $mgkg^{-1}$ Vanadium, 1.71 ± 0.00 $mgkg^{-1}$ Tantalum, (1.62 ± 0.00 $mgkg^{-1}$) Chromium, 0.80 ± 0.00 $mgkg^{-1}$ Nickel and 0.27 ± 0.02 $mgkg^{-1}$ Lead, occurred as trace constituents of the activated avocado seeds (Table 4.2). XRF analysis of the activated avocado seeds showed changes in the quantities of the elemental

constituents after the adsorption process (Table 4.2). The observed changes in the composition of the activated avocado seeds before and after the metal-ion adsorption process could be attributed to surface coverage of the activated avocado seeds by metal ions, as reported by Ezeokonkwo et al. (2018).

4.1.3 FTIR analysis

The functional groups on the surface of the activated avocado seeds used were also determined before and after the adsorption process. The functional group determination was done using Fourier Transform Infrared (FTIR) analysis. The results obtained before and after the metal-ion adsorption are presented in Figures 4.5 and 4.6 and the interaction of the absorption bands.

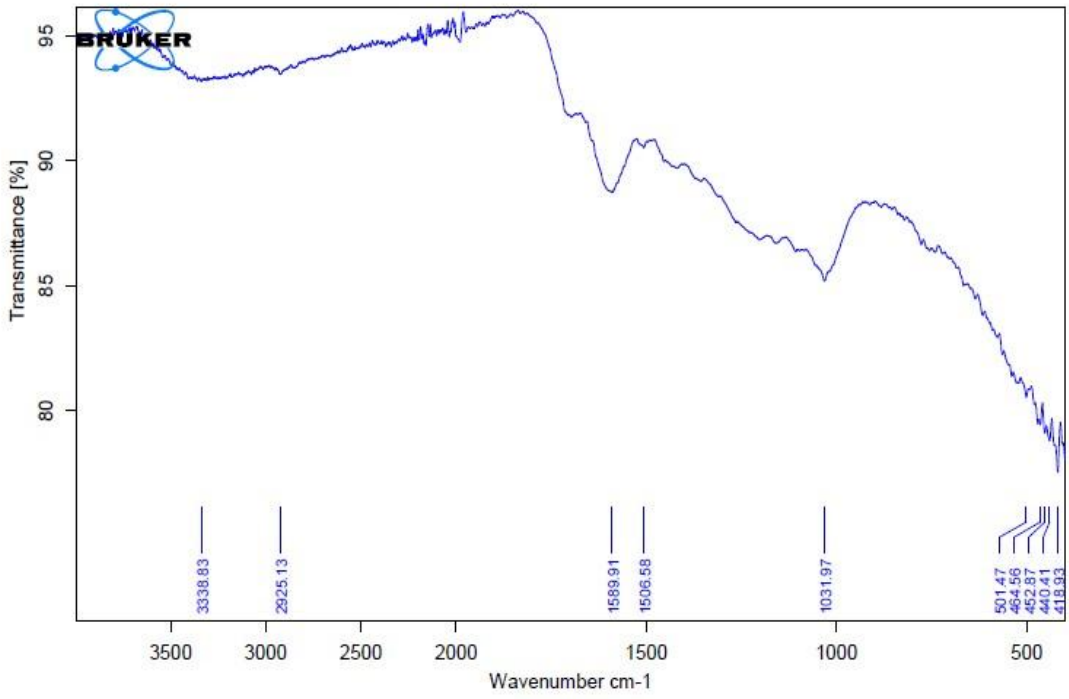

Figure 4.5: Image of FTIR spectrum of activated avocado seeds prior to application

The FTIR spectrum recorded for the activated avocado seeds before it was used in the metal-ion adsorption process (Figure 4.5) showed absorption bands at different wave

numbers. Peaks occurred at wave numbers 3338.83, 2925.13, 2000, 1589.91 and 1031.97 cm^{-1}. A broad and weak absorption band at 3338.83 cm^{-1} could be attributed to the stretching vibration of the O-H bond in the structure of cellulose as reported by Awwad et al. (2021).

A sharp and weak absorption band at 2925.13 cm^{-1} might have originated from the stretching vibration of C-H bonds in alkanes as reported by Adegoke et al. (2017). Aromatic overtones also occurred at 2000 cm^{-1} might have originated from aromatic functional groups present in the structure of cellulose as indicated in a similar study (Azargohar & Dalai, 2006). A sharp and strong absorption band at 1589.91 cm^{-1} might be attributed to the stretching vibration of C=O bonds of cellulose, as has been reported by Awwad et al. (2021). A sharp and weak band at 1506.58 might have originated from the C-C vibrations of aromatic groups in the cellulose structure. A sharp and strong absorption band observed at 1031.97cm^{-1} might have resulted from the C-O stretching vibration related to holocellulose and lignin structures as reported by Adegoke et al. (2017).

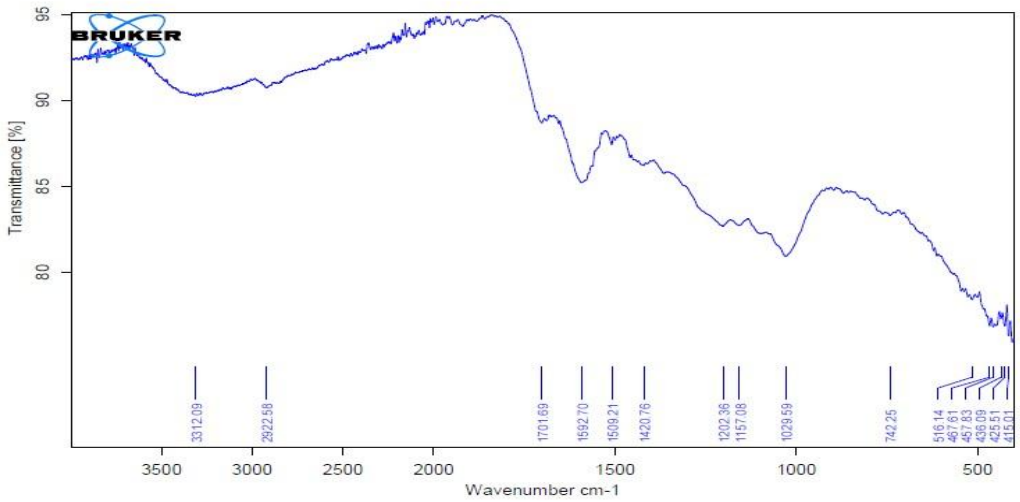

Figure 4.6: Image of FTIR spectrum of activated avocado seeds post application

The FTIR assessment of the activated carbon avocado seeds after its application in the adsorption process (Figure 4.6) showed similar adsorption bands as those in activated avocado seeds before use (Figure 4.6) but at different wave numbers. Peaks occurred at wave numbers 3312.09, 2922.58, 2000, 1701.69, 1592.70 and 1509.21 cm^{1} (Figure 4.6). A broad but weak absorption band at 3312.09 cm^{-1} may be due to O-H stretching vibrations of cellulose as reported by Awwad et al. (2021). A sharp and weak absorption band observed at 2922.58 cm^{-1} could be attributed to the stretching vibration of the C-H bond of alkanes as indicated by Gorzin & Ghoreyshi (2013) and Adegoke et al. (2017). Aromatic overtones were also seen at 2000 cm^{-1} and they might have resulted from aromatic groups within the cellulose structure as reported in a similar study (Azargohar & Dalai, 2006).

A sharp band at 1701.69 cm^{-1} might be due to the stretching vibration of the C-H bond of the aromatic groups in the cellulose structure. A strong absorption band at 1592.70 cm^{-1} could be attributed to the stretching vibration of C=O bonds in the cellulose structure as reported by Adegoke et al. (2017). A sharp band at 1509.21cm^{-1} could be related to the vibrations of C-C bonds of aromatic groups. A sharp and strong absorption band observed at 1029.59cm^{-1} might have resulted from the C-O stretching vibration, which might have originated from holocellulose and lignin structures within the cellulose structures of the avocado seeds, as reported by Nazifa et al. (2019).

Comparing the FTIR spectrum of the activated avocado seeds before and after its use in the adsorption process showed changes in the positions of the absorption bands. For instance, a broad absorption band observed at 3338.83 cm^{-1} before the activated carbon produced was used (Figure 4.5) in the absorption process was shifted to

3312.09cm^{-1} after being used in the adsorption process (Figure 4.6). This observed shift in the absorption band could be due to complexation between the metal ions and the OH groups, as reported in a similar study (Wang et al., 2019).

The changes in the absorption positions may also be due to the interaction of the metal ions with the different functional groups on the surface of the activated avocado seeds as interpreted by Ezeokonkwo et al. (2018). This shift in absorption band positions agreed with the findings seen in FTIR spectra of chitosan adsorbent for phenol adsorption before and after its application as reported by Alves et al. (2020).

4.2 Physico-Chemical Parameters of Samples

The physicochemical properties of the samples involved in this study were obtained onsite, their mean values were evaluated and then compared with the allowable standards set by the World Health Organization (WHO) (Appendix 1). The data obtained were presented and reported in the form mean ± standard deviation (mean ± SD) (Table 4.4).

4.2.1 Temperature

The temperature of the water samples ranged from 26.3 ± 0.12 ºC to 30.3 ± 0.05 ºC (Table 4.4). The highest mean temperature (30.3 ± 0.05 ºC) occurred in the water samples from unprotected well 3 collected from Amafie, whilst the sample collected from borehole 1 at Amafie had lowest mean temperature (26.3 ± 0.12 ºC) (Table 4.4). These results corresponded favourably to those reported in similar studies by Agbalagba et al. (2011), Akinbile &Yusoff (2011) and Ismaila et al. (2017).

The relatively high temperatures of the water sample from the unprotected well may be due to direct exposure to the sunlight, as reported in a similar study by Adesiyan et al. (2018). An increase in the rate of interaction with the water resources could also have accounted for the elevated temperatures recorded for the unprotected well water samples. Effluent discharged from mining and other activities into the environment might have also contributed to the high temperatures of the water sampled from the unprotected $well_b$ for this study, as reported in a similar study by Adefemi & Awukuni (2010).

A temperature difference (3.17ºC) occurred between the temperature of sample from the unprotected $well_a$ and that of the protected well water resources sampled for this study. This temperature difference agrees with that reported in a similar study by Adefemi & Awukuni (2010). Though the temperature of drinking water is often not a major human issue, as it depends on individual taste and preference, increase in water temperature could promote the growth of microorganisms that could change the taste, odour and colour of water as reported by Adefemi & Awukuni (2010).

4.2.2 pH

The mean pH of the water sources sampled for this study ranged from 5.49 ± 0.03 to 6.82 ± 0.03 (Table 4.4). Unprotected well (a-type) sample collected from well 2 at Amafie had the highest mean pH (6.82 ± 0.03), whilst the groundwater collected from protected well 1 at Amafie had lowest pH (5.49±0.03). Except for the pH for borehole 3 (5.50±0.08), protected well (5.49±0.03) and protected well 2 (5.78±0.05), which had pH below the permissible (6.5-8.5) limit for drinking water, the pH of all the other water samples used in this study were within the 6.5-8.5 permissible limit set by WHO

(Appendix 1). The observed pH within the permissible limit (6.5-8.5) might have resulted from no or lower levels of dissolved carbonate and hydroxide ions in the water sources as reported by Maju-Oyovwikowhe & Shuaib (2019). However, the pH of groundwater sources that were below 6.5-8.5 permissible limits for drinking water might be due to leaching of sulphate ions from fertilizers and pesticides into the groundwater from cultivated farmlands, as reported in a similar study by Ismaila et al. (2017).

4.2.3 Turbidity

With the exception of boreholes 2 and 3 and the protected well 3 water sources that recorded mean turbidity within the permissible turbidity (5 NTU) level set by WHO (Appendix 1), all other water samples used in this study had mean turbidity above permissible turbidity (5 NTU) level.

Table 4.4: Physico-Chemical Parameters of Samples Used in the Study

Parameter Sample	Temperature (ºC)	pH	Turbidity (NTU)	Conductivity (µS/cm)	TDS (mg/L)
BH 1	26.3 ± 0.12	6.46±0.08	10.7 ± 0.15	30.2 ± 0.36	30.3 ± 0.02
BH 2	26.5 ± 0.01	6.30±0.01	1.10 ±0.02	29.4 ±0.53	29.8 ± 0.03
BH 3	26.4 0.01	5.50±0.08	0.6 ± 0.01	111.0 ± 0.10	26.1 ±0.02
UWa 1	30.0 ± 0.10	6.75±0.08	336.0 ± 0.01	251.0 ± 0.35	26.6 ± 0.36
UWa 2	30.2 ± 0.05	6.82±0.03	991.0 ± 0.12	254.0 ±0.10	29.2 ±0.19
UWa 3	30.3± 0.05	6.55±0.06	371.0 ± 0.58	157.0 ± 0.12	28.4 ±0.02
PW 1	27.5 ± 0.10	5.49±0.03	18.7 ± 0.10	96.1 ± 0.08	27.2 ± 0.01
PW 2	26.7± 0.06	5.78±0.05	76.3 ± 1.76	116.0 ±0.20	28.2 ± 0.02
PW 3	27.1± 0.06	6.61±0.00	1.10 ± 0.03	157.0 ± 0.12	31.0 ± 0.20
PW 4	26.8± 0.02	6.17±0.01	60.5 ± 0.49	196.0 ± 0.20	28.5 ± 0.04
UW_b 1	29.8 ± 0.02	6.51±0.07	361.0 ± 0.58	315.0 ± 0.21	32.6 ± 0.11
UW_b 2	29.8 ± 0.10	6.60±0.01	368.0 ± 0.29	314.0 ±0.30	28.6 ± 0.06

BH = Borehole, UWa = Unprotected well type a, PW = Protected well, UWb = Unprotected well type b

The sample collected from unprotected well$_a$ 2 (Amafie) had the highest mean turbidity (991.0 ± 0.012 NTU) whilst the groundwater collected from borehole 3 (Kojina) had the least mean turbidity (0.6± 0.01 NTU) (Table 4.4).

Mean turbidities of unprotected well$_b$ 1 and 2 from Amafie and Kojina water sources (36.1 ± 0.58 to 991.0 NTU) were generally high compared with those of other groundwater sources (0.6 ± 0.01 -76.3 NTU). The high turbidities of the unprotected well$_b$ water sources may be due to run-off of soil particles into the water bodies and galamsey activities as reported by Haftu & Sathishkumar (2020). Elevated turbidity level is a major concern as turbid water habours micro and macro-organisms, which are a potential cause of diseases.

4.2.4 Electrical conductivity

Mean conductivity of the water samples used in this study ranged from 29.4 ± 0.53 to 315.0 ± 21 µS/cm (Table 4.4). Water collected from the unprotected well$_b$ from Amafie and Kojina had the highest electrical conductivity (315.0 ±0.21 µS/cm), whilst that of the water from borehole 2 (Amafie) had the least mean conductivity (29.4 ± 0.53 µS/cm). The electrical conductivity of the water samples used in this study was below the 500 µS/cm permissible limit set by WHO (Appendix 1) and corresponded favourably with that reported by Maju-Oyovwikowhe & Shuaib (2019). High electrical conductivity level of a drinking water is an indication of inorganic pollution load, due to high salinity and high mineral content (Mitra et al., 2018). However, the prolonged intake of high-salt-containing water may cause kidney stone formation (Garg et al., 2009).

4.2.5 Total dissolved solids

Mean TDS of the water samples used in this study ranged from 26.1± 0.02 to 32.6 ± 0.11 mg/L (Table 4.4). The water samples collected from borehole 3 (Kojina) had the lowest mean TDS (26.1 ± 0.02 mg/L), whilst the water samples collected from unprotected well$_b$ 1 and 2 from Amafie and Kojina had the highest mean TDS (32.6 ±0.11 mg/L) (Table 4.4). Generally, the TDS of water samples were below the 500 mg/L permissible level TDS set by WHO (Appendix 1). Even though TDS were low, anthropogenic activities such as farming and mining observed at the sampling sites might have contributed to the TDS recorded for the water samples and agreed favourably with that observed in similar study by Agbalagba et al. (2011). High concentration of TDS in drinking water has a tearing effect on persons suffering from kidney and heart diseases (Sarala & Mageswari, 2014).

4.3 Heavy Metal Concentration

Levels of As, Cd and Pb in water sources for this study were treated statistically, and data obtained were reported in the form mean ± standard deviation (mean ± SD) and presented (Table 4.4). These mean levels were compared with permissible levels
(Appendix 2) set by WHO, EC and USEPA.

4.3.1 Cadmium concentration in samples

The results obtained (Table 4.5) showed that cadmium concentration in the water samples collected from the borehole and protected well were below the detection limit (<2.00E-03 mg/L) of the method used. This finding agreed well with the results reported by Agbalagba et al. (2011).

Table 4.5: Mean Concentration (mg/L) of As, Cd and Pb in sample before adsorption

Metal	Water Sample	Mean ± SD	Max	Min	Standard Error
Cadmium	BH	< 0.002(BDL)	-	-	-
	UWa	0.019 ± 0.014	0.030	0.003	0.008
	PW	<0.002(BDL)	-	-	-
	UWb 1	0.041 ± 0.001	0.042	0.040	0.006
	UWb 2	0.043 ± 0.003	0.045	0.040	0.001
Lead	BH	0.033 ± 0.010	0.043	0.024	0.005
	UWa	0.053 ± 0.016	0.065	0.034	0.009
	PW	0.039 ± 0.017	0.053	0.020	0.009
	UWb 1	0.064 ± 0.001	0.065	0.063	0.006
	UWb 2	0.049 ± 0.006	0.050	0.043	0.003
Arsenic	BH	0.029 ± 0.003	0.031	0.026	0.001
	UWa	0.026 ± 0.006	0.031	0.019	0.003
	PW	0.042 ± 0.002	0.043	0.040	0.008
	UWb 1	0.039 ± 0.002	0.041	0.038	0.001
	UWb 2	0.037 ± 0.001	0.038	0.037	0.005

BDL = Below detection limit, BH = Borehole, UWa = Unprotected well type a, PW = Protected, UWb = Unprotected well type b

Mean cadmium concentration in water samples collected from unprotected $well_a$ was 0.018 ± 0.014 mgL^{-1} (unprotected $well_a$), 0.041 ± 0.001 mgL^{-1} (Unprotected $well_b$ from Kojina) and 0.043 ± 0.003 mgL^{-1} (Unprotected $well_b$ from Amafie). Cd levels were above WHO (0.003 mgL^{-1}), EC (0.005 mgL^{-1}) and USEPA (0.005 mgL^{-1}) permissible levels of drinking water (Appendix 2). These observations were similar to that reported by Ehi-Eromosele & Okiei (2012).

Boreholes and protected wells Cd level (0.0002) was low, and this might have resulted from possible adsorption of Cd onto soil particles and organic matter components of the soil as reported by Kodom et al. (2012). However, elevated Cd levels were found in the samples from unprotected $well_b$ from Amafie and Kojina, and this might have resulted from agricultural activities observed at sampling sites or from the chemical used in the

galamsey gold mining observed at the sampling sites. The high levels of Cd in drinking water sources are a major public health issue since exposure to high Cd level could cause prostate enlargement, stillbirth, low birth weight and spontaneous abortion as reported by EhiEromosele & Okiei (2012).

Inhalation of cadmium oxide (CdO) fumes causes severe irritation to the respiratory system (Chakraborty et al., 2020). Cd also causes low progesterone and prolactin levels and lowers testosterone in men (Chakraborty et al., 2020). High level of Cd in water could also negatively affects life, as reported in a similar study (Adelekan & Abegunde, 2011).

4.3.2 Lead concentration in samples

The results (Table 4.5) also showed higher concentrations of Pb above 0.010 mgL^{-1} permissible lead levels in drinking water set by the World Health Organisation, (WHO, 2020). Mean concentration of Pb in the groundwater sampled from borehole and protected wells water resources were 0.033 ± 0.010 mgL^{-1} and 0.038 ± 0.017 mgL^{-1} respectively whilst unprotected $well_a$ and the unprotected $well_b$ had mean lead levels of 0.053 ± 0.016 mgL-^{1} (unprotected $well_a$), 0.064 ± 0.001mgL^{-1} (unprotected $well_b$ 1) and 0.049 ± 0.006 mgL^{-1} (unprotected $well_b$ 2). These findings were similar to those reported in a similar study by Agbalagba et al. (2011).

The high levels of Pb in the unprotected $well_b$ water resources may be due to surface run-offs and leaching of Pb ions from nearby dumping sites, galamsey sites and farming activities. However, the results agreed with those reported in similar studies done by Akinbile & Yusoff (2011) and Ehi-Eromosele & Okiei (2012). The high level of Pb seen

in drinking water sources is a serious public health issue, as Pb can damage nervous system in infants and could also cause blood and brain disorders, as reported by Ehi-Eromosele & Okiei (2012).

Consumption of these water resources over an extended time could cause Pb accumulation in soft tissues and bones, as reported by Ehi-Eromosele & Okiei (2012). Pb does not have any known human health benefit(s) (Ehi-Eromosele & Okiei (2012). Regular consumption of water with high Pb levels could damage the nervous and reproductive systems as well as the kidneys, as reported by WHO (2012). Hence, continuous consumption of water from the boreholes and wells in the study area with the elevated Pb level, as indicated by WHO (2012), could cause unwanted health issues in the individuals who depend on those water sources for their daily water needs.

4.3.3 Arsenic concentration in sample

Mean levels of As (Table 4.5) in all the samples studied were above the permissible limit (0.010 mgL^{-1}) recommended by WHO, USEPA and EC. The mean concentrations of As in the groundwater samples were 0.028 ± 0.003 mgL^{-1} (borehole) and 0.041 ± 0.002 mgL^{-1} (protected well), whilst the water samples from unprotected $well_a$ and the unprotected $well_b$ also had mean As concentrations of 0.026 ± 0.006 mgL^{-1}, 0.039 ± 0.002 mgL^{-1} and 0.037 ± 0.001 mgL^{-1} respectively. The results corresponded with those found in similar studies reported by Garba et al. (2012) and Senila et al. (2017).

The elevated level of As concentrations in the investigated water resources might have resulted from leaching from nearby farmlands and dumping sites observed at sampling sites and these observations were similar to those made by Cobbina et al. (2015). The high concentrations of As found in the water sources might have also originated from

water-soluble compounds such as arsenopyrites, other naturally occurring As ores and other minerals that might be present at the sampling site, as reported by Pal et al. (2009) and Senila et al. (2017).

This finding shows that the residents in these communities, where the samples were collected, may be at risk of As poisoning through continuous consumption of polluted water. Long-term exposures to the elevated levels of As via ingestion could result in cancer of the skin, bladder and lungs in the inhabitants of the gold mining communities as reported in several similar studies done on mining communities (Aloke et al., 2019; Mantey et al., 2020; Asare et al., 2021).

Furthermore, individuals consuming waters with such high levels of As could also develop health issues such as diabetes, pulmonary diseases, among others as reported by IEPA (2016).

4.4 Remediation of As, Cd and Pb

The efficiency of the activated avocado seeds under specific conditions of contact time, adsorbent dosage, pH, and temperature was investigated as reported in adsorption studies by Anyinka et al. (2017) and Asare et al. (2021). This was done to assess the possibility and efficiency of using the activated avocado seeds to remove As, Cd and Pb that have progressively contaminated drinking water sources in Ghana. The data generated from the As, Cd and Pb remediation processes were recorded and presented (Table 4.6).

***Table 4.6: Percentage of As, Cd and Pb Removed from Samples using* activated Avocado Seeds**

Water Sample	Metal	Initial metal conc. (mg/L)	Conc. of metal removed (mg/L)	Residual metal Conc. (mg/L)	Percentage (%) of metal removed
Bore hole	Cadmium	<0.002	<0.002	<0.002	0.0
	Lead	0.044	0.043	0.001	97.7
	Arsenic	0.031	0.030	0.001	96.8
Unprotected well$_a$	Cadmium	0.031	0.029	0.002	93.5
	Lead	0.067	0.066	0.001	98.5
	Arsenic	0.032	0.031	0.001	96.9
Potected well	Cadmium	<0.002	<0.002	<0.002	0.0
	Lead	0.055	0.054	0.001	98.2
	Arsenic	0.043	0.042	0.001	97.7
Unprotected well$_b$	Cadmium	0.043	0.041	0.002	95.3
	Lead	0.049	0.048	0.001	98.0
	Arsenic	0.037	0.036	0.001	97.3

<0.002, Below detection limit

Levels of Cd in the water sampled from the borehole and the protected well water source were below the detection limit (<0.002) of the metal extraction method used. After the adsorption process, quantities of Cd removed from the samples collected from unprotected well$_a$ and the unprotected well$_b$ were 93.5% (0.029 mgL^{-1}) and 95.3 % (0.041 mgL^{-1}) respectively (Table 4.6).

Maximum quantity of Pb removed from the water samples was 97.7 % (0.043 mgL^{-1}), 98.5 % (0.066 mgL^{-1}), 98.5 % (0.054 mgL^{-1}), and 98.2 % (0.048 mgL^{-1}) from Borehole, unprotected well$_a$, protected well and unprotected well$_b$. (Table 5). For As, percentage removals after water treatment were 96.8 % (0.030 mgL^{-1}), 96.9 % (0.031mgL^{-1}), 97.7%

(0.042 mgL^{-1}) and 97.3 % (0.036 mgL^{-1}) from Borehole, unprotected $well_a$, Protected well and Unprotected $well_b$ (Table 4.6).

Reductions seen in concentrations of the metals As, Cd and Pb in the water samples were due to adsorption of the metals onto the porous active adsorptive surfaces of the activated avocado seeds. The results obtained after samples were treated agreed with the results reported in similar studies by Benard et al. (2013) and Buah et al. (2016).

4.5 Contact Time Effect on As, Cd and Pb Adsorption onto Activated Avocado Seeds

Effect of contact time (20, 40, 60, 80 and 100 min) on removal efficiency of the activated avocado seeds was investigated at initial conditions of 1g of the activated avocado seeds at 25^{o} C, agitation speed of 100 rpm and pH 7 on all samples used in this study. Percentages of As, Cd and Pb removed were plotted as a function of the adsorption parameters (Figure 4.7).

At optimum contact time (60 minutes) for each of the samples (Borehole, unprotected $well_a$, protected well, and Unprotected $well_b$ (Figures 4.7) approximately 80 % of the heavy metals investigated were removed when samples and activated avocado seeds used were in contact for 60 minutes. The amounts of metal ions removed were generally high in the first 40 minutes (Figures 4.7), after which the quantities of metal ions adsorbed slowed down gradually till equilibrium was reached at 60 minutes.

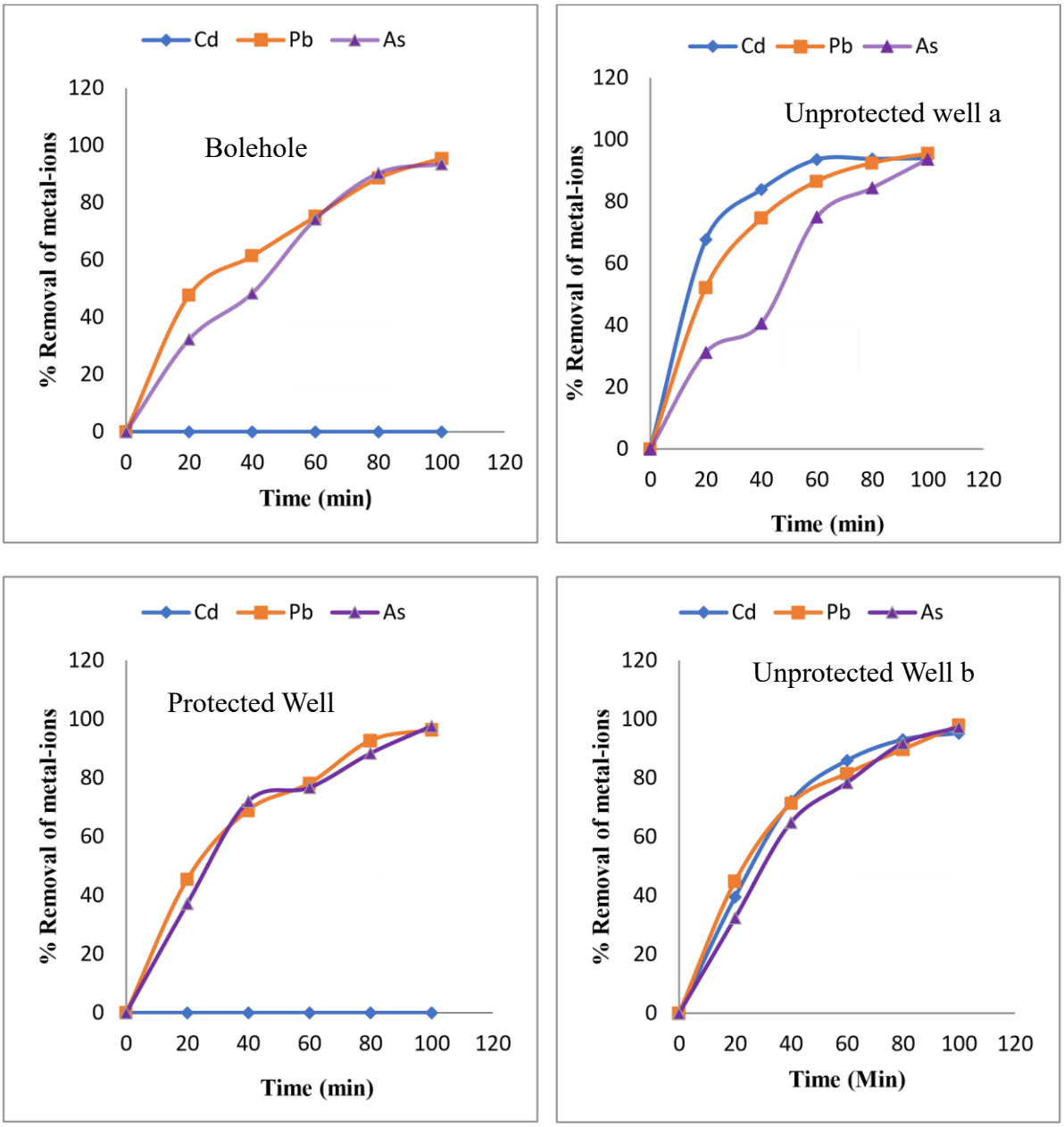

Figure 4.7: Contact time effect on As, Cd and Pb removal efficiency of the activated avocado seeds

The percentage of As removed in Unprotected well a, declined after the first 30 minutes, after which it rose gradually at 40 minutes to reach equilibrium after 60 minutes, where the quantities of As removed were high. This observation corresponded favourably with similar studies done by Oluyemi et al. (2012) and Gorzin & Ghoreyshi (2013).

Initially, adsorption of As, Cd and Pb was rapid, and that might have resulted from availability of large number of active adsorption sites on the surfaces of activated

avocado seeds particles on the onset of the adsorption process, as reported by Asare et al. (2018). However, a progressive decrease in the quantities of metal ions removed was observed as the process continued. This observed reduction in the removal efficiency of the activated avocado seeds could have also originated from a reduction in the active sites on the surfaces of the activated avocado seeds particle as adsorption progressed (Asare et al., 2021).

4.5.1 Adsorbent dose effect on adsorption of As, Cd and Pb

Effect of adsorbent dose on uptake of As, Cd and Pb ions was investigated using 1, 1.5, 2, 2.5 and 3 g of the activated avocado seeds contact time of 60 min, pH 7, temperature (25 ºC) and agitation speed of 100 rpm. The data obtained were reported graphically (Figures 4.8).

The data generated from the effect of the dose of activated avocado seeds on adsorption of As, Cd and Pb (Figures 4.8) showed a gradual increase in the adsorption capacity of the activated avocado seeds. Generally, As, Cd and Pb ions removal efficiency of the activated avocado seeds increased progressively until approximately 90 % removal was achieved. However, after the approximated 90 % removal, the removal efficiency of the activated avocado seeds declined progressively until equilibrium was established when 2.5g of the activated avocado seeds was used. After this, further increasing the dosage of the activated avocado seeds produced no further increase in quantities of As, Cd and Pb ions removed.

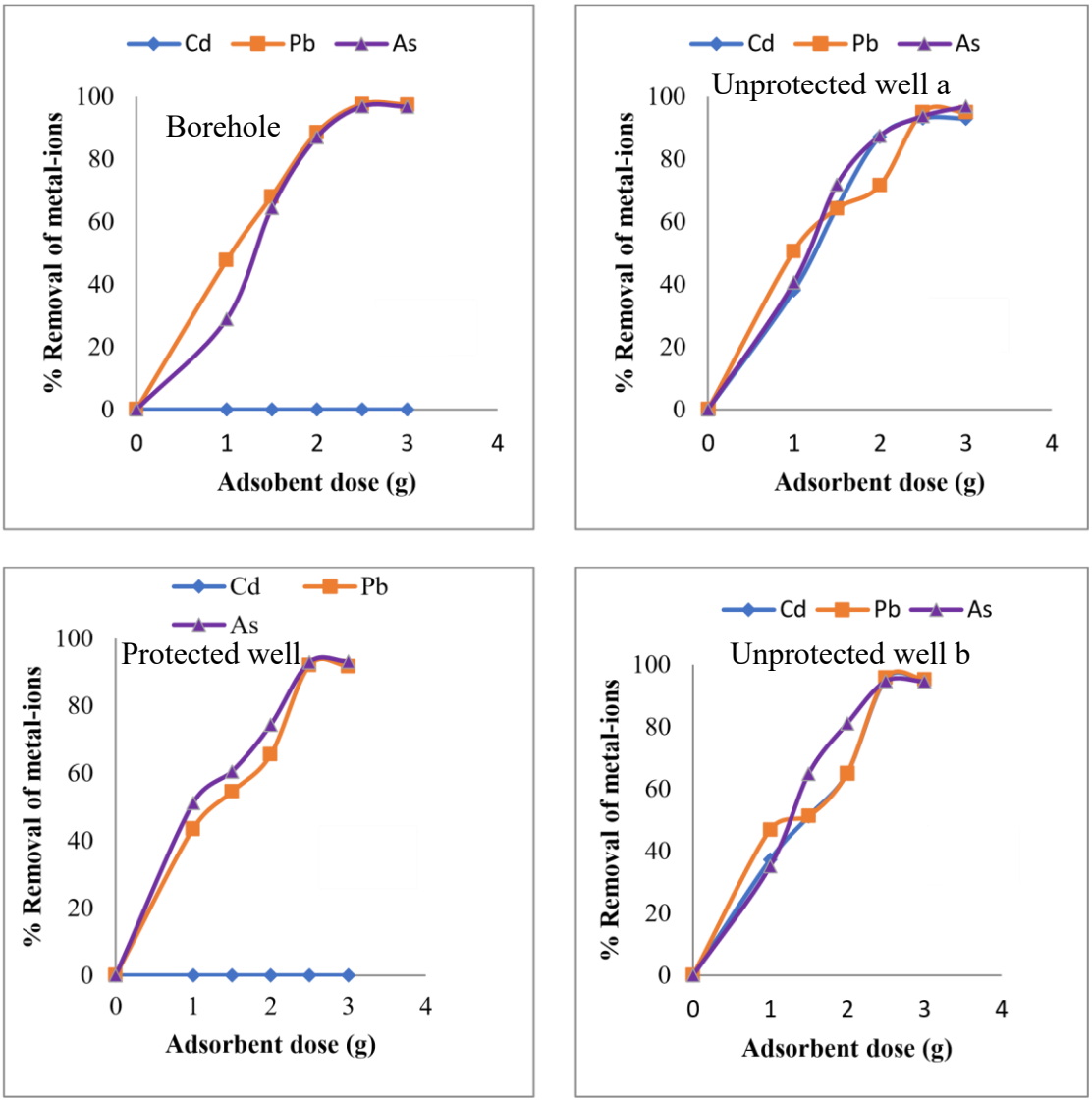

***Figure 4.8**: Adsorbent dose effect on adsorption of As, Cd and Pb samples*

Maximum amounts of As and Pb ions removed from the borehole were 97.7% (0.043 mgL^{-1}) and 96.8 % (0.031 mgL^{-1}) respectively (Figure 4.8), with the optimum adsorbent dose of 2.5g. Quantities of As, Cd and Pb ions removed from water sampled from Unprotected well$_a$ also were 93.5 % (0.029), 98.5 % (0.066 mgL^{-1}) and 96.9 % (0.030 mgL^{-1}) (Figure 4.8), respectively, with the optimum dose (2.5g) of the activated avocado seeds. Maximum amount of As and Pb ions removal from protected well water sample was 96.4% (0.053 mgL^{-1}) and 97.7 % (0.042 mgL^{-1}) respectively (Figure 4.8). Similarly, maximum quantities of As, Cd and Pb ions removed from water sampled from the

Unprotected well$_b$ were 95.3 % (0.041 mgL^{-1}), 93.9 % (0.041 mgL^{-1}) and 94.6 % (0.036 mgL^{-1}) respectively when the optimum amount (2.5 g) of the activated avocado seeds was used (Figure 4.8). These adsorption trends observed corresponded with observations made in similar studies done by Onundi et al. (2010) and Bernard et al. (2013).

The initial increment in the removal efficiency of the activated avocado seeds was expected as the quantity of the activated avocado seeds was increased. This is because active adsorption sites on the surfaces of the activated avocado seed particles were expected to increase as the quantity of activated avocado seeds increased, as reported by Asare et al. (2018). Further increase in adsorbent dose beyond the optimum quantity (2.5 g) resulted in a decline in the quantities of metal ions removed (Figure 4.8). This reduction in the adsorption capacity of the activated avocado seeds could be due to the overlapping of the adsorption sites as a result of overcrowding of adsorbent particles as reported by Najua et al. (2008) and Onundi et al. (2010). The decline seen in the removal efficiency of the activated avocado seeds could also be due to screening effects on the outer layers of the activated avocado seeds particles due to high activated avocado seeds dose as reported by Onundi et al. (2010). This screening by the activated avocado seed particles might have shielded the binding sites on activated avocado seeds from being accessed by the metal ions, as reported in a similar study by Onundi et al. (2010).

4.5.2 pH effect on As, Cd and Pb removal by activated avocado seeds

pH plays a vital role in heavy metals adsorption from aqueous systems as indicated by Srivastava et al. (2006). Changes in pH of aqueous solution affect metal-ion uptake by adsorbents due to dissociation of functional groups on active sites of the adsorbents as pH increases (Srivastava et al., 2006). The effect of pH on adsorption process was also

investigated in this study by varying pH of the water samples from 5 to 9 and the data generated were presented graphically (Figure 4.9). The results showed that increasing the pH of the water sample from 5 to 9 decreased the metal-ion removal efficiency of the activated avocado seeds. The maximum amount of As, Cd and Pb removed occurred between pH 5 and 6 and as observed in all the samples.

The maximum amounts of Cd ions removed from the samples collected from Unprotected $well_a$ and the Unprotected $well_b$ water source (Figure 4.9) were 90.3% (0.028 mgL^{-1}) and 95.3 % (0.041 mgL^{-1}), respectively, and that occurred at pH 5. However, the percentage of Cd ions removed from the samples collected from Borehole and Protected well (Figure 4.9) were below detection limit. The maximum amounts of Pb ions removed in samples collected from Borehole, unprotected $well_a$ and unprotected $well_b$ water source (Figure 4.9) were 97.7 % (0.043 mgL^{-1}), 95.5 % (0.064 mgL^{-1}), and 98.2 % (0.054 mgL^{-1}) respectively and occurred at pH 5. However, 98.0 % (0.048 mgL^{-1}) of Pb ions was removed when the pH was adjusted to 6 (Figure 4.9).

Similarly, maximum amounts of As ions removed from samples collected from Unprotected $well_a$, Protected well and Unprotected $well_b$ were 96.9 % (0.031 mgL^{-1}), 95.3% (0.041 mgL^{-1}), and 97.3% (0.036 mgL^{-1}) respectively and they occurred at pH 5 (Figure 10) whilst 93.3 % (0.028 mgL^{-1}) of As ions was removed from samples collected from borehole water (Figure 4.9) when pH was increased to 6.

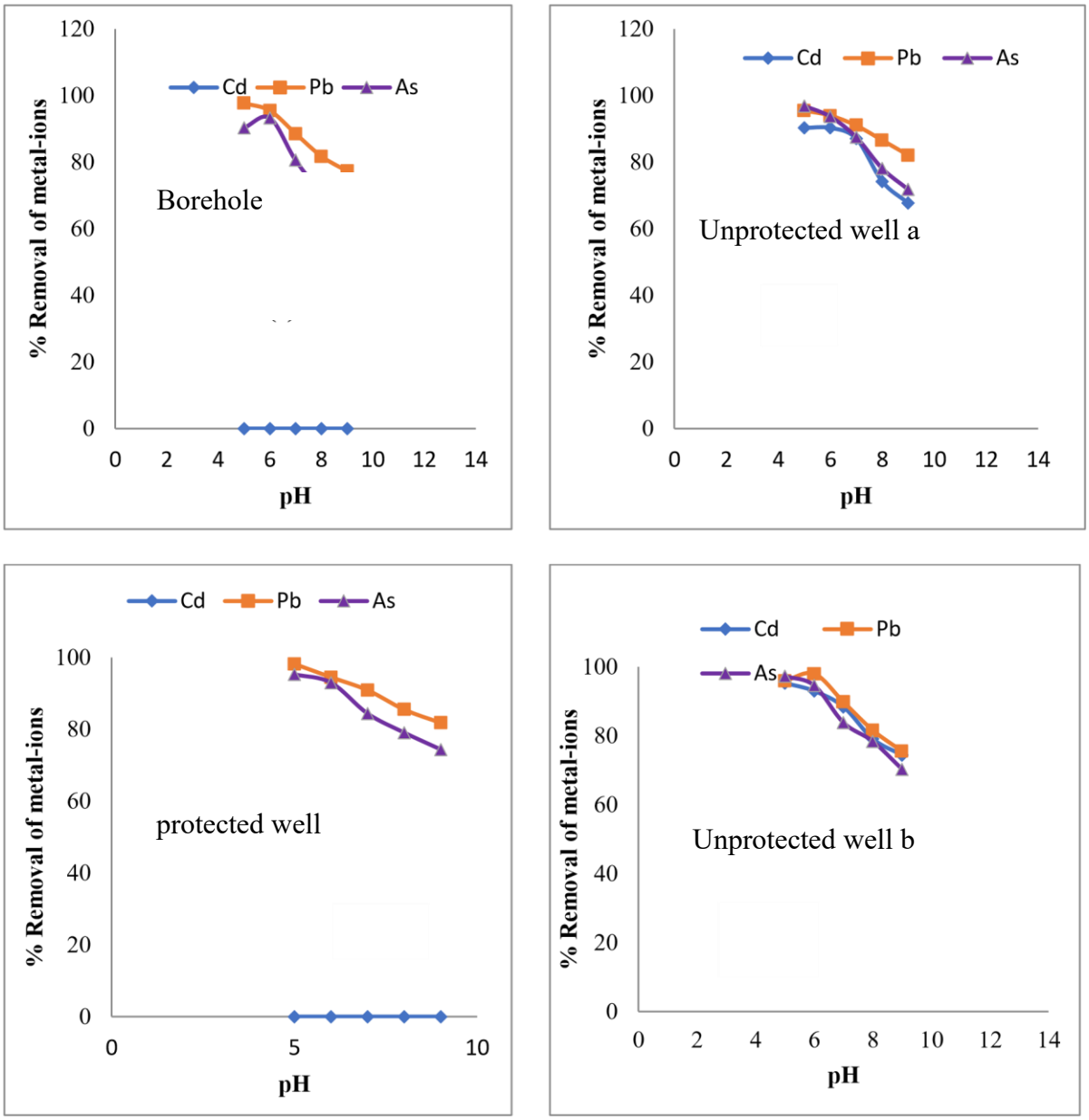

Figure 4.9: pH effect on adsorption of As, Cd and Pb in samples.

The reductions seen in the percentages of Cd ions in the samples collected from the borehole and protected well (Figure 4.9) may be due to fact that level of Cd ions in the water samples were probably below detection limit of the metal extraction method used. The maximum quantity of metal ions removed from all the samples occurred at pH 5 and 6. These could partly be due to low the mobility of H^+ ions compared with As, Cd and Pb ions for the limited active adsorption sites on the activated avocado seeds as reported

in a similar study by Onundi et al. (2010). Also, as pH increases from 2 to 7, more negatively charged surfaces of the activated avocado seeds become available and thus facilitate greater uptake of metals, as seen in similar studies done by Onundi et al. (2010) and Jimoh et al. (2011).

The reduction in metal ion uptake (Figure 4.9) by the activated avocado seeds (pH>7) may be due to precipitation of the metal ions and the immediate replacement of the metal ions by the hydroxyl groups present on the surfaces of the activated avocado seeds. This might have resulted in the formation of metal-ion complexes with organic ligands such as hydroxyl groups present on the surface of the activated avocado seeds as indicated in similar studies done by Gaikwad (2004), Tumin et al. (2008) and Jimoh et al. (2011).

4.5.3 Temperature effect on the adsorption of As, Cd and Pb

The effect of temperature on the adsorption of As Cd and Pb was studied at varied temperatures (25, 30, 35, 40 and 45^{o}C). This was carried out using 1g of the activated avocado seed, agitation speed (100 rpm) and contact time of 60 minutes at pH 7. The data obtained were presented graphically (Figure 4.10).

Quantities of Cd ions removed (Figure 4.10) were below the detection limit of method used in the extraction of Cd ions from the samples. However, quantities of Cd ions removed from water sampled from Unprotected well$_a$ and Unprotected well$_b$ (Figures 4.10) increased from 71% (0.022 mgL^{-1}) and 51.2 % (0.029 mgL^{-1}) at 25^{o}C to 96.7 % (0.029 mgL^{-1}) and 95.4 % (0.041 mgL$^{-1)}$ respectively, when the temperature was increased to 40 ºC.

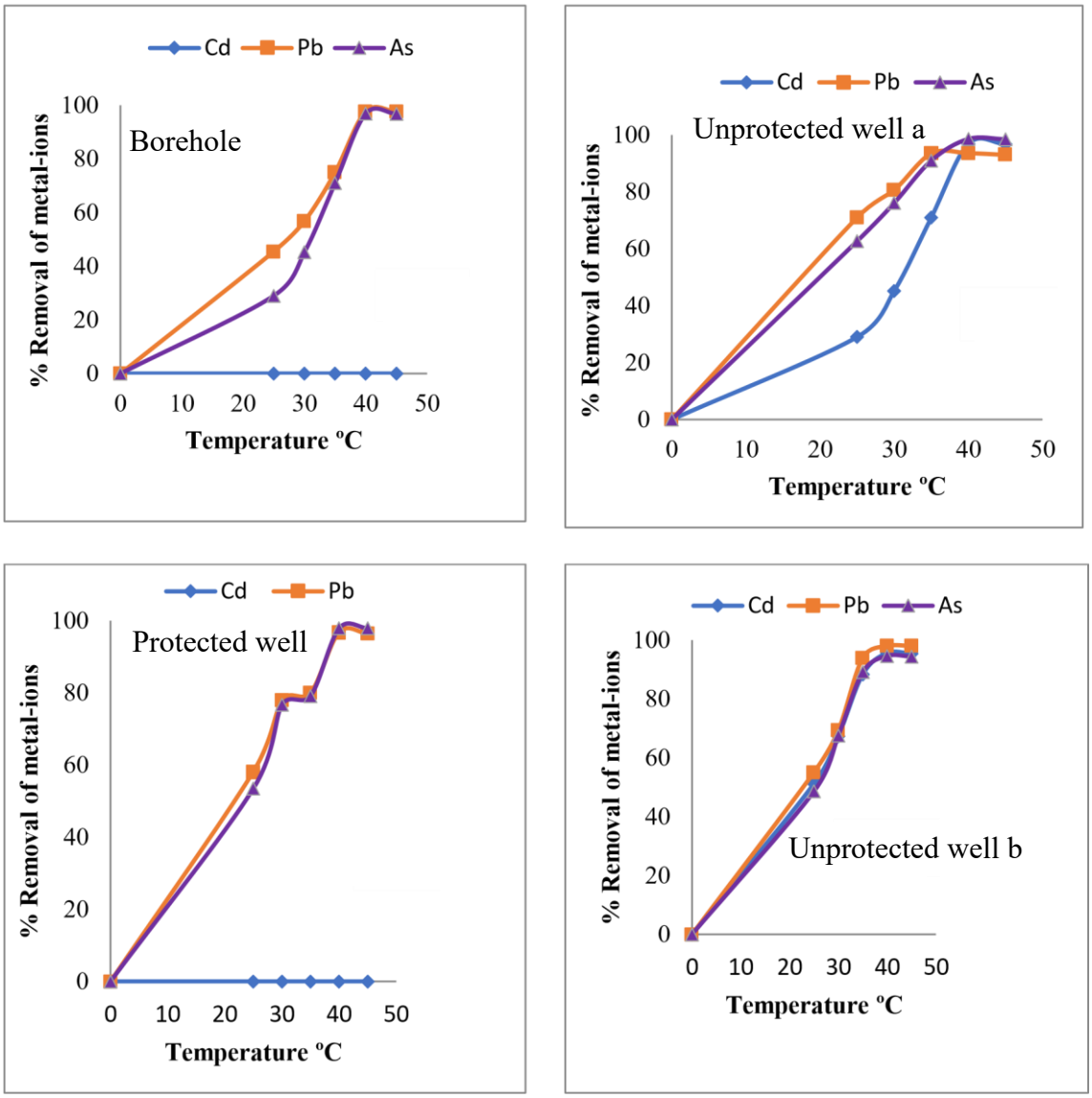

Figure 4.10: Temperature effect on adsorption of As, Cd and Pb

Further increase in temperature progressively increased the quantity of Cd ions removed. Adsorption continued until 93.5 % (0.030 mgL^{-1}) and 93.0 % (0.040 mgL^{-1}) of Cd were eliminated from water sampled from Unprotected $well_a$ and Unprotected $well_b$ respectively as the temperature increased to 45 ºC.

Similarly, Pb ions removed from water sampled from Borehole, Unprotected $well_a$, protected well and unprotected $well_b$ increased from 45.5 % (0.020 mgL^{-1}), 62.7 % (0.042 mgL^{-1}), 58.2% (0.032 mgL^{-1}) and 48.8% (0.027 mgL^{-1}) respectively at 25ºC to 97.7 %

(0.043 mgL^{-1}), 98.6 % (0.066 mgL^{-1}), 98.1% (540 mgL^{-1}) 96.8 % (0.048 $mgL^{-}1$) at the optimum temperature of 40 ºC (Figure4.10). The amount of Pb ions removed in borehole (0.042 mgL^{-1}), unprotected $well_a$ (0.065 mgL^{-1}), protected well (0.053 mgL^{-1}) and unprotected $well_b$ (0.048 mgL^{-1}) reduced to a very minimal extent with temperature increase of 5°C; 95.5 % to 95 %; 98.5 % to 98 %; 96.4 % to 96 % and 96.8 %.

The proportion of As ions also went up quite significantly: 29.0 % (0.090 mg/L^{-1}) to 96.7 % (0.030 mgL^{-1}) of water sampled at Borehole, 21.9 % (0.070 mgL^{-1}) to 97.9 % (0.031 mgL^{-1}) of water sampled at $well_a$, 53.5 % (0.023 mgL^{-1}) to 97.9 % (0.042 mgL^{-1}) An additional incremental temperature to a level of 45°C led to a slight cutdown of the amount of As ions eliminated in Borehole (93.5 %, 0.029 mgL^{-1}), unprotected $well_a$ (97.5 %, 0.034 mgL^{-1}), protected well (95.4 %, 0.031 mgL^{-1}) and unprotected $well_b$ (96.4 %, 0.034 mgL^{-1}) (Abdel et al., 2015; Liu et al., 2017; Zhu et al., 2023).

The amount of metal ions extracted by the activated avocado seed increased proportional with the increase in the temperature (Abdel et al., 2015). The observation is in line with that of a prior study (Liu et al., 2017), which showed that metal ions bonded the activated avocado seeds at moderately high temperatures rapidly. The migration of metal ions to the avocado seed surfaces could have proceeded much faster at high temperatures of thermal energies (Zhu et al., 2023). As a result, the slow decreasing rate of metal-ion removal above the maximum temperature (40°C) could possibly be ascribed to possible deterioration of the surfaces that would adversely decrease the adsorption capacity on the activated avocado seeds (Liu et al., 2017). The observed reduction in the quantities of metal ions removed by the activated avocado seeds may also have been due to weakening

of the adsorptive forces between the active sites of the activated avocado seeds and the metal ions during the adsorption process as (Kumari & Singh, 2019; Abdel et al., 2015).

4.6 Data Modelling

Adsorption isotherms were used to describe the adsorption equilibrium data obtained by the uptake of As, Cd and Pb ions onto the surface of the activated avocado seeds. Langmuir and the Freundlich isotherm models have been used by several researchers to interpret adsorption of heavy metals onto different adsorbents, as reported by Jimoh et al. (2011), Gorzin et al. (2013), Asare et al. (2018) and Asare et al. (2021). In this study, Langmuir and Freundlich isotherm models were applied to the adsorption of As, Cd and Pb ions on activated avocado seeds. The equilibrium data generated were presented graphically using linear versions of the Langmuir and the Freundlich isotherm models (Figures 4.11 and 4.12).

4.6.1 Langmuir isotherm

The Langmuir isotherm model describes monolayer adsorption of contaminants onto distinct localised adsorption sites on the surfaces of the adsorbent (Bulut et al., 2007; Liu et al., 2017; Ho, et al., 1999). Arsenic (As), cadmium (Cd) and lead (Pb) were adsorbed onto fixed adsorption sites with the same energy (homogeneous adsorption surface) on the surface of the activated avocado seeds used in a similar study by Liu et al., (2017).

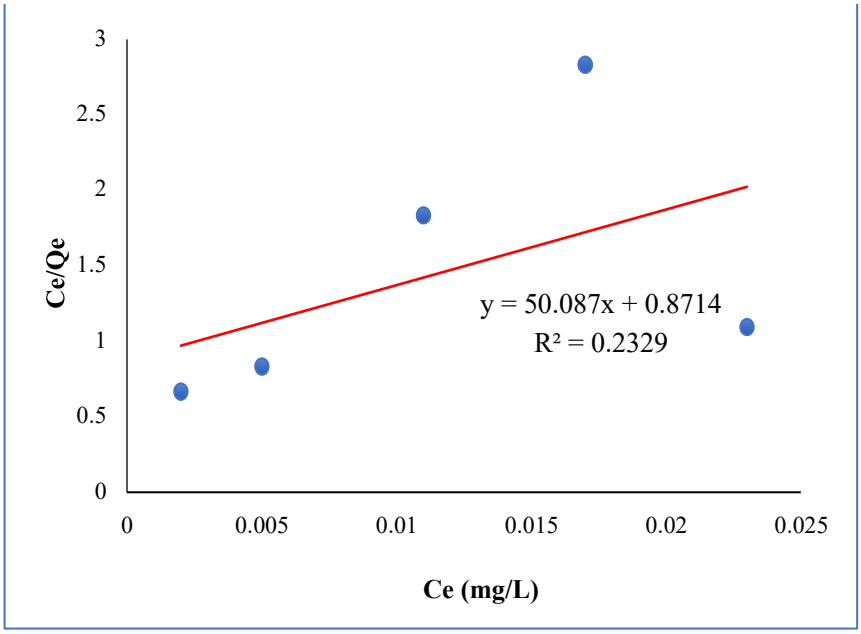

Figure 4.11: A plot of Langmuir isotherm for equilibrium data obtained from activated avocado seeds produced

According to the observations made by Foo and Hameed (2010), the Langmuir adsorption isotherm asserts that no migration of metal ions takes place in the plane of the adsorption surfaces. Furthermore, it assumes a uniform distribution of the adsorbing energy on the metal ions at the homogenous surface of the activated carbon. This principle is widely applied in metal adsorption studies (Ho & McKay, 1999; Abdel et al., 2015; Edet & Ifelebuegu, 2020)

The linearized Langmuir isotherm produced a straight line when Ce/Qe was plotted against Ce (Figure 4.11). The slope and intercept were used to calculate the values of qm (maximum amount of metal ions removed) and b (Langmuir isotherm constant) in accordance with standard procedures reported by by Onundi et al., (2010); Ho & McKay (1999); Foo & Hameed (2010) and Edet & Ifelebubuegu (2020). The resulting parameters derived from the linearized plot (Figure 4.11), i.e., adsorption energy, b (l/mg), maximum

adsorption capacity, qm (mg/g), and the associated coefficient of determination (R^2) are presented in Table 4.7.

Table 4.7 : Langmuir Isotherms Parameters determined for As, Cd and Pb adsorption study

		Langmuir Isotherm Parameters		
Sample	Metals	b (L/mg)	q_m (mg/g)	R^2
BH	Pb	57.5	0.020	0.232
	As	552	0.007	0.550
UWa	Cd	17.2	0.023	0.120
	Pb	5.35	0.161	0.331
	As	48.6	0.006	0.436
PW	Pb	14.0	0.066	0.060
	As	37.9	0.011	0.353
UWb	Cd	0.939	0.841	0.001
	Pb	22.5	0.050	0.131
	As	109	0.016	0.771

BH = Bore hole, UWa = Unprotected well (a-type), PW = Protected well and UWb = Unprotected well (b-type)

The values obtained for Langmuir constant (b) (Lmg^{-1}) on equilibrium data for Borehole were 57.5 Lmg^{-1} (Pb) and 552 Lmg^{-1} (As) (Table 6). The corresponding values of R^2 were 0.233 (Pb) and 0.550 (As). Also, the Langmuir constants (b) of the unprotected well-water samples were as follows: 17.2 Lmg^{-1} (Cd), 5.35 Lmg^{-1} (Pb) and 48.6 Lmg^{-1} (As). The R^2 were 0.119 (Cd), 0.331 (Pb) and 0.436 (As) (Table 6). For protected well, the Langmuir isotherm constants were 14.0 Lmg^{-1} (Pb) and 37.9 Lmg^{-1} (As) and R^2 were 0.060 (Pb) and 0.353 (As) (Table 6). The data obtained for the unprotected $well_b$ had Langmuir constant (b) 0.939 Lmg^{-1}(Cd), 22.5 Lmg^{-1} (Pb) and 109 Lmg^{-1} (As) and R^2 via the linear form of Langmuir isotherm model were 0.001 (Cd), 0.131 (Pb) and 0.771 (As)

(Table 4.7). These high values of Langmuir constants (b) indicate that the activated avocado seeds produced had strong affinity for As, Cd and Pb ions as reported in similar studies (Abdel et al., 2015; Edet & Ifelebuegu, 2020; Onundi et al., 2010; Ho & McKay, 1999). However, the high value of the Langmuir constant (b) and the negative maximum adsorption capacity for (q_m) for both unprotected and protected well water sources indicated that the Langmuir isotherm did not adequately describe the adsorption behaviour of As and Pb in the analysed samples as reported in a similar study by Abdel et al., (2015).

4.6.2 Freundlich isotherm

To examine whether the process of metals adsorption took place on definite adsorptive sites of heterogeneous adsorptive surface and to explain the heterogeneous distribution of energies that are related to these sites, the Freundlich model of the isotherm was used. Through this isotherm, adsorption of the metal ions on the activated avocado seeds was evaluated to justify whether a multilayer adsorption mechanism was present, as alluded to earlier by Edet & Ifelebuegu (2020); abdel et al., (2015); Onundi et al., (2010); Foo & Hameed, (2010).

A plot of log Qe against log Ce yielded a straight line (Figure 4.12) from which the constants (n and k) were determined from the slope and intercept respectively as done in similar studies by Abdel et al., (2015); Ho & McKay, (1999); Edet & Ifelebuegu (2020). From the linearized Freundlich isotherm model (Figure 4.12), the adsorption parameters including the Freundlich constants (k_f, mg/g), the adsorption intensity (n), which reflects the favorability and heterogeneity of the adsorption process, and (R^2), which indicates

the goodness of fit of the model, were calculated. The computed values are presented in Table 4.8.

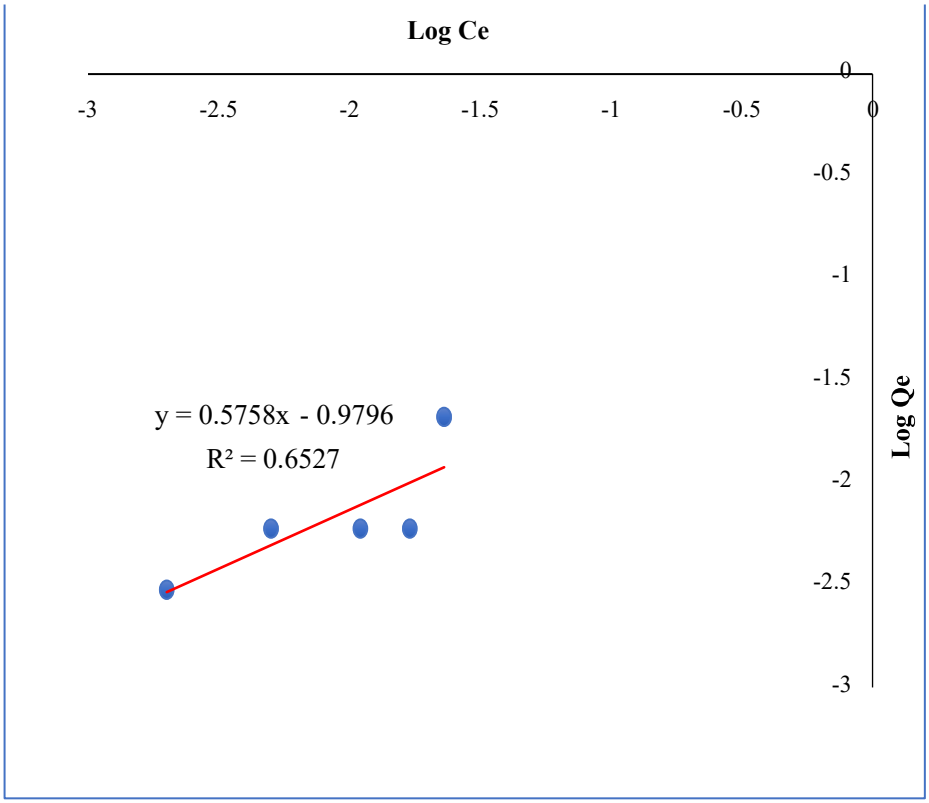

Figure 4.12: Freundlich isotherm plot for adsorption of selected metals onto activated avocado seeds

The Freundlich constants (k_f) calculated on the adsorption equilibrium data (Table 4.8) of Borehole were 9.54 mgg^{-1} (Pb), and 4.87 mgg^{-1} (As). The respective values of R^2 were 0.653 (Pb) and 0.758 (As). The Freundlich isotherm constants of Unprotected $Well_a$ water samples, determined at 219 mgg^{-1} (Cd), 1.08 mgg^{-1} (Pb), 48.5 mgg^{-1} (As) and the coefficient determinations (R^2) 0.179 (Cd), 0.989 (Pb) and 0.256 (As) were calculated (Table 4.8).

Table 4.8: Freundlich Isotherm Parameters determined for As, Cd and Pb adsorption study

Freundlich Isotherm Parameters				
Sample	Metal	k_F (mg/g)	n	R^2
BH	Pb	9.54	1.740	0.653
	As	4.87	0.405	0.758
UWa	Cd	219.00	0.614	0.179
	Pb	1.080	0.968	0.989
	As	48.50	3.24	0.256
PW	Pb	3.780	1.340	0.738
	As	25.30	2.700	0.264
UWb	Cd	14.70	0.659	0.979
	Pb	11.00	1.980	0.663
	As	9.810	1.800	0.889

BH = Bore hole, UWa = Unprotected well (a-type), PW = Protected well and UWb = Unprotected well (b-type)

As explained by equilibrium data, activated avocado seeds had Freundlich constants (k_f) of 3.780 mgg^{-1} (Pb) and 25.30 mgg^{-1} (As) with R^2 of 0.738 (Pb) and 0.264 (As) applied to the water samples taken in the Protected well. The measured removals of metal ions, from Unprotected $well_a$, allowed calculation of the Freundlich constants (k_f) of 14.70 mgg^{-1} (Cd), 11.00 (mgg^{-1}) (Pb) and 9.810 (mgg^{-1}) (As) with R^2 of 0.979 (Cd), 0.663(Pb) and 0.889 (As).

When the same methodology was applied on a different water source, i.e., Unprotected $well_b$, Freundlich constants and coefficients of determination were obtained as 12.50 mgg^{-1} (Cd), 19.30 mgg^{-1} (Pb) and 9.170 mgg^{-1} (As) with R^2 0.663 (Cd), 0.771 (Pb) and 0.889 (As).

This observation shows that adsorption of selected metal ions on activated avocado seeds is a distinguishable phenomenon and thus, makes the biomaterial a good bio-adsorbent of these pollutants in aqueous environments.

The coefficients of determination Freundlich were usually higher than the ones connected with the Langmuir isotherm model. Freundlich Linear determinations (R^2) were in the range of 0.264 to 0.738 with the Protected well data and 0.179 to 0.989 with the Unprotected $well_a$ data, 0.663 to 0.979 with the Unprotected $well_b$ data, 0.653 to 0.758 with the Borehole data, whereas Langmuir R^2 ranged between 0.353 to 0.604 with the Protected well. The Freundlich isotherm constants (k_f) estimated for the equilibrium adsorption data recorded in this study (Table 4.8) were also generally higher than the corresponding Langmuir isotherm constant (b) (Table 4.7). Freundlich constant (k_f) falls in the following ranges: 4.870 to 9.540 mgg^{-1} (borehole), 1.080 to 219.0 mgg^{-1} (unprotected $well_a$), 3.780 to 25.30 mgg^{-1} (protected well) and 11.00 to 14.70 mgg^{-1} (unprotected $well_b$). Langmuir constant (b) values ranged between 57.50 and 552 mgL^{-1} (borehole), 5.350 and 48.60 mgL^{-1} (unprotected $well_a$), 37.90 and 14.00 mgL^{-1} (protected well) and 22.50 to 109.0 mgL^{-1} (unprotected $well_b$) (Table 4.7).

The estimated coefficient of determination R^2 of each adsorption isotherm shows that the Freundlich isotherm model gives a better fit with the experimentally developed values compared with the Langmuir isotherm model, similar to the study done by Abdel et al., (2015). This is evidenced by the R^2 values of the Freundlich isotherm being much closer to unity than those of the Langmuir isotherm. Also, the best fit of the Freundlich isotherm model to describe the experimental data indicates that the examined metal ions were

absorbed on the heterogeneous surface of the activated avocado seed, and these findings are confirmed by the expert work of Abdel et al., (2015) and Foo & Hameed, (2010).

4.7 Kinetics Modelling of the Adsorption Process

The evaluation of the kinetic process provides useful information with regard to the mechanism of adsorption as well as the step that ultimately dominates the total adsorption process. The given issue can be well summarized in Gorzin and Ghoreyshi (2013).

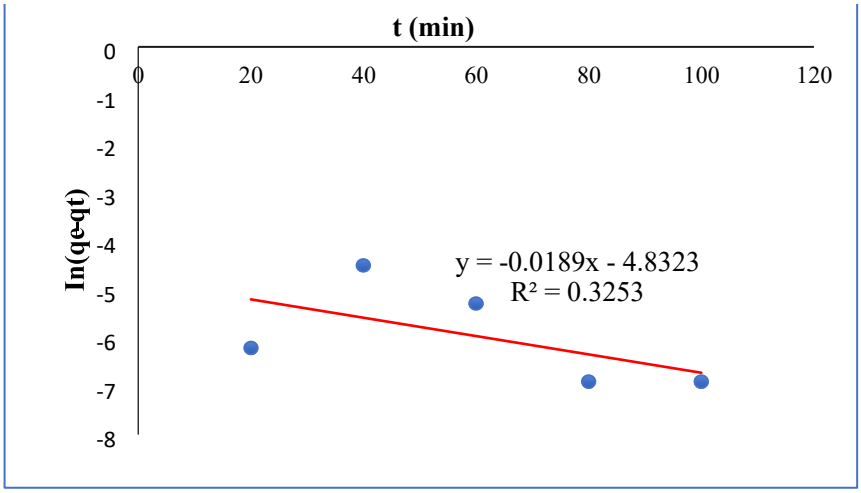

***Figure 4.13: First order pseudo kinetic plot for adsorption of Cd, Pb and As onto* activated avocado seeds**

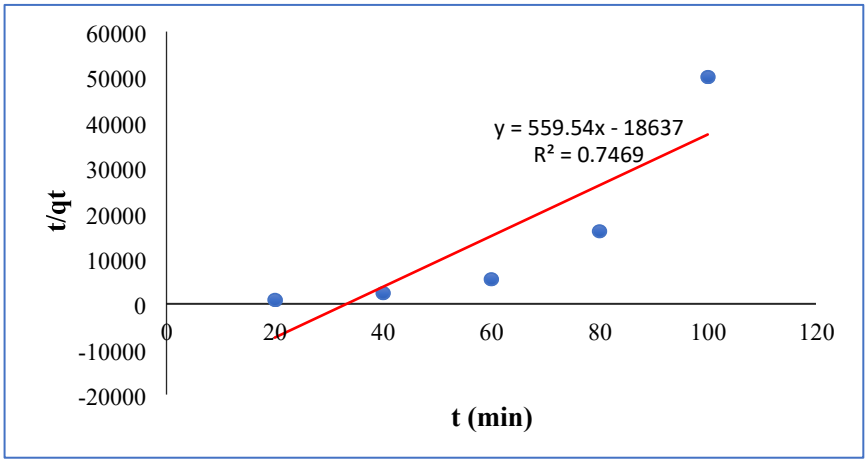

Figure 4.14: Second order pseudo kinetic plot for adsorption of As, Cd and Pb onto activated avocado seeds

To study the kinetics process in the adsorption of the selected metals onto the activated avocado seeds, the use of, the pseudo-first-order kinetic model and the pseudo-second-order model was employed as used by Bulut & Tez, (2007); Febrianto et al., (2009) and Ho & McKay, (1999). The pseudo-first-order model is applicable to the process of physical adsorption, where weak forces are present between the metal ions and adsorbent surfaces (Bulut & Tez, 2007); the association of this model is thoroughly reported by Plazinski et al., (2009). The plot of ln (qe - qt) against time was linear as illustrated in Figure 14 and the equilibrium adsorption capacity (qe) and the rate constant (k_1) were calculated using the intercept and the slope of the plot, following similar protocol by Bulut & Tez, (2007) and Febrianto et al., (2009). The estimate of equilibrium concentration of Cd ions was measured at 0.152 mgg^{-1} (Unprotected $well_a$) and 0.020 mgg^{-1} (Unprotected $well_b$) and R^2 was 0.293 (Unprotected $well_a$) and 0.004 (Unprotected $well_b$). Upon application of pseudo-first-order, it was predicted that the Cd removals would be 0.008mgg^{-1} (borehole), 0.0002 mgg^{-1} (Unprotected $well_a$), 0.001 mgg^{-1} (Protected well) and 0.003 mgg^{-1} (Unprotected $well_b$) with respective R^2 values of 0.325, 0.374, 0.490 and 0.426 respectively. Similar findings were achieved with Pb ions in which the model was able to predict that the removals will be 0.0003 mgg^{-1} (borehole), 0.00001 mgg^{-1} (Unprotected $well^a$), 0.0004 mgg^{-1} (Protected well), and 0.0002 mgg^{-1} (Unprotected $well_b$) with R^2 values 0.463, 0.442, 0.567, and 0.403, respectively (Table 8). Similarly, the first order pseudo kinetic model again predicted amounts of As ions removed from the water sampled for this study to be 0.279 mgg^{-1} (Borehole), 0.034 mgg^{-1} (Unprotected $well_a$), 0.006 mgg^{-1} (Protected well) and 0.010 mgg^{-1} (Unprotected $well_b$) with coefficient of determinations of 0.921 (borehole), 0.856 (Unprotected $well_a$), 0.044 (Protected well) and 0.044 (Unprotected $well_b$) (Table 8), using first order pseudo kinetic model.

Table 4.9: Estimated parameters of first and second order pseudo kinetic models for As, Cd and Pb Uptake by Activated avocado seeds

Sample	Metal	Initial Conc. (mg. g^{-1})	Pseudo-first-order				Pseudo-Second-order		
			qe, exp (mg. g^{-1})	K1 (min^{-1})	qe,cal (mg. g^{-1})	R^2	K 2 ($gmg^{-1}min^{-1}$)	qe,cal (mg. g^{-1})	R^2
BH	Pb	0.044	0.003	0.019	0.008	0.325	0.002	0.173	0.747
	As	0.031	0.010	0.031	0.028	0.921	0.002	0.179	0.859
UWa	Cd	0.031	0.010	0.048	0.152	0.293	0.002	0.227	0.971*
	Pb	0.067	0.020	0.058	0.0002	0.374	0.002	0.174	0.760
	As	0.032	0.030	0.035	0.034	0.856	0.002	0.175	0.763*
PW	Pb	0.055	0.020	0.053	0.001	0.490	0.001	0.166	0.626
	As	0.043	0.040	0.016	0.006	0.044	0.002	0.174	0.790
UWb	Cd	0.043	0.010	0.067	0.020	0.004	0.002	0.182	0.886
	Pb	0.049	0.040	0.005	0.003	0.426	0.001	1.660*	0.629
	As	0.037	0.020	0.022	0.009	0.440	0.001	0.169*	0.707

Note: BH = Bore hole, UWa = Unprotected well (a-type), PW = Protected well and UWb = Unprotected well (b-type)

Equilibrium adsorption data were also examined using 2nd order pseudo kinetic model whereby the 2nd order pseudo kinetic rate constant (k_2) and the calculated values of As, Cd and Pb ions removed (qecal), was computed based on the values obtained from the plot (Figure 4.14). The model-estimated levels of Cd ions removal were 0.227 mgg^{-1} (Unprotected $well_a$) and 0.182 mgg^{-1} (Unprotected $well_b$), with the corresponding R^2 value of 0.885 (Unprotected $well_a$) and 0.971 (Unprotected $well_b$) (Table 4.9). The predicted amounts of Pb ions removed at equilibrium from water samples using the second order pseudo kinetic model plot (Figure 4.14) were 0.173 mgg^{-1} (Borehole), 0.174 mgg^{-1} (Unprotected $well_a$), 0.166 mgg^{-1} (Protected well) and 1.66 mgg^{-1} (Unprotected $well_b$) whilst the associated coefficient of determination (R^2) were 0.747 (Borehole), 0.760 (Unprotected $well_a$), 0.626 (Protected well) and 0.629 (Unprotected $well_b$) (Table 4.9). The calculated quantities of A s ions removed at equilibrium

from water sampled for this study were found to be 0.179 mgg^{-1} (Borehole), 0.175 mgg^{-1} (Unprotected $well_a$), 0.174 mgg^{-1} (Protected well), 0.169 mgg^{-1} (Unprotected $well_b$) with corresponding coefficient determination (R^2) were 0.859 (Borehole), 0.763 (Unprotected $well_a$), 0.790 (Protected well) and 0.707 (Unprotected $well_b$) (Table 4.9). The second-order pseudo kinetic plot (Figure 4.14) provided coefficients of determination (R^2) values that were greater than the corresponding values representing the first-order pseudo kinetic plot (Figure 4.13) in all of the metals. However, the second-order pseudo-kinetic model, which had the coefficients of determination approaching unity, fitted better (Bulut et al., 2007) and Ho & McKay, (1999).

Most of the findings obtained in the current kinetic study were also consistent with those given by Gorzin & Ghoreyshi (2013) and Edet & Ifelebuegu (2020). Because the second-order pseudo model is based on the assumption that adsorption is chemisorption-controlled, which is supported by Plzinski et al. (2009). The good fit between the second-order pseudo model and the equilibrium adsorption data collected in the current study justifies the argument that adsorption of As, Cd, and Pb ions onto the activated avocado seeds was occurring via chemisorption was created between the activated avocado surface and the adsorbed ions throughout the adsorption process (Bulut & Tez, 2007).

4.8 Thermodynamics Analysis

Thermodynamic analysis was conducted to investigate the scientific viability of using an adsorption technique on water polluted with heavy metals, as done by Jock et al. (2018). A Van 't Hoff plot was made from the obtained data to determine $\Delta G°$ $\Delta S°$, and $\Delta H°$; following a similar protocol by Haghighi & Irannajad (2021); Jock et al. (2018), Edet & Ifelebuegu (2020). The plots of In Kd against 1/T produced straight lines (Fig.

4.15) and provided data that were used to obtain values of these parameters (Table 4.10). The standard Gibbs free energy change of each metal was within the range of -9.59 to -6.00 kJ/mol with a favourable trend of the borehole water towards adsorption (Table 4.10). The results of negative values of ΔG^{o} prove the viability of the processes of adsorbing heavy metals as discussed in Gorzin & Ghoreyshi (2013); Asare et al. (2018); Edet & Ifelebuegu (2020); Zhang et al. (2020).

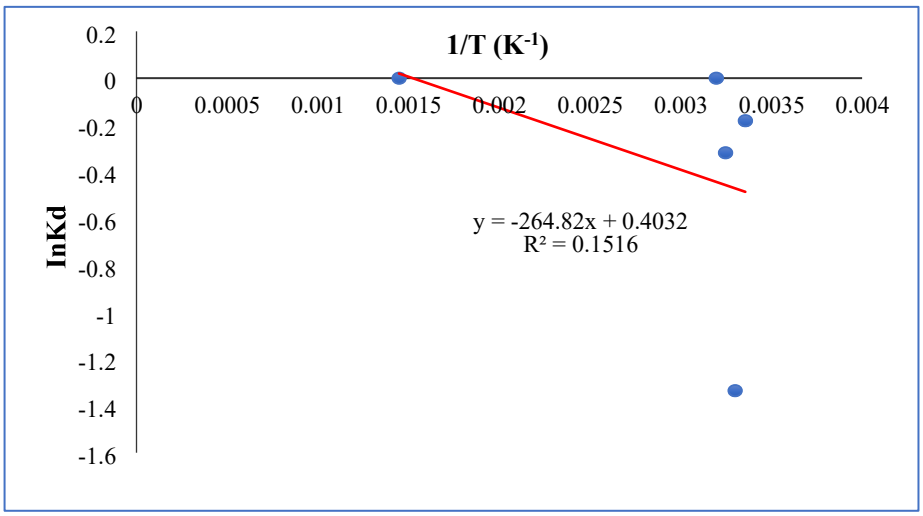

Figure 4.15: Van't Hoff plot for thermodynamic parameters determination.

Table4. 9: Thermodynamic Parameters for the Adsorption of As, Cd and Pb Activated avocado seeds

Sample	Metals	Initial Conc. Mg/L	ΔH ($kJ \cdot mol^{-1}$)	ΔS ($kJ \cdot mol^{-1}K^{-1}$)	ΔG ($kJ \cdot mol^{-1}$)	R^2
BH	Pb	0.044	-2.20	0.003	-3.20	0.152
	As	0.031	-5.37	0.014	-9.59	0.358
UWa	Cd	0.031	-1.12	0.002	-1.65	0.031
	Pb	0.067	-3.13	0.010	-6.23	0.118
	As	0.032	-6.33	0.002	-1.11	0.005
PW	Pb	0.055	-1.66	0.002	-2.31	0.019
	As	0.043	-46.3	0.001	-8.31	0.146
UWb	Cd	0.043	-19.8	0.008	-4.49	0.160
	Pb	0.049	-0.98	0.002	-1.45	0.021
	As	0.037	-0.003	0.0002	-0.06	0.0000003

BH = Bore hole, UWa = Unprotected well (a-type), PW = Protected well and UWb = Unprotected well (b-type)

This finding also proves that the adsorption mechanisms of the metal ions under investigation were spontaneous and agree with the results provided by Jock et al. (2010); Haghighi & Irannaja (2021).

The standard enthalpy change (ΔH°) measured during the adsorption of both metals was between negative three kilojoules per mole (unprotected $well_b$) and a negative one kilojoule per mole (unprotected $well_a$) (Table 4.10). The adsorption in question was exothermic as the values of ΔH, as cited by Jock et al. (2018) and Edet and Ifelebuegu (2020), were negative.

Table 4.10 shows standard changes of entropy (ΔS°) during the adsorption process. These values were between 0.0002 kJmol-1K-1 (Unprotected $well_b$) and 0.0104 $kJmol^{-1}K^{-1}$(Unprotected $well_a$). The positive values of the ΔS° show that at the boundary of activated avocado seeds and water, a higher speed of movement of the metals to available sites of the surface of the activated avocado seeds occurred. The findings of this study can be aligned with the results of Asare et al. (2021) and prove the fact that the activated avocado seeds used have good affinity towards the metals under study. As a result, the activated avocado seeds may serve as a potential adsorbent for exhausting high levels of metal contaminants in the water systems. The findings collected during this research are favourable to the findings of Gorzin & Ghoreyshi (2013), Asare et al. (2018), and Asare et al. (2021).

CHAPTER FIVE

SUMMARY, CONCLUSION, AND RECOMMENDATIONS

Chapter five involves a summary of the work, a conclusion, and suggestions to be made concerning future research works.

5.1 Summary

This study was conducted to develop activated avocado seeds, characterise the activated avocado seeds, and use them to remove As, Cd, and Pb from groundwater sources obtained from Sefwi Wiawso and its surrounding towns.

The activated avocado seeds were produced using a physical activation method on washed and dried avocado seeds. This activation was done at 60ºC for 24 hours, and the granular activated avocado seeds were grounded and bagged in polythene ziplock bags, sealed tightly, and then stored.

The analysis of activated carbon avocado seed surface properties was studied.
Before and after use of the activated avocado seeds in the metals adsorption, JSM-6380 (USA) SEM-XRF, Rigaku NEX CG II (USA) X-ray fluorescent spectroscopy, and Shimadzu, IR Affinity1 (Japan) Fourier Transform Infrared spectroscopy were taken. The pore size, volume, and the functional groups composition of the activated avocado seeds were characterised through the conduction of surface characterisation studies, as done in a similar study by Molina-Balmaceda et al. (2024).

Probe determinants were also used to carry out a determination of physico-chemical parameters (Temperature, pH, Electrical conductivity, Total dissolved solids, and

Turbidity) in various samples (Hadzi et al., 2015). This was performed to assess the physical characteristics of samples incorporated in the present research (Hadzi et al., 2015). The capability of the activated avocado seeds to adsorb water contaminants under different conditions was also determined by an adsorption study, as done in a similar study by Gomez-Naranjo et al. (2024). The time impact, different amounts of adsorbent, pH, and temperature on the system phenomenon of metals were determined (Leite et al., 2018).

The adsorption data were modeled using Langmuir and Freudlich isotherm equations by following the same protocol as in Bulut & Tez (2007); Febrianto et al. (2009). Kinetic studies were conducted using pseudo-first-order and pseudo-second-order models (Bulut et al., 2007) and Ho & McKay (1999).

Thermodynamic parameters, including standard enthalpy change, standard entropy change, and standard Gibbs free energy change, were estimated using the Van't Hoff plot to analyse the process (Haghighi & Irannajad, 2021; Jock et al., 2018). Isotherm equations of Langmuir and the Freundlich adsorption were used to model the data obtained on the basis of the adsorption study. Pseudo-first-order and pseudo-second-order kinetics models have been applied to establish the kinetics of the adsorption process. The activated avocado seeds had an irregular, elongated, and porous surface of different sizes and shapes before use, as seen from SEM images taken. This porous surface and its associated irregular surface projections contributed greatly to the As, Cd, and Pb metal uptake as indicated literature Hussein et al., 2015; Buah et al., 2016; Anyika et al., 2017). However, the morphological structures of the activated avocado seeds were modified into relatively smooth surfaces after they had been used in the

adsorption process. This observed surface smoothness resulted from the surface coverage of the activated avocado seeds by the metals adsorbed, as reported by Hussein et al. (2015).

The EDX spectrum of the activated avocado seeds demonstrated that carbon, potassium, and oxygen atoms were present, because they were found to constitute the predominant elemental components. The metals are immobilised by the Carbon constituent of the activated avocado seeds in ambient conditions since they offer an adsorptive surface to the metals (Bashkova et al., 2005). Surface oxygen groups provide acidic carbon surfaces (Bandosz et al., 2006), which decompose to provide active sites at the edges of the graphene layer (Bandosz et al., 2006). Also, the potassium component combines with oxides and hydroxides of the aqueous phase to provide basic surfaces of the activated avocado seeds (Williams & Aydinlik, 2020). The basic surfaces of the activated avocado seeds enhance their adsorption capacity (Williams & Aydinlik, 2021). Therefore, carbon, potassium, and oxygen components would contribute to the effectiveness of the activated avocado seeds to adsorb metals as reported by Uddin & Nasar (2021). After the activated avocado seeds had been used, the EDX spectrum recorded showed changes in the elemental constituents of the activated avocado seeds, with calcium found to be a major elemental constituent.

The XRF results revealed that CaO (44.0 ± 0.01 mg kg-1) and SiO (24.3 ± 0.07 mg kg-1) were the major chemical constituents of the activated avocado seeds. The XRF Analysis also showed significant amounts of MgO (9.39 ± 0.12 $mgkg^{-1}$), SO_3 (8.56 ± 0.04$mgkg^{-1}$), Al_2O_3 (7.98 ± 0.11 $mgkg^{-1}$), and P_2O_5 (5.84 ± 0.04$mgkg^{-1}$) were present as chemical constituents of the activated avocado seeds. High lime (CaO) content was also found in the activated avocado seeds, and that signifies that the activated avocado

seeds have high neutralizing capacity for acidic effluents and thus have the ability to also precipitate metals as indicated by Shirin et al. (2021).

Aluminium oxide, silicon oxides, Iron (III) oxide, and Magnesium oxide components of the activated avocado seeds played major roles in precipitation and contaminant transport in the adsorption process of As, Cd, and Pb metals as reported by Dove et al. (2005); Goldberg et al. (2007). Sulphur trioxide and Phosphorus pentoxide components, of the activated avocado seeds, also provided negative surface charge characteristics, which enhanced the adsorption capacity of the metal ions on the activated avocado seeds as reported by Choi et al. (2009) and Kuang et al. (2020).

Thus, Al_2O_3, CaO, MgO, P_2O_5, SiO_2, and SO_3, components of the activated avocado seeds used in this study, were revealed as key chemical constituents, and they contributed to the elimination of the selected metals in the samples treated. Changes in the amounts of the constituent oxides of the activated avocado seeds were observed after they had been used in the metal's adsorption process. Except for the Iron (III) oxide, the quantities of the other chemical constituents decreased gradually after the application. These observed properties were attributed to the interaction of the oxides with the metals as reported by Ezeokonkwo et al. (2018). The interactions might have caused the metals to be deposited onto the porous surface structures of the activated avocado seeds for attachment and removal.

The XRF analysis of the activated avocado seeds used showed 12 elemental constituents before use and 19 elemental components after the adsorption process. The elemental As, Cd, and Pb constituent elements were not detected to have absorption

elements in activated avocado seeds during this experiment, before use in the adsorption system of metals. Nonetheless, according to the XRF report on the activated avocado seeds [as the material used in the adsorption process], the elemental composition revealed Lead, Vanadium, Chromium, Thallium, Tantalum, and Antimony as the constituents of the activated avocado seeds. Zirconium, scandium, and chlorine were observed to be the major elemental constituents, whilst Rubidium, Titanium, Strontium, Zinc, Tin, and Tellurium were also found to be the minor elemental constituents of the activated avocado seeds after their use. The XRF analysis of the avocado seeds showed changes in the concentrations of its elemental components after its use in the adsorption process. These changes could be due to the surface coverage of the activated avocado seeds by metals in the investigated samples.

The activated avocado seeds exhibited a weak broad absorption at 3338.83 cm^{-1} as a result of the stretching vibration of the O-H bond in the hemicellulose structure (Abidi et al., 2014). A strong and sharp absorption band at 2925.13 cm^{-1} is also ascribed to the stretching vibration of C-H bonds in alkanes as denoted by Adegoke et al. (2017). An aromatic overtone at 2000 cm^{-1} was also blamed on the presence of aromatic functional groups in the hemicellulose structure as reported by Nanda et al. (2013) and Azargohar & Dalai (2006). A very intense and sharp infrared band centred at 1589.91 cm^{-1} was absorbed, which was attributed to the C=O stretching vibrations of the hemicellulose (Azargohar & Dalai, 2006). Weak and sharp absorption at 1506.58cm^{-1} was assigned to the C-C stretching of functional groups aromatic in the structure of hemicellulose, whilst the sharp and strong absorption band observed at 1031.97cm^{-1} was assigned to C-O stretches linked to the holocellulose and lignin structures as indicated by Azargohar & Dalai (2006).

The product of the activated avocado seeds also had carbonyl, hydroxyl, and aromatic functional groups, which were also present on the surface of activated carbon that was used in similar research by Abidi et al. (2014). Although the FTIR on the activated seed of the avocado after the metal's adsorption process displayed absorption bands resembling the same as before the use of the activated avocado seed, the bands shifted. These shifts in positions of the absorption peaks in the FTIR spectrum of the used avocado seeds were attributed to metallic interaction with the various functional groups on the activated avocado seeds (Abidi et al., 2014).

The physico-chemical parameters tested in the samples employed had their values below the allowable limit prescribed by WHO, except for turbidity. Unprotected wellb water samples had the highest temperature, and it ranged from 29.8± 0.02 to 30.3 ± 0.05 ºC. It was obvious that the elevated temperatures might have resulted from direct exposure of the Unprotected well water sources to the sunlight. An increase in the rate of chemical reactions within the Unprotected well water sources could have also accounted for the elevated temperatures of the waters. The temperature rise observed for the Unprotected well water sources could only promote the growth of microorganisms, which would impair the quality of drinking water as reported by Nkansah et al. (2010).

Except for two of the water samples (Borehole 3 and protected well 1), the pH of the samples was generally within the 6.5-8.5 permissible limit for human consumption. The water sources had low pH, and they ranged from 5.50 ± 0.08 to 6.46 ± 0.08. The low pH could be attributed to the leaching of sulphate ions from fertilizers and pesticides from observed nearby cultivated farmlands into the groundwater at the

sampling site. The low pH of the water might have also originated from moving effluent released into the environment by galamsey operators, as stated by Ismaila et al. (2017). The overall Mean turbidity (189.0 NTU) value of the sample was deemed above the WHO allowable limit of 5 NTU. There were high turbidity values recorded for Unprotected well$_b$ and protected well water sources, which may be due to surface run-off from nearby farmlands observed at galamsey sites into the water bodies. Electrical conductivities determined on the water samples were generally low compared to the 400 μS/cm set by WHO (WHO, 2022). Generally, TDS values of the water samples used in this study were lower than the 500 mg/L WHO permissible level (WHO, 2022). Although TDS were low, it was possible that farming and mining activities noticed at the sampling site led to some TDS addition as noted in the water sources (Hao et al.,2024; Wang, 2021). The levels of arsenic (As), cadmium (Cd), and lead (Pb) in the water generally exceeded the WHO, EC, and USEPA permissible levels (WHO, 2022; EC, 2024; USEPA, 2009) for drinking water, except Cd in boreholes and protected well waters. The elevated arsenic (As), cadmium (Cd), and lead (Pb) levels in the samples might have resulted from surface run-offs and seepage of the metals from nearby dumping sites, farmlands, and chemicals used in galamsey gold mining (Hilson et al., 2014; Armah et al., 2016; Bortey-Sam et al., 2015; Owusu-Nimo et al., 2018). The higher concentrations of these selected heavy metals in the water resources could be hazardous to human beings consuming the same (Tchounwou et al., 2012; Saha & Paul, 2019; Armah et al., 2010). As cadmium has been reported to cause prostate enlargement, still birth, low birth weights, spontaneous abortion, and others EhiEromosele & Okiei, 2012).

Consumption of high-level lead (Pb) contaminated water could damage the nervous and reproductive systems and the kidney, as well as long-term exposures to arsenic (As) via water could result in skin, bladder and lung cancer (Environmental Health Perspectives, 2013; Smith et al., 2017; USEPA & ATSDR, 2007-2012). It has been identified that contact time, adsorbent dosage, pH as well and temperature can positively affect the efficiency of the activated avocado seeds (Sulaiman et al., 2018). The highest percentages of removed metal by using the parameters studied were more than 90%.

The study of equilibrium adsorption data, using the Isotherm study, indicated Freundlich isotherm constants (kf), estimates (ranged between 1.08 mg/kg to 219), were usually higher than their Langmuir isotherm constants (b) (ranged between -5.35 and 552 L/mg). The Freundlich parameter of affinity constant (kf) demonstrated that the assimilation of As, Cd, and Pb metals with activated avocado seeds is a potential phenomenon. The avocado seeds that have been activated, therefore, serve as the prospective adsorption avenue towards absorption of arsenic (As), cadmium (Cd), and lead (Pb) ions in water bodies (Chimdessa &Ejeta, 2022; Mquehe-Nedzivhe et al., 2018). The estimated coefficient determinations (R^2) of the Freundlich isotherm model (ranged between 0.179 and 0.989) were, in most cases, nearer to 1 in comparison to that of the Langmuir adsorption isotherm model (ranged between 0.120 and 0.770). Accordingly, the Freundlich isotherm model fitted the experimental data better and therefore, the Freundlich isotherm model would best explain how the ion concentration of selected heavy metals at equilibrium is related to the amount of ion adsorbed by the activated avocado seeds (Abdel et al., 2015). The experiment also reveals that the ions

were adsorbed on the heterogeneous surface of the activated avocado seeds (Abdel et al., 2015).

The kinetic data revealed that the parameters predicted by the pseudo-second-order model corresponded more closely to the experimentally observed values than those predicted by the pseudo-first-order model (Bulut & Tez, 2007; Febrianto et al., 2009). This observation was supported by the coefficient of determination (R^2), which ranged from 0.626 to 0.971 for the pseudo-second-order model, while the pseudo-first-order model yielded a wider and less reliable range of 0.004 to 0.921. Consequently, the pseudo-second-order model was considered to provide a more accurate representation of the adsorption kinetics in the study (Bulut & Tez, 2007).

The second-order pseudo kinetic parameter fit of the adsorption generated in this study also denoted that metal-ion adsorption was chemisorption and fitted perfectly with one of the observations stated by Foo & Ahmeed (2010). In the thermodynamics investigation of this study, it was also possible to predict the standard change in the Gibbs free energy (ΔG°) of the adsorption process to have a negative value (Crini & Lichtfouse, 2019). The obtained negative values of ΔG°, produced by the metal ions, meant that the adsorption processes being studied by the researchers were possible (Haghighi & Irannajad,2021; Jock et al., 2018; Edet & Ifelebuegu, 2020)

The standard enthalpy change (ΔH°) approximated in the chosen metal ions in all the sources of water was negative. The negative nature of the ΔH° indicated that energy was lost when As, Cd and Pb ions got attached to the activated avocado seeds surfaces for removal Jock et al., (2018) The positive values of the ΔS° indicated the that there was an overwhelming displacement of the metal ions to the active sites on the surfaces

of the activated avocado seeds, which were employed during the adsorption process (Haghighi & Irannajad,2021; Jock et al., 2018); Edet & Ifelebuegu, 2020).

5.2 Conclusion

The study revealed that the activated avocado seeds have an affinity with the metals of As, Cd, and Pb. Activated avocado seeds possessed an irregular, elongated, uneven porous surface structure of various sizes and forms, which was revealed through surface characterisation. The activated avocado seeds yield similar chemical and elemental compositions, indicating that the resultant adsorbent is comparably more effective and efficient than other activated carbons in the market.

Both the chemical and physical characteristics of the samples under study were at admissible levels as per the WHO standard, except for turbidity (WHO, 2024). The metal levels of selected metals in the samples exceeded the WHO threshold, with the exception of Cd in the boreholes and the protected wells (WHO, 2022). The significant cause of these amounts of metals in the water samples that were examined was discovered to be the galamsey activities (Hilson et al., 2014; Armah et al., 2016; Bortey-Sam et al., 2015; Owusu-Nimo et al., 2018).

The adsorption tests carried out on As, Cd, and Pb also indicated that time impact, adsorbent quantity, pH, and temperature condition positively affected the efficiency of the activated avocado seeds (Mqehe-Nedzvhe et al., 2018). Under those optimum adsorption conditions, the maximum concentration of metals removed was more than 90% on each ion studied.

Adsorption isotherms modelling analyses were carried out to determine the equilibrium relationship between As, Cd, and Pb metals in the samples and their amounts that were removed using the activated avocado seeds, revealing that the Freundlich isotherm model was able to fit the experimental data rather than the Langmuir isotherm (Al-othman et al., 2018; Chimdessa & Ejeta, 2022). Kinetic studies revealed that the pseudo-second-order kinetics model fitted most perfectly to the data, hence could explain the mechanism of metals adsorption on the surface of the avocado seeds that had been activated prior to the avocado seeds being employed in the study in terms of As, Cd, and Pb metals (Al-othman et al., 2018; Chimdessa & Ejeta, 2022). This kinetic model also suggested that the chemisorption mechanism controlled the adsorption process of the study. Another observation made in the thermodynamics studies on As, Cd, and Pb demonstrated that the adsorption was a possible process since negative standard Gibbs free energy changes (ΔG°) were recorded (Mqehe-Nedzivhe et al., 2018). The standard enthalpy changes (ΔH°) computed on the adsorption process of the selected metals also reported that generated energy was lost by the activated avocado seeds-water system to the environment in the process of adsorbing metals (Chimdessa & Ejeta, 2022). The standard entropy change (ΔS°) estimated also indicated that there was a massive rush of the metals onto the surface of the activated avocado seeds to attach and detach Tan et al., 2008; Al-Othman et al., 2012; Chimdessa & Ejeta, 2022).

5.3 Recommendations

1 Even though the activated avocado seeds were very effective at removing selected metals from water resources at galamsey sites in Sefwi Wiawso and its environs, the scope of the galamsey sites was small. Hence, further

investigations by the water research institute and other research institutions should examine the adsorption capacity of the activated avocado seeds on heavy metal contaminants across the entire country.

2 A low-cost activated carbon must be produced by research institutions in Ghana from cocoa pods, since cocoa pods are the most abundant agricultural waste materials at galamsey sites in Ghana, and no study of that sort has been made.

3 Future study must be made by AAMUSTED research students to assess turbidity impact on metal-ion remediations in water resources using activated carbons, since most water resources observed at the galamsey sites had elevated turbidity due to galamsey activities.

4 I also suggested that the isotherm studies should be extended to other isotherm models on similar equilibrium data generated to obtain best best-fitted isotherm by future researchers.

5 Municipal and District Assemblies must investigate the proper disposal of activated carbons after use, since used adsorbents are a potential source of environmental contaminants.

REFERENCES

Abas, S. N. A., Ismail, M. H. S., Kamal, M. L., & Izhar, S. (2013). Adsorption process of heavy metals by low-cost adsorbent: a review. *World Applied Sciences Journal*, *28*(*11*), 1518-1530.

Abidemi, O. O. (2011). Levels of Pb, Fe, Cd and Co in Soils of Automobile Workshop in Osun State, Nigeria. *Journal Application Science Environmental Management*, *15* (*2*), 279 – 282.

Adefemi, S. O. & Awokunmi, E. E. (2010). Determination of physico-chemical parameters and heavy metals in water samples from Itaogbolu area of OndoState, Nigeria. *African Journal of Environmental Science and Technology*, *4*(*3*):145-148.

Adegoke, H. I., Adekola, F. A., Olowookere, I. T., & Yaqub, A. L. (2017). Thermodynamic studies on adsorption of lead (II) Ion from aqueous solution using magnetite, activated carbon and composites. *Journal of Applied Sciences and Environmental Management*, *21*(*3*), 440-452.

Adelekan, B. A. & Abegunde, K. D. (2011). Heavy Metals Contamination of Soil and Groundwater at Automobile Mechanic Villages in Ibadan, Nigeria**.** *International Journal of the Physical Sciences*, *6*(*5*): 1045-1058.

Adesiyan, I. M., Bisi-Johnson, M., Aladesanmi, O. T., Okoh, A. I., & Ogunfowokan, A. O. (2018). Concentrations and human health risk of heavy metals in rivers in southwest Nigeria. *Journal of Health and Pollution, 8*(*19*):1-14.

Agbalagba, O. E., Agbalagba, O. H., Ononugbo, C. P., & Alao, A. A. (2011). Investigation into the physico-chemical properties and hydrochemical processes of groundwater from commercial boreholes In Yenagoa, Bayelsa State, Nigeria. *African Journal of Environmental Science and Technology*, *5*(*7*), 473481.

Agbor, R. B., Ekpo, I. A., Ekaluo, U. B., Okpako, E. C., Okigbo, A. U., Osang, J. E., & Kalu, S. E. (2013). Groundwater quality assessment of some selected boreholes in Calabar. *World Rural Observe*, *5*(*3*), 37-41.

Agwaramgbo, L., Agwaramgbo, E., Mercadel, C., Edwards, S., & Buckles, E. (2011). Lead remediation of contaminated water by charcoal, LA red clay, spinach, and mustard green. *Journal of Environmental Protection*, *2*(*9*), 1240.

Ahmaruzzaman, M. (2011). Industrial wastes as low-cost potential adsorbents for the treatment of wastewater laden with heavy metals. *Advances in colloid and interface science*, *166*(*1-2*), 36-59.

Akinbile, C. O., & Yusoff, M. S. (2011). Environmental impact of leachate pollution on groundwater supplies in Akure, Nigeria. *International Journal of Environmental Science and Development*, *2*(*1*), 81-86.

Akpor, O. B., & Muchie, M. (2010). Remediation of heavy metals in drinking water and wastewater treatment systems: processes and applications. *International Journal of Physical Sciences*, *5*(*12*), 1807-1817.

Alfarra, R. S., Ali, N. E., & Yusoff, M. M. (2014). Removal of heavy metals by natural adsorbent. *International Journal of Biosciences*, *4*(*7*), 130-139.

Al-Ghouti, M. A., & Da'ana, D. A. (2020). Guidelines for the use and interpretation of adsorption isotherm models: A review. *Journal of hazardous materials*, *393*,1-22.

Aljlil, S. A., & Alsewailem, F. D. (2014). Adsorption of Cu & Ni on bentonite clay from waste water. *Athens Journal of Natural & Formal Sciences*, *1*(*1*), 21-30.

Aloke, C., Uzuegbu, I. E., Ogbu, P. N., Ugwuja, E. I., Orinya, O. F., & Obasi, I.

O. (2019). Comparative assessment of heavy metals in drinking water sources from Enyigba Community in Abakaliki Local Government Area, Ebonyi State, Nigeria. *African Journal of Environmental Science and Technology*, *13*(*4*), 149-154.

Alves, D. C., Coseglio, B. B., Pinto, L. A., & Cadaval Jr, T. R. (2020). Development of Spirulina/chitosan foam adsorbent for phenol adsorption. *Journal of Molecular Liquids*, *309*, 1-6.

Anyika, C., Asri, N. A. M., Majid, Z. A., Jaafar, J., & Yahya, A. (2017). Batch sorption desorption of As (III) from waste water by magnetic palm kernel shell activated carbon using optimized Box–Behnken design. *Applied Water Science*, *7*(*8*), 4573- 4591.

Arah, I. (2015). Monitoring water quality in river bodies of mining communities in Ghana. *Asian Journal of Humanities and Social Sciences*, *3*(*1*), 20-8.

Armah, F. A., Quansah, R., & Luginaah, I. (2014). A systematic review of heavy metals of anthropogenic origin in environmental media and biota in the context of gold mining in Ghana. *International scholarly research notices, 1*, 1-37.

Arivoli, S., Hema, M., & Barathiraja, C. (2008). Comparative study on metal ions adsorption on a low-cost carbonaceous adsorbent kinetic equilibrium and mechanistic studies. *Ranian Journal of Environmental Health Science and Engineering*, *5*, 1-10.

Asad, M., et al. (2024). Field testing of an affordable zero-liquid-discharge arsenic-removal technology for a small- community drinking water system in rural California.

Asamoah, D. N., & Amorin, R. (2011). Assessment of the quality of bottled/sachet water in the Tarkwa-Nsuaem municipality (TM) of Ghana. Research Journal of Applied Sciences, *Engineering and Technology*, *3*(*5*), 377-385.

Asare, E. A., Essumang, D. K., Dodoo, D. K., & Tagoe, S. (2018). Utilization of Bacillus thuringiensis MC28 as a biosorbent for mercury in groundwaters from some selected gold mining communities in the Wassa West District of the Western Region of Ghana. *Environmental Nanotechnology, Monitoring & Management*, *9* (*2018*): 95-106.

Asare, E. A., Dartey, E., Sarpong, K., Effah-Yeboah, E., Amissah-Reynolds, P. K., Tagoe, S., & Balali, G. I. (2021). Adsorption Isotherm, Kinetic and Thermodynamic Modelling of Bacillus subtilis ATCC13952 Mediated Adsorption of Arsenic in Groundwaters of Selected Gold Mining Communities in the Wassa West Municipality of the Western Region of Ghana. American *Journal of Analytical Chemistry*, *12*(*5*), 121-161.

Attua, E. M., Annan, S. T., & Nyame, F. (2014). Water quality analysis of rivers used as drinking sources in artisanal gold mining communities of the Akyem Abuakwa area: A multivariate statistical approach. *Ghana Journal of Geography*, *6*, 24-41.

ATSDR (2009). Draft toxicological profile for cadmium, Alanta, Georgia: US Department of Health and Human service.

Awe, A. A., Opeolu, B. O., Fatoki, O. S., Ayanda, O. S., Jackson, V. A., & Snyman, R. (2020). Preparation and characterisation of activated carbon from Vitis vinifera leaf litter and its adsorption performance for aqueous phenanthrene. *Applied Biological Chemistry*, *63*(1), 1-17.

Awwad, A. M., Maisa'a, W., & Amer, M. W. (2021). Fe $(OH)_3$/kaolinite nanoplatelets: Equilibrium and thermodynamic studies for the adsorption of Pb (II) ions from aqueous solution. *Chemistry International*, *7*(*2*), 90-102.

Azargohar, R., & Dalai, A. K. (2006). Biochar as a precursor of activated carbon. In Twenty- seventh symposium on biotechnology for fuels and chemicals. *Humana Press*.*129,* 762-773.

Azanu, D., & Voegborlo, R.B. (2013). Sorption of inorganic mercury on soils from ankobra basin in the south - western part of Ghana. *Journal of Science and Technology*, *3* (*33*),1-15.

Azis, A., Yusuf, H., Faisal, Z., & Suradi, M. (2015). Water turbidity impact on discharge decrease of groundwater recharge in recharge reservoir. *Procedia Engineering*, *125*, 199-206.

Bandosz, T. J., & Ania, C. O. (2006). Surface chemistry of activated carbons and its characterization. *In Interface Science and Technology*,*7*,159-229.

Bashkova, S., Bagreev, A., & Bandosz, T. J. (2005). Catalytic properties of activated carbon surface in the process of adsorption/oxidation of methyl mercaptan. *Catalysis Today*, *99*(*3-4*), 323-328.

Bashir, N., Saeed, R., Afzaal, M., Ahmad, A., Muhammad, N., Iqbal, J., Khan, A., Maqbool., & Y Hameed, S. (2020). Water quality assessment of lower Jhelum canal in Pakistan by using geographic information system (GIS). *Groundwater for Sustainable Development*, 10, 1-9.

Barsbay, M., Kavaklı, P. A., Tilki, S., Kavaklı, C., & Güven, O. (2018). Porous cellulosic adsorbent for the removal of Cd (II), Pb (II) and Cu (II) ions from aqueous media. *Radiation Physics and Chemistry*, *142*, 70-76.

Beatrice, N. A., Brell, M. K., Aboubakar, A., Stéphanie, Y. Y. A., Armelle, M. Y. D., Bertrand, Z. Z., & Clarisse, M. M. Y. (2019). Assessment of physico-chemical and heavy metal properties of groundwater in Edéa (Cameroon). American *Journal of Water Resources*, 7(1), 1-10.

Bernard, E., Jimoh, A., & Odigure, J. (2013). Heavy metals removal from industrial wastewater by activated carbon prepared from coconut shell. *Research Journal of Chemical Sciences*, *3*(*8*), 3-9.

Bhatnagar, A., & Minocha, A. K. (2009). Utilization of industrial waste for cadmium removal from water and immobilization in cement. *Chemical Engineering Journal*, *150*(*1*), 145-151.

Bobade, V., & Eshtiagi, N. (2015). Heavy metals removal from wastewater by adsorption process: A review. In Asia Pacific Confederation of Chemical Engineering Congress. *Engineers Australia, 312*. 1-7

Bashkova, S., Bagreev, A., & Bandosz, T. J. (2005). Catalytic properties of activated carbon surface in the process of adsorption/oxidation of methyl mercaptan. *Catalysis Today*, *99*(*3-4*), 323-328.

Bodurtha, P.& Brassard, P. (2000) Neutralization of Acid by Steel-Making Slags. *Environmental Technology*, *21* (*11*): 1271-1281.

Boadu, K. O., Joel, O. F., Essumang, D. K., & Evbuomwan, B. O. (2018). Comparative Studies of the Physicochemical Properties and Heavy Metals adsorption Capacity of Chemical Activated Carbon from Palm Kernel, Coconut and Groundnut Shells. Journal of Applied Sciences and Environmental Management, *22*(*11*), 1833-1839.

Brookes, J. D., & Carey, C. C. (2015). Ensure availability and sustainable management of water and sanitation for all. *United Nation Chronicle*, *51*(*4*), 15-16.

Buah, W., MacCarthy, J. & Ndur, S. (2016). Conversion of Corn Cobs Waste into Activated Carbons for Adsorption of Heavy Metals from Minerals Processing Wastewater. *International Journal of Environmental Protection and Policy*, *4*(*4*), 98-103.

Bubanale, S., & Shivashankar, M. (2017). History, method of production, structure and applications of activated carbon. *International Journal of Engineering and Technical Research, 6*, 495-498.

Burlakovs, J., & Vircavs, M. (2011). Heavy metal remediation technologies: review. In Conference, *Ecobaltica*.

Chaemiso, T. D., & Nefo, T. (2019). Removal methods of heavy metals from laboratory wastewater. *Journal of Natural Sciences Research*, *9*(2), 36-42.

Chakraborty, R., Asthana, A., Singh, A. K., Jain, B., & Susan, A. B. H. (2020). Adsorption of heavy metal ions by various low-cost adsorbents: a review. *International Journal of Environmental Analytical Chemistry*, 1-38. Chaudhry, F. N., & Malik, M. F. (2017). Factors affecting water pollution: a review. *Journal Ecosyst Ecography*, *7*(*225*), 1-3.

Chen, M., Cui, Y., Bai, F. and Wang, J. (2013). Effect of two biogas residues' application on copper and zinc fractionation and release in different soils. *Journal of Environmental Science*, *25*(*9*): 1865-1873.

Choi, H. D., Jung, W. S., Cho, J. M., Ryu, B. G., Yang, J. S., & Baek, K. (2009). Adsorption of Cr (VI) onto cationic surfactant-modified activated carbon. *Journal of Hazardous Materials*, *166*(*2-3*), 642-646.

Christine, A. A., Kibet, J. K., Kiprop, A. K., & Were, M. L. (2018). The assessment of bore-hole water quality of Kakamega County, Kenya. *Applied water science*, *8*(*1*), 1-8.

Cobbina, S. J., Duwiejuah, A. B., Quansah, R., Obiri, S., & Bakobie, N. (2015). Comparative assessment of heavy metals in drinking water sources in two small-scale mining communities in northern Ghana. International journal of environmental research and public health, *12*(*9*), 10620-10634.

Daci-Ajvazi, M., Thaçi, B., Daci, N., & Gashi, S. (2017). Biosorbents as Healthy Challenge for the Environment. *International Journal of Environmental and Science Education*, *12*(*3*), 415- 425.

Daily Guide Newspaper, 08/02/2013, 'Ghana faces water crisis-Within 20 years due to activities of galamsey operators. Retrieved 21-07-24. Available at https://www.graphic.com.gh/news/general-news/ghana-faces-water-crisiswithin-20-years-due-to-activities-of-galamsey-operators.html.

De Gisi, S., Lofrano, G., Grassi, M., & Notarnicola, M. (2016). Characteristics and adsorption capacities of low-cost sorbents for wastewater treatment: A review. *Sustainable Materials and Technologies*, *9*, 10-40.

Delkash, M., Bakhshayesh, B. E., & Kazemian, H. (2015). Using zeolitic adsorbentsTo cleanup special wastewater streams: A review. *Microporous and Mesoporous Materials, 214*, 224-241.

Dizge, N., Keskinler, B., & Barlas, H. (2009). Sorption of Ni (II) ions from aqueous solution by Lewatit cation-exchange resin. *Journal of hazardous materials, 167*(*1-3*), 915-926.

Dove, P. M., Han, N., & De Yoreo, J. J. (2005). Mechanisms of classical crystal growth theory explains quartz and silicate dissolution behavior. Proceedings of the National Academy of Sciences, *102*(*43*), 15357-15362.

Dyer, C. A. (2007). Heavy metals as endocrine-disrupting chemicals. *Humana Press*. 111-133.

Food Print. (2025). How industriall agriculture affects our water. https://foodprint.org/issues/how-industrial-agriculture-affects-our-water/

Edet, U. A., & Ifelebuegu, A. O. (2020). Kinetics, isotherms, and thermodynamic modeling of the adsorption of phosphates from model wastewater using recycled brick waste. *Processes*, *8*(*6*), 665.

ElBastamy, E., Ibrahim, L. A., Ghandour, A., Zelenakova, M., Vranayova, Z., & Abu Hashim, M. (2021). Efficiency of Natural Clay Mineral Adsorbent Filtration Systems in Wastewater Treatment for Potential Irrigation Purposes. *Sustainability*, *13*(*10*), 1-18.

El-Kady, A. A., & Abdel-Wahhab, M. A. (2018). Occurrence of trace metals in foodstuffs and their health impact. *Trends in food science & technology*, *75*, 36-45.

Ehi-Eromosele, C. O., & Okiei, W. O. (2012). Heavy metal assessment of ground, surface and tap water samples in Lagos metropolis using anodic stripping voltammetry. *Heavy Metal Assessment of Ground, Surface and Tap Water Samples in Lagos Metropolis Using Anodic Stripping Voltammetry, 2*(*3*), 82-86.

El-Gaayda, J., Titchou, F. E., Oukhrib, R., Yap, P. S., Liu, T., Hamdani, M., & Akbour, R. A. (2021). Natural flocculants for the treatment of wastewaters containing dyes or heavy metals: a state-of-the-art review. *Journal of Environmental Chemical Engineering*, *9*(*2021*).1-22.

Eltayeb, N., & Khan, A. (2019). Design and preparation of a new and novel nanocomposite with CNTs and its sensor applications. *Journal of Materials Research and Technology, 8*(*2*), 2238–2246.

Elumalai, V., Nethononda, V. G., Manivannan, V., Rajmohan, N., Li, P., & Elango, L. (2020). Groundwater quality assessment and application of multivariate statistical analysis in Luvuvhu catchment, Limpopo, South Africa. *Journal of African Earth Sciences*, *171*, 1-14.

Engwa, G. A., Ferdinand, P. U., Nwalo, F. N., & Unachukwu, M. N. (2019). Mechanism and health effects of heavy metal toxicity in humans. *Poisoning in the modern world-new tricks for an old dog, 10* (*2*),1-81.

Eruola, A. O., & Ogunyemi, I. O. (2014). Evaluation of the adsorption capacity of the coconut shell and palm-kernel shell adsorbents powder for the sorption of cadmium (II) ions from aqueous solution. *IOSR Journal of Environmental Science, Toxicology and Food Technology 8*(*6*), 55-63.

Es'haghi, Z., Khalili, M., Khazaeifar, A., & Rounaghi, G. H. (2011). Simultaneous extraction and determination of lead, cadmium and copper in rice samples by a new pre-concentration technique: Hollow fiber solid phase microextraction combined with differential pulse anodic stripping voltammetry. *Electrochimica Acta, 56*(*9*), 3139-3146.

Ewusi, A., Apeani, B. Y., Ahenkorah, I. and Nartey, R. S. (2017), "Mining and Metal Pollution: Assessment of Water Quality in the Tarkwa Mining Area", *Ghana Mining Journal*, *17*(*2*), 17 – 31.

Ezeokonkwo, M. A., Ofor, O. F., & Ani, J. U. (2018). Preparation and evaluation of adsorbents from coal and Irvingia gabonensis seed shell for the removal of Cd (II) and Pb (II) ions from aqueous solutions. *Frontiers in Chemistry*, *132*(*5*), 1-14.

Febrianto, J., Kosasih, A. N., Sunarso, J., & Ju, Y. H., Indraswati, N., & Ismadji, S. (2009). Equilibrium and kinetic studies in adsorption of heavy metals using biosorbent: a summary of recent studies. *Journal of hazardous materials*, *162*(*2-3*), 616-645.

Fianko, J. R., Osae, S., Adomako, D., Adotey, D. K., & Serfor-Armah, Y. (2007). Assessment of heavy metal pollution of the Iture Estuary in the central region of Ghana. *Environmental Monitoring and Assessment*, *131*(*1*), 467-473.

Folarin, O. M., & Sadiku, E. R. (2011). Thermal stabilizers for poly (vinyl chloride): A review. *International journal of physical sciences*, 6, 4323-4330.

Gaikwad, R. W. (2004). Removal of Cd (II) from aqueous solution by activated charcoal derived from coconut shell. *Eelectronic Journal of Environmental, Agricultural and Food chemistry*, *3*(*4*), 702-709.

Gao, Y., Yue, Q., Gao, B., Sun, Y., Wang, W., Li, Q., & Wang, Y. (2013). Comparisons of porous, surface chemistry and adsorption properties of carbon derived from Enteromorpha prolifera activated by $H_4P_2O_7$ and KOH. *Chemical Engineering Journal*, *232* (*1*), 582-590.

Garba, Z.N., Gimba, C.E., & Galadima, A. (2012). Arsenic Contamination of Domestic Water from Northern Nigeria. *International Journal of Science and Technology, 2*(*1*), 55 – 60.

Garg, V. K., Suthar, S., Singh, S., Sheoran, A., & Jain, S. (2009). Drinking water quality in villages of southwestern Haryana, India: assessing human health risks associated with hydrochemistry. *Environmental Geology*, *58*(6), 1329-1340.

Gautam, R. K., Sharma, S. K., Mahiya, S., & Chattopadhyaya, M. C. (2014). Contamination of heavy metals in aquatic media: transport, toxicity and technologies for remediation. in Heavy Metals in Water: *Presence, Removal and Safety*. 1-24.

Gedik, K. & Imamoglu, I. (2008). Removal of cadmium from aqueous solutions using clinoptilolite: influence of pretreatment and regeneration. *Journal of Hazardous Matter. 155*(*1–2*), 385–392.

Genç-Fuhrman, H., Tjell, J. C., & McConchie, D. (2004). Adsorption of arsenic from water using activated neutralized red mud. *Environmental science & technology, 38*(*8*), 2428-2434.

Georgescu, B., Georgescu, C., Dărăban, S., Bouaru, A., & Paşcalău, S. (2011). Heavy metals acting as endocrine disrupters. Scientific Papers Animal Science and Biotechnologies, 44(2), 89-93.

Ghana Statistical Service. (2010). Population & Housing Cencus, District Analytical Report-Sefwi Wiawso Municipal. Retrieved on 05-08-23. Available at https://www2.statsghana.gov.gh/docfiles/2010_District_Report/Western/Sefwi Wiawso.pdf

Giraldo-Gutiérrez, L., & Moreno-Piraján, J. C. (2008). Pb (II) and Cr (VI) adsorption from aqueous solution on activated carbons obtained from sugar cane husk and sawdust. *Journal of Analytical and Applied Pyrolysis, 81*(*2*), 278-284.

Goldberg, S., Criscenti, L. J., Turner, D. R., Davis, J. A., & Cantrell, K. J. (2007). Adsorption–desorption processes in subsurface reactive transport modeling. *Vadose Zone Journal*, 6(*3*), 407-435.

Gorzin, F., & Ghoreyshi, A. A. (2013). Synthesis of a new low-cost activated carbon from activated sludge for the removal of Cr (VI) from aqueous solution: Equilibrium, kinetics, thermodynamics and desorption studies. *Korean Journal of Chemical Engineering, 30*(*8*), 1594-1602.

Grace, W. R. (2010). Co. Enriching Lives, everywhere. *Zeolite Structure Archived February*, *15*, 2009.

Green-Ruiz, C., Rodriguez-Tirado, V., & Gomez-Gil, B. (2008). Cadmium and zinc removal from aqueous solutions by Bacillus jeotgali: pH, salinity and temperature effects. *Bioresource technology*, *99*(*9*), 3864-3870.

Guilherme, M. R., Aouada, F. A., Fajardo, A. R., Martins, A. F., Paulino, A. T., Davi, M. F., & Muniz, E. C. (2015). Super absorbent hydrogels based on polysaccharides for application in agriculture as soil conditioner and nutrient carrier: A review. *European Polymer Journal*, *72*, 365-385.

Gunatilake, S. K. (2015). Methods of removing heavy metals from industrial wastewater. *Methods*, 1(1), 14.

Haftu, Z., & Sathishkumar, P. (2020). Determination of Physicochemical Parameters and Heavy Metals Concentration in Drinking Water at Asgede Tsimbila District, Tigray, Ethiopia. *Chemistry Africa*, 3(*2*), 419-426.

Hamdaoui, O. (2009). Removal of copper (II) from aqueous phase by Purolite C100 MB cation exchange resin in fixed bed columns: Modeling. *Journal of hazardous materials*, *161*(*2-3*), 737-746.

Hansen, B., Thorling, L., Schullehner, J., Termansen, M., & Dalgaard, T. (2017). Groundwater nitrate response to sustainable nitrogen management. *Scientific Reports*, *7*(1), 1-12.

Hazourli, S., Ziati, M., & Hazourli, A. (2009). Characterization of activated carbon prepared from lignocellulosic natural residue: -Example of date stones. *Physics Procedia*, *2*(*3*), 1039-1043.

He, S., & Wu, J. (2019). Hydrogeochemical characteristics, groundwater quality, and health risks from hexavalent chromium and nitrate in groundwater of Huanhe Formation in Wuqi county, northwest China. *Exposure and Health*, *11*(2), 125-137.

HSDB (Hazardous Substance Data Bank). (2009). Diisooctyl phthalate. National Library of Medicine HSDB Database. (Retrieved on 01/06/2020).

Hu, Z., & Qi, L. (2014). 15.5-Sample digestion methods. Treatise on Geochemistry. *Elsevier, Oxfo*rd, *1*(*2*), 87-109.

Hussein, F. H., Halbus, A. F., Lafta, A. J., & Athab, Z. H. (2015). Preparation and characterization of activated carbon from Iraqi Khestawy date palm. *Journal of chemistry*, *2015*, 1-8.

IEPA (2014). Drinking Water Parameters. Retrieved on 20-04-2020. Available at https://www.ie/pubs/advice/drinkingwater/2015_04_21_parametersstandalonedoc.pdf.

Ibrahim, W. M. (2011). Biosorption of heavy metal ions from aqueous solution by red macroalgae. *Journal of Hazardous Materials*, 192(3), 1827-1835.

Ilkunur, S., & Hanife, B., 2013. Equilibrium and Kinetic Studies on the Biosorption of 2-chlorophenol and 4-chlorophenol by live Aspergillus niger. *Ekoloji 22,* (*88*),1–12.

IARC. (2012). Arsenic, metals, fibres and dusts. IARC monographs on the evaluation of carcinogenic risks to humans.

Ismaila, O. S., Samsudeen, O. A., Yusuf, O. A., & Gunu, U. C. (2017). Assessment of Physicochemical Characteristics of Selected Borehole Waters in Oke-Oyi Community, Ilorin East Local Government Area, Kwara State. *Journal of Applied Sciences and Environmental Management, 21*(*6*), 1127-1129.

Jakhrani, S. H., Soni, H. L., & Shar, N. Z. (2019). Analysis of Total Dissolved Solids and Electrical Conductivity in Different Water Supply Schemes of Taluka Chachro, District Tharparkar. *Quaid-E-Awam University Research Journal of Engineering, Science & Technology, Nawabshah.*, *17*(01), 1-5.

Jhariya, D., Khan, R., & Thakur, G. S. (2016). Impact of mining activity on water resource: an overview study. *Proceedings of the Recent Practices and Innovations in Mining Industry, Raipur, India*, 19-20.

Ji, Y., Li, T., Zhu, L., Wang, X., & Lin, Q. (2007). Preparation of activated carbons by microwave heating KOH activation. *Applied surface science, 254*(*2*), 506512.

Jia, S., Jia, R., Zhang, K., Sun, S., Lu, N., Wang, M., & Zhao, Q. (2020). Disinfection characteristics of Pseudomonas peli, a chlorine-resistant bacterium isolated from a water supply network. *Environmental research*, *185*, 1-8.

Jimoh, T., Egila, J. N., Dauda, B. E. N., & Iyaka, Y. A. (2011). Preconcentration and removal of heavy metal ions from aqueous solution using modified charcoal. *Journal Environtal Chemical Ecotoxicol*, *3*, 236-41.

Jiang, C., Wang, X., Qin, D., Da, W., Hou, B., Hao, C., & Wu, J. (2019). Construction of magnetic lignin-based adsorbent and its adsorption properties for dyes. *Journal of hazardous materials*, *369*, 50-61.

Johnson, P. D., Girinathannair, P., Ohlinger, K. N., Ritchie, S., Teuber, L., & Kirby, J. (2008). Enhanced removal of heavy metals in primary treatment using coagulation and flocculation. *Water environment research*, *80*(*5*), 472-479.

Kastali, M., Mouhir, L., Assou, M., Anouzla, A., & Abrouki, Y. (2020). Diagnosis of leachate from a closed landfill, impact on the soil, and treatment by coagulation flocculation with alginate and ferric chloride. *Desalination and Water Treatment*, *206*, 307-314.

Kameda, K., Hashimoto, Y., & Ok, Y. S. (2018). Stabilization of arsenic and lead by magnesium oxide (MgO) in different seawater concentrations. *Environmental Pollution*, *233*, 952-959.

Kennedy, K. K., Maseka, K. J., & Mbulo, M. (2018). Selected adsorbents for removal of contaminants from wastewater: towards engineering clay minerals. *Open Journal of Applied Sciences*, *8*(*8*), 355-369.

Kesici, G. G. (2016). Arsenic ototoxicity. *Journal of otology*, 11(1), 13-17.

Khan, N. A., Ibrahim, S., & Subramaniam, P. (2004). Elimination of heavy metals from wastewater using agricultural wastes as adsorbents. *Malaysian journal of science*, *23*(*1*), 43-51.

Kodom, K., Preko, K., & Boamah, D. (2012). X-ray fluorescence (XRF) analysis of soil heavy metal pollution from an industrial area in Kumasi, Ghana. *An International Journal, 21*(*8*), 1006-1021.

Králik, M. (2014). Adsorption, chemisorption, and catalysis. *Chemical Papers, 68*(*12*), 1625-1638.

Kuang, Y., Zhang, X., & Zhou, S. (2020). Adsorption of methylene blue in water onto activated carbon by surfactant modification. *Water,* 12(2), 587.

Kubicki, J. D., Sofo, J. O., Skelton, A. A., & Bandura, A. V. (2012). A new hypothesis for the dissolution mechanism of silicates. *The Journal of Physical Chemistry, 116*(*33*), 17479-17491.

Kuffour, R. A., Tiimub, B. M., & Agyapong, D. (2018). Impacts of illegal mining (galamsey) on the environment (water and soil) at Bontefufuo area in the Amansie West district. *Journal of Environment and Earth Science 8*(*7*), 98-107.

Kumar, K. V., Gadipelli, S., Wood, B., Ramisetty, K. A., Stewart, A. A., Howard, C.

A. & Rodriguez-Reinoso, F. (2019). Characterization of the adsorption site energies and heterogeneous surfaces of porous materials. *Journal of materials chemistry*, *7*(*17*), 10104-10137.

Lago-Vila, M., Rodríguez-Seijo, A., Arenas-Lago, D., Andrade, L., & Vega, M. F. A. (2017). Heavy metal content and toxicity of mine and quarry soils. *Journal of Soils and Sediments*, *17*(*5*), 1331-1348.

Lakshmi, T., Rajendran, R., Ezhilarasan, D. (2015). Atomic Absorption Spectrophotometric Analysis of Heavy Metals in Acacia catechu willd. *International Journal of Pharmacognosy and Phytochemical Research*, *7*(*4*); 777-781.

Lenntech, I. (2005). FAQ air pollution frequently asked questions. The questions library on air related questions. *Lenntech Water Treatment and Air Purification Holding BV Rotterdam sewege, 402*.

Li, P., Karunanidhi, D., Subramani, T., & Srinivasamoorthy, K. (2021). Sources and consequences of groundwater contamination. *Archives of Environmental Contamination and Toxicology, 80,*1–10.

Liu, H., Chen, W., Liu, C., Liu, Y. U., & Dong, C. (2014). Magnetic mesoporous clay adsorbent: preparation, characterization and adsorption capacity for atrazine. *Microporous and mesoporous materials, 194,* 72-78.

Liu, J., Wu, X., Hu, Y., Dai, C., Peng, Q., & Liang, D. (2016). Effects of Cu (II) on The adsorption behaviors of Cr (III) and Cr (VI) onto kaolin. *Journal of Chemistry, 2016*,1-11.

Liu, J., Mwamulima, T., Wang, Y., Fang, Y., Song, S., & Peng, C. (2017). Removal of Pb (II) and Cr (VI) from aqueous solutions using the fly ash-based adsorbent material-supported zero-valent iron. *Journal of Molecular Liquids*, *243*, 205-211.

Loi, Q. K., Horikawa, T., Do, D. D., & Nicholson, D. (2021). Characterization of non-graphitized carbon blacks: a model with surface crevices. *Physical Chemistry Chemical Physics*, *23*(22), 12569-12581.

Maju-Oyovwikowhe, G. E., & Shuaib, I. I. (2019). Physiochemical characteristics and heavy metal levels of water from hand dug wells in Ikiran-Ile, Akoko Edo Local Government Area, Edo State, Nigeria. *Journal of Applied Sciences and Environmental Management*, 23(2), 283-290.

Mandal, N. K. (2014). Performance of low-cost bio adsorbents for the removal of metal ions-A review. *International Journal of Science and Research* (*IJSR*)*, 3*(*1*), 177-180.

Mandel, J. S., McLaughlin, J. K., Schlehofer, B., Mellemgaard, A., Helmert, U., Lindblad, P. & Adami, H. O. (1995). International renal-cell cancer study. IV. Occupation. International journal of cancer, 61(5), 601-605.

Mann, A. G., Tam, C. C., Higgins, C. D., & Rodrigues, L. C. (2007). The association between drinking water turbidity and gastrointestinal illness: a systematic review. *BMC public health, 7*(*1*), 1-7.

Mantey, J., Nyarko, K. B., Owusu-Nimo, F., Awua, K. A., Bempah, C. K., Amankwah, R. K., & Appiah-Effah, E. (2020). Influence of illegal artisanal small-scale gold mining operations (galamsey) on oil and grease (O/G) concentrations in three hotspot assemblies of Western Region, Ghana. *Environmental Pollution*, 263, 114251.

Meride, Y., & Ayenew, B. (2016). Drinking water quality assessment and its effects on residents' health in Wondo genet campus, Ethiopia. *Environmental Systems Research, 5*(*1*), 1-7.

Mitra, P., Pal, D. K., & Das, M. (2018). Does quality of drinking water matter in kidney stone disease: A study in West Bengal, India. *Investigative and clinical urology*, *59*(3), 158- 165.

Mohammed, M. A., Shitu, A., Tadda, M. A., & Ngabura, M. (2014). Utilization of various Agricultural waste materials in the treatment of Industrial wastewater containing Heavy metals: A Review. *International Reserach Jounal Environmental Science*, *3*(*3*), 62-71.

Mohan, S., & Gandhimathi, R. (2009). Removal of heavy metal ions from municipal solid waste leachate using coal fly ash as an adsorbent. *Journal of hazardous materials, 169*(1-3), 351-359.

Mohan, D., & Pittman Jr, C. U. (2007). Arsenic removal from water/wastewater using adsorbents-a critical review. *Journal of hazardous materials*, *142*(1-2), 1-53. Moss, B. (2008). Water pollution by agriculture. Philosophical Transactions of the *Royal Society B: Biological Sciences*, *363*(*1491*), 659-666.

Motsara, M. R., & Roy, R. N. (2008). Guide to laboratory establishment for plant nutrient analysis (19). 1-183.

Nabi, S. A., Bushra, R., Naushad, M., & Kahn, A. M. (2015). Synthesis, characterization and analytical applications of a new cation exchange eaterial poly-o-toluidine stannic molybdate for the separation of toxic metal ions. *Chemical Engineering Journal*, 165, 529–536.

Najua, D. T.; Luqman, C. A.; Zawani, Z.; Suraya, & A. R. (2008). Adsorption of copper from aqueous solution by ElaisGuineensis kernel activated carbon, *Journal Engineering Science & Technology*, 3(2), 180-189.

Nazifa, T. H., Hadibarata, T., Yuniarto, A., Elshikh, M. S., & Syafiuddin, A. (2019). Equilibrium, kinetic and thermodynamic analysis petroleum oil adsorption from aqueous solution by magnetic activated carbon. In *IOP Conference Series: Materials Science and Engineering* 1(495), 1-13.

Niu, M., Li, G., Cao, L., Wang, X., & Wang, W. (2020). Preparation of sulphate aluminate cement amended bentonite and its use in heavy metal adsorption. *Journal of Cleaner Production*, *256*, 1-16.

NTP. (2004). Lead and Lead Compounds. Retrieved on 12-06-2020 Available at www.ntp.niehs.nih.gov/ntp/roc/content/profiles/lead.pdf.

Obiefuna, G. I., & Sheriff, A. (2011). Assessment of shallow ground water quality of Pindiga Gombe Area, Yola Area, NE, Nigeria for irrigation and domestic purposes. *Research Journal of Environmental and Earth Sciences*, 3(2), 131-141.

Obiri, S., Dodoo, D. K., Okai-Sam, F., & Essumang, D. K. (2006). Cancer health risk assessment of exposure to arsenic by workers of AngloGold Ashanti–Obuasi Gold Mine. *Bulletin of environmental contamination and toxicology, 76*(*2*), 195-201.

Obiri, S., Dodoo, D. K., Armah, F. A., Essumang, D. K., & Cobbina, S. J. (2010). Evaluation of lead and mercury neurotoxic health risk by resident children in The Obuasi municipality, Ghana. *Environmental toxicology and pharmacology, 29*(*3*), 209-212.

Ojekunle, Z. O., Adeyemi, A. A., Taiwo, A. M., Ganiyu, S. A., & Balogun, M. A. (2020). Assessment of physicochemical characteristics of groundwater within selected industrial areas in Ogun State, Nigeria. *Environmental Pollutants and Bioavailability*, 32(*1*), 100-113.

Olasoji, S. O., Oyewole, N. O., Abiola, B., & Edokpayi, J. N. (2019). Water quality assessment of surface and groundwater sources using a water quality index method: A case study of a peri-urban town in southwest, Nigeria. *Environments, 6*(*2*), 23.

Oluyemi, E.A., Adekunle, A.S., Adenuga A. A., Makinde, W, O., (2010). Physico-chemical properties and heavy metal content of water sources in Ife North Local Government Area of Osun State, Nigeria. *African Journal Environmental Science Technology, 4*(*10*),691-697.

Oluyemi, E. A., Adeyemi, A. F., & Olabanji, I. O. (2012). Removal of Pb^{2+} and Cd^{2+} ions from wastewaters using palm kernel shell charcoal (PKSC). Research *Journal in Engineering and Applied Sciences*, *1*(*5*), 308-313.

Onundi, Y. B., Mamun, A. A., Al Khatib, M. F., & Ahmed, Y. M. (2010). Adsorption of copper, nickel and lead ions from synthetic semiconductor industrial wastewater by palm shell activated carbon. *International Journal of Environmental Science & Technology*, *7*(*4*), 751-758.

Othman, M.N., Abdullah, M.P., & Aziz, Y.F. (2010). Removal of Aluminium from Drinking Water. *Sains Malaysiana*, *39*, 51-55.

Owlad, M., Aroua, M. K., Daud, W. A. W., & Baroutian, S. (2009). Removal of hexavalent chromium-contaminated water and wastewater: a review. *Water, air, and soil pollution*, *200*(*1*), 59-77.

Oyelude, E. O., & Appiah-Takyi, F. (2012). Removal of methylene blue from aqueous solution using alkali-modified malted sorghum mash. *Turkish Journal of Engineering and Environmental Sciences, 36*(*2*), 161-169.

Pal, P., Sen, M., Manna, A., Pal, J., Pal, P., Roy, S., & Roy, P. (2009). Contamination of groundwater by arsenic: a review of occurrence, causes, impacts, remedies and membrane-based purification. *Journal of Integrative Environmental Sciences, 6*(*4*), 295-316.

Park, Donghee, Yeoung-Sang Yun, & Jong Moon Park. (2010) "The past, present, and future trends of biosorption." *Biotechnology and Bioprocess Engineering 15*, (*1*) 86-102.

Patlolla, A. K., & Tchounwou, P. B. (2005). Serum acetyl cholinesterase as a Biomarker of arsenic induced neurotoxicity in sprague dawley rats. *International Journal of Environmental Research and Public Health*, *2*, 80-83

Peng, J., Song, Y., Yuan, P., Xiao, S., & Han, L. (2013). A novel identification method of the environmental risk sources for surface water pollution accidents in chemical industrial parks. *Journal of Environmental sciences, 25*(*7*), 1441-1449.

Pereira, A. G. B., Martins, A. F., Paulino, A. T., Fajardo, A. R., Guilherme, M. R., Faria, M. G. I. & Muniz, E. C. (2017). Recent advances in designing hydrogels from chitin and chitin-Derivatives and their impact on environment and agriculture: *Revista Virtual Quimica, 9*(*1*), 370-386.

Prahas, D., Kartika, Y., Indraswati, N., & Ismadji, S. J. C. E. J. (2008). Activated carbon from jackfruit peel waste by H3PO4 chemical activation: Pore Structure and surface chemistry characterization. *Chemical Engineering Journal, 140* (*1-3*), 32-42.

Pyrzynska, K. (2019). Removal of cadmium from wastewaters with low-cost adsorbents. *Journal of Environmental Chemical Engineering*, 7(1), 1-29.

Radnia, H., Ghoreyshi, A. A., Younesi, H., & Najafpour, G. D. (2012). Adsorption of Fe (II) ions from aqueous phase by chitosan adsorbent: equilibrium, kinetic, and thermodynamic studies. *Desalination and Water Treatment, 50*(*1-3*), 348359.

Rahmanian, N., Ali, S. H. B., Homayoonfard, M., Ali, N. J., Rehan, M., Sadef, Y., & Nizami, A. S. (2015). Analysis of physiochemical parameters to evaluate the drinking water quality in the state of Perak, Malaysia. *Journal of Chemistry*, *1*, 1-10.

Rao, K. S, Mohapatra, M. Anand, S. & Venkateswarlu, P. (2010) Review on cadmium removal from aqueous solutions. *International Journal of Engineering, Science and Technology, 2*, 81-103.

Rao, M. M., Ramana, D. K., Seshaiah, K., Wang, M. C., & Chien, S. C. (2009). Removal of some metal ions by activated carbon prepared from Phaseolus aureus hulls. *Journal of hazardous materials*, *166*(2), 1006-1013.

Repo, E., Warchoł, J. K., Bhatnagar, A., & Sillanpää, M. (2011). Heavy metals adsorption by novel EDTA-modified chitosan–silica hybrid materials. *Journal of colloid and interface science, 358*(*1*), 261-267.

Salam, O. E. A., Reiad, N. A., & ElShafei, M. M. (2011). A study of the removal characteristics of heavy metals from wastewater by low-cost adsorbents. *Journal of Advanced Research, 2(4), 297-303.*

Salama, A., & Abou-Zeid, R. E. (2021). Ionic chitosan/silica nanocomposite as efficient adsorbent for organic dyes. *International Journal of Biological Macromolecules*, *188*, 404-410.

Saloua, J., Mohamed, T., Ahmed, M., & Khadija, M. (2020). Industrial rejection: removal of heavy metals based on chemical precipitation and research for recoverable material in by-products. *International Journal of Engineering Technologies and Management Research, 7*(*2*), 39-52.

Samie, A., Makonto, O. T., Mojapelo, P., Bessong, P. O., Odiyo, J. O., & Uaboi-Egbenni, P. O. (2013). Physico-chemical assessment of borehole water used by schools in Greater Giyani Municipality, Mopani district, South Africa. *African Journal of Biotechnology, 12(30*), 4858-4865.

Sarala Thambavani, D., & Uma Mageswari, T. S. R. (2014). Water quality indices as indicators for potable water. *Desalination and Water Treatment*, *52*(25-27), 4772-4782.

Saravanan, A., Sundararaman, T. R., Jeevanantham, S., Karishma, S., Kumar, P. S., & Yaashikaa, P. R. (2020). Effective adsorption of Cu (II) ions on sustainable adsorbent derived from mixed biomass (Aspergillus campestris and agro waste): optimization, isotherm and kinetics study. *Groundwater for Sustainable Development, 11*(*1-15*).

Satarug, S., Vesey, D. A., & Gobe, G. C. (2017). Current health risk assessment practice for dietary cadmium: Data from different countries. *Food and Chemical Toxicology, 106*, 430-445.

Savić, I., Stojiljkovic, S., & Gajić, D. (2014). Industrial application of clays and clay minerals. In Clays and Clay Minerals: Geological Origin, Mechanical Properties and Industrial Applications. *Nova Science Publishers, New York,* 379-402.

Sekabira, K., Origa, H. O., Basamba, T. A., Mutumba, G., & Kakudidi, E. (2010). Assessment of heavy metal pollution in the urban stream sediments and its tributaries. *International Journal of Environmental Science & Technology*, *7*(*3*), 435-446.

Senila, M., Levei, E., Cadar, O., Senila, L. R., Roman, M., Puskas, F., & Sima, M. (2017). Assessment of availability and human health risk posed by arsenic contaminated well waters from Timis-Bega area, Romania. *Journal of analytical methods in chemistry*, *1*, 1-7.

Sharma, H., Rawal, N., & Mathew, B. B. (2015). The characteristics, toxicity and effects of cadmium. *International Journal of Nanotechnology and Nanoscience, 3,* 1-9.

Shih, R. A., Hu, H., Weisskopf, M. G., & Schwartz, B. S. (2007). Cumulative lead dose and cognitive function in adults: a review of studies that measured both blood lead and bone lead. *Environmental Health Perspectives*, *115*(*3*), 483492.

Shirin, S., Jamal, A., Emmanouil, C., & Yadav, A. K. (2021). Assessment of Characteristics of Acid Mine Drainage Treated with Fly Ash. *Applied Sciences*, *11*(9), 1-10.

Singh, N., Kumar, D., & Sahu, A. P. (2007). Arsenic in the environment: effects on human health and possible prevention. *Journal of Environmental Biology*, *28*(*2*), 359.

Srivastava, V. C., Mall, I. D., & Mishra, I. M. (2006). Characterization of mesoporous rice husk ash (RHA) and adsorption kinetics of metal ions from aqueous solution onto RHA. *Journal of hazardous materials*, *134*(*1-3*), 257-267.

Staneva, D., Koutzarova, T., Vertruyen, B., Vasileva-Tonkova, E., & Grabchev, I. (2017). Synthesis, structural characterization and antibacterial activity of cotton fabric modified with a hydrogel containing barium hexaferrite nanoparticles. *Journal of Molecular Structure*, *1127*, 74-80.

Sud, D., Mahajan, G., & Kaur, M. P. (2008). Agricultural waste material as potential adsorbent for sequestering heavy metal ions from aqueous solutions–A review. *Bioresource technology, 99*(*14*), 6017-6027.

Sulyman, Y. I., Abdulrazak, S., Oniwapele, Y. A., & Ahmad, A. (2015). Concentration of heavy metals in some selected cereals sourced within Kaduna state, Nigeria. *IOSR Journal of Environmental Science, Toxicology and Food Technology*, *9*(*10*), 17-19.

Su, Z., Wu, J., He, X., & Elumalai, V. (2020). Temporal changes of groundwater quality within the groundwater depression cone and prediction of confined groundwater salinity using Grey Markov model in Yinchuan area of northwest China. *Exposure and Health*, *12*(3), 447-468.

Sun, S., Feng, C., Tong, S., Zhao, Y., Chen, N., & Zhu, M. (2021). Evaluation of advanced phosphorus removal from slaughterhouse wastewater using industrial waste-based adsorbents. *Water Science and Technology*, *83*(6), 1407-1417.

Tadda, M. A., Ahsan, A., Shitu, A., ElSergany, M., Arunkumar, T., Jose, B., Abdur R. M., & Nik, N. N. (2016). A review on activated carbon: process, application and prospects. *Journal of Advanced Civil Engineering Practice and Research, 2*(*1*):7-13.

Tinkov, A. A., Filippini, T., Ajsuvakova, O. P., Skalnaya, M. G., Aaseth, J., Bjørklund, G., Gatiatulinai, E.R., Popovaj E.V., Nemereshinai, O.N., Huangk, P.T., Vincetid, M. Anatoly & Skalny, A. V. (2018).

Tizo, M. S., Blanco, L. A. V., Cagas, A. C. Q., Cruz, B. R. B. D., Encoy, J. C., Gunting, J. V., Renato O. Arazo, Val I. F. & Mabayo, V. I. F. (2018). Efficiency of calcium carbonate from eggshells as an adsorbent for cadmium removal in aqueous solution. *Sustainable Environment Research, 28*(*6*), 326-332.

Tumin, N. D., Chuah, A. L., Zawani, Z., & Rashid, S. A. (2008). Adsorption of copper from aqueous solution by Elais Guineensis kernel activated carbon. *Journal of Engineering Science and Technology, 3*(*2*), 180-189.

Trivunac, K., & Stevanovic, S. (2006). Removal of heavy metal ions from water by complexation-assisted ultrafiltration. *Chemosphere, 64*(*3*), 486-491. Uddin, M. K., & Nasar, A. (2020). Walnut shell powder as a low-cost adsorbent for methylene blue dye: isotherm, kinetics, thermodynamic, desorption and response surface methodology examinations. *Scientific Reports*, *10*(*1*), 1-13.

UNICEF, & WHO. (2025). Fast fact: 1 in 4 people globally still lack access to safe drinking water-WHO, UNICEF. https://www.unicef.org/press-releasess/fast-facta-1-4-people-globally-still-lack-acess-safe-drinking-water-who-unicef

Upadhyay, U., Sreedhar, I., Singh, S. A., Patel, C. M., & Anitha, K. L. (2021). Recent advances in heavy metal removal by chitosan-based adsorbents. *Carbohydrate Polymers*, *251*, 1-29.

Upfold, N. S., Luke, G. A., & Knox, C. (2021). Occurrence of human enteric viruses in water sources and shellfish: A focus on Africa. *Food and Environmental Virology*, 1-31.

USEPA (2009). National primary drinking water regulations (Retrieved 17-23-23) Available at: https://www.nrc.gov/docs/ML1307/ML13078A040.pdf.

Vafakhah, S., Bahrololoom, M. E., Bazarganlari, R., & Saeedikhani, M. (2014). Removal of copper ions from electroplating effluent solutions with native corn cob and corn stalk and chemically modified corn stalk. *Journal Environmental & Chemical Engineering*, 356–361.

Wang, J., Zhang, Y., Liu, Z., Norris, P., Romero, C. E., Xu, H., & Pan, W. P. (2017). Effect of coordinated air pollution control devices in coal-fired power plants on arsenic emissions. *Energy & Fuels, 31*(*7*), 7309-7316.

Wang, J., Zhang, W., & Wei, J. (2019). Fabrication of poly (β-cyclodextrin) conjugated magnetic graphene oxide by surface-initiated RAFT polymerization for synergetic adsorption of heavy metal ions and organic pollutants. *Journal of Materials Chemistry A*, *7*(5), 2055-2065.

Wang, L., Shi, C., Pan, L., Zhang, X., & Zou, J. J. (2020). Rational design, synthesis, adsorption principles and applications of metal oxide adsorbents: A review. *Nanoscale, 12*(*8*), 4790-4815.

Wani, A. L., Ara, A., & Usmani, J. A. (2015). Lead toxicity: a review. *Interdisciplinary toxicology*, *8*, (*2*), 55-64.

World Health Organization. (2011). Guidelines for Drinking-water Quality, Fourth Edition-WHO.Retrieved on 08-10-24. Available at https://www.who.int/water_sanitation_health/publications/2011/9789241548151ch12.pdf .

World Health Organization. (2010). Preventing disease through healthy environments: exposure to Arsenic: A major public health concern. Retrieved on 11/06/24. Available at www.who.int/ipcs/features/arsenic.pdf.

World Health Organization. (2019). Guidelines for Drinking-water Quality. Retrieved on 11/05/24. Availabel at www.who.int/news-room/fact-sheets/detail/drinking-water.

Williams, N. E., & Aydinlik, N. P. (2021). KOH ratio effect, characterization, and kinetic modeling of methylene blue from aqueous medium using activated carbon from Thevetia peruviana shell. *Chemical Engineering Communications*, *208*(8), 1189-1208.

Wikipedia contributors. (2023). Water resources. In Wikipedia. https://en.wikipedia.org/wiki/Water_resources

Xia, M., Chen, Z., Li, Y., Li, C., Ahmad, N. M., Cheema, W. A., & Zhu, S. (2019). Removal of Hg (II) in aqueous solutions through physical and chemical adsorption principles. *RSC advances, 9*(*36*), 20941-20953.

Xiaolong, W., Jingyi, H., Ligang, X., & Qi, Z. (2010). Spatial and seasonal variations of the contamination within water body of the Grand Canal, China. Environmental Pollution, 158(5), 1513-1520.

Xu, J., Chen, L., Qu, H., Jiao, Y., Xie, J., & Xing, G. (2014). Preparation and characterization of activated carbon from reedy grass leaves by chemical activation with H3PO4. *Applied Surface Science*, *320*, 674-680.

Yadav, M., Gupta, R., Arora, G., Yadav, P., Srivastava, A., & Sharma, R. K. (2020). Current Status of Heavy Metal Contaminants and Their Removal/Recovery Techniques. *In Contaminants in Our Water: Identification and Remediation Methods*, *3*, 41-64.

Yahaya, M. I., Ezeh, G. C., Musa, Y. F., & Mohammad, S. Y. (2010). Analysis of heavy metals concentration in road sides soil in Yauri, Nigeria. African Journal of Pure and Applied Chemistry, 4(3), 022-030.

Ye, X., & Wong, O. (2006). Lead exposure, lead poisoning, and lead regulatory standards in China. *Regulatory Toxicology and Pharmacology, 46*(*2*), 157-162.

Yin, G., Song, X., Tao, L., Sarkar, B., Sarmah, A. K., Lin, Q., Xiao, R., Liu, Q., Zhang, W. & Wang, H. (2020). Novel Fe-Mn binary oxide-biochar as an adsorbent for removing Cd (II) from aqueous solutions. *Chemical Engineering Journal, 389*, 1-9.

Yu, C., & Han, X. (2015). Adsorbent Material Used in Water Treatment-A Review. In 2015 2nd International Workshop on Materials Engineering and Computer Sciences. *Atlantis Press*. 290-293.

Zereg, S., Boudoukha, A., & Benaabidate, L. (2018). Impacts of natural conditions and anthropogenic activities on groundwater quality in Tebessa plain, Algeria. *Sustainable Environment Research, 28*(*6*), 340-349.

Zhang, W., An, Y., Li, S., Liu, Z., Chen, Z., Ren, Y.,Wang, X., Zhang, X. & Wang, X. (2020). Enhanced heavy metal removal from an aqueous environment using an eco-friendly and sustainable adsorbent. *Scientific reports*, *10*(*1*), 1- 19.

Zhu, J., Shi, B., Zhu, J., Chen, L., Zhu, J., Liu, D., & Liang, H. (2009). Production, characterization and properties of chloridized mesoporous activated carbon from waste tyres. *Waste management & research, 27*(*6*), 553-560.

Zulum, U., Bulakarima, A. U., & Chandan, V. (2017). Assessment of Health Effect of Water Pollution in Maiduguri Metropolis. *International Journal of Sciences & Applied Research*, 4(4) 40-45.